Chemical Engineering Journal Advances 14 (2023) 100460

Contents lists available at ScienceDirect

Chemical Engineering Journal Advances

journal homepage: www.sciencedirect.com/journal/chemical-engineering-journal-advances

Review on green biomass-synthesized metallic nanoparticles and composites and their photocatalytic water purification applications: Progress and perspectives

Shahid-ul-Islam [a,b,*], Satyaranjan Bairagi [c], Mohammad Reza Kamali [d]

[a] Department of Biological and Agricultural Engineering, University of California, Davis, CA, 95616, United States
[b] Department of Textile and Fibre Engineering, Indian Institute of Technology Delhi, Hauz Khas, New Delhi, 110016, India
[c] Materials and Manufacturing Research Group, James Watt School of Engineering, University of Glasgow, Glasgow, G12 8QQ, United Kingdom
[d] Process and Environmental Technology Lab, Department of Chemical Engineering, KU Leuven, J. De Nayerlaan 5, Sint-Katelijne-Waver, 2860, Belgium

ARTICLE INFO

Keywords:
Green synthesis
Metallic nanoparticles
Photocatalysis
Dyes
Heavy metals
Antibiotics

ABSTRACT

In recent years, the use of biomass for the cost-effective synthesis of nanoparticles has emerged as a promising green technology. Because of their remarkable properties, such as tunable surface plasmon resonance characteristics and high surface areas, bio-synthesised nanomaterials are receiving more scientific and academic attention for their use in various application sectors, especially as catalysts in environmental remediation. Green synthesized nanomaterial's can efficiently contribute to the degradation of a wide range of organic pollutants, including dyes, into harmless by-products. These particles have a cure for recalcitrant organic and inorganic pollutants due to their photocatalytic properties, which largely depend on the production of reactive oxygen species under sunlight or UV illumination. This comprehensive review systematically covers up-to-date knowledge on recent developments in the green synthesis of nanoparticles and composites using plants and microorganisms, unravels underlying mechanisms, and highlights their application areas. It then provides detailed information on their applications in the degradation of potentially toxic organic dyes and the removal of other emerging pollutants, including heavy metals and antibiotics. Finally, the current challenges and perspectives of this technology for future applications are discussed.

1. Introduction

With the growth of the worldwide population and advancements in industrialization and urbanization, the demand for chemicals, materials, and energy has increased enormously [1]. As a result, a massive amount of unwanted manmade waste is released into the environment, resulting in polluting environmental systems. More specifically, an aquatic system gets hampered due to these undesirable wastes. Water is a valuable commodity for human life, industrial use, and national economic growth [2]. Different types of wastes, like heavy metals, organic compounds, fertilizers, industrial effluents, etc., are the major concerns for environmental contamination [3]. Therefore, protecting the environment from various contaminants should be the main target for the whole community in the world. There are different technologies by which environmental contamination can be reduced, such as adsorption of the contaminants, chemical reactions, photocatalysis, filtration of the contaminants, etc. Conventional methods for the removal of environmental contaminants have some limitations, such as higher energy consumption, higher cost, tendency to generate toxic biproducts, requiring high temperature, etc. Moreover, conventional methods have lower reactivity and are volatile in nature, which are not desirable for the degradation of environmental contaminants [3]. Recently, nanotechnology has drawn great attention in the research community to overcome these problems with conventional methods. Nanotechnology is nothing but a process by which materials in the nanoscale range can be synthesized and utilized in different fields such as biology, chemistry, material science, and engineering [4,5]. In recent years, nanotechnology has become a more attractive research area in the field of environmental concerns. The properties and efficacy of the nanomaterials make them an appropriate candidate for reducing environmental pollution since they have significant catalysing activity and a higher surface to volume ratio, which results in higher reactivity of the nanomaterials. [6,7].

* Corresponding author.
E-mail address: shads.jmi@gmail.com (Shahid-ul-Islam).

https://doi.org/10.1016/j.ceja.2023.100460

Available online 26 January 2023

Nanoparticles have higher surface area and surface energy, which causes them to easily absorb a huge number of environmental pollutants [6,7].

In recent years, amongst different nanomaterials, metallic nanoparticles have attracted more attention in the different fields of applications like environmental remediation, catalysis, imaging, gene therapy, drug delivery, electronics, cosmetics, space industry, and many more shown in Fig. 1 [8–11]. Their attractive characteristics, like higher surface area, surface energy, and chemical reactivity, make them suitable for different applications. Moreover, their chemical reactivity can be controlled by changing their size, shape, and dispersion. They also have diverse magnetic, optical, thermal, and mechanical properties [12]. The global synthesis of metallic nanoparticles is estimated to be 13.7 billion US dollars, with a projected value of 50 billion US dollars by 2026 [2]. The metal nanoparticles (MNPs) can be synthesized by different techniques like physical, chemical, and biological methods. In physical and chemical synthesis methods, precursor materials react to produce metal nanoparticles in the presence of reducing agents such as sodium borohydride, hydrazine, etc. These reducing agents are generally toxic in nature, which causes human health issues and environmental pollution [13]. To overcome problems with the physical and chemical synthesis of metallic nanoparticles, the biological synthesis method has attracted more attention from researchers because this method is more facile, biocompatible, less toxic, energy efficient, greener, and eco-friendly for synthesizing nanoparticles. Therefore, green nanotechnology is a prominent solution to synthesizing nanoparticles while maintaining environmental quality. Green nanotechnology, along with the principles of green chemistry, is utilized to maintain a pollution-free environment. In addition, green nanotechnology provides nanomaterials through safer, greener, and eco-friendly pathways. Green nanotechnology-based synthesis is more advantageous compared to chemical synthesis for metallic nanoparticles because synthesized nanoparticles are more stable at room temperature for a long time in green synthesis than in chemical synthesis. Using a suitable process, the green synthesis method's cost can be decreased by 1/10th compared to the chemical synthesis method. Furthermore, because surface capping agents (which are present during synthesis) on the surface of green nanoparticles can remove a greater number of contaminants than nanoparticles. So far, different biological sources such as microorganisms (bacteria, fungi, and algae), bio wastes, agro-wastes, plant derivatives (leaves, fruits, and seeds) and different biodegradable polymers have been utilized for the synthesis of metallic nanoparticles. Single metallic nanoparticles can be categorized into two broad groups, namely single metallic nanoparticles and compound metallic nanoparticles [14–21].

To date, a number of review papers have been published on the green synthesis of metal and metal oxide nanoparticles, but a comprehensive and systematic review where all metallic, metal oxide, bimetallic, core-shell, and composite-based nanoparticles have been discussed is rare [6,15,29,21,30]. Therefore, the present review will first summarise the green synthesis of nanoparticles in detail by outlining the key discoveries in the green synthesis of metal, metal oxide, and composite nanoparticles and making an attempt to resolve their probable synthesis mechanisms. This review then focuses on green chemistry and its mechanisms for the remediation of environmental pollution. Moreover, the catalytic activity of different metallic nanoparticles in environmental pollution remedies has also been covered in detail.

2. Green synthesis of metal and metal oxide nanoparticles

The green synthesis route for the preparation of metal and metal oxide nanoparticles has attracted significant attention as it can offer toxicity free living organisms and a pollution-free environment, unlike physical and chemical synthesis routes [31]. Moreover, green synthesis can present further gains like reducing input energy in the synthesis process and lower product costs compared to the conventional synthesis methods (physical and chemical), which leads to an easy commercialization of the nanoparticles. There are various green sources such as microorganisms (bacteria, fungi, algae, etc.), biowaste, agricultural waste, and plant components (leaves, fruits, and seeds) that can be used for the synthesis of nanoparticles [31,32].

2.1. Green synthesis of monometallic nanoparticles

Metal nanoparticles that are commonly used include gold, silver, copper, platinum, iron, and others. So far, various approaches for the preparation of these metal nanoparticles through green routes (plant-based synthesis and microorganism-based synthesis) have been explored by the different research groups. In the microbe-based synthesis method,

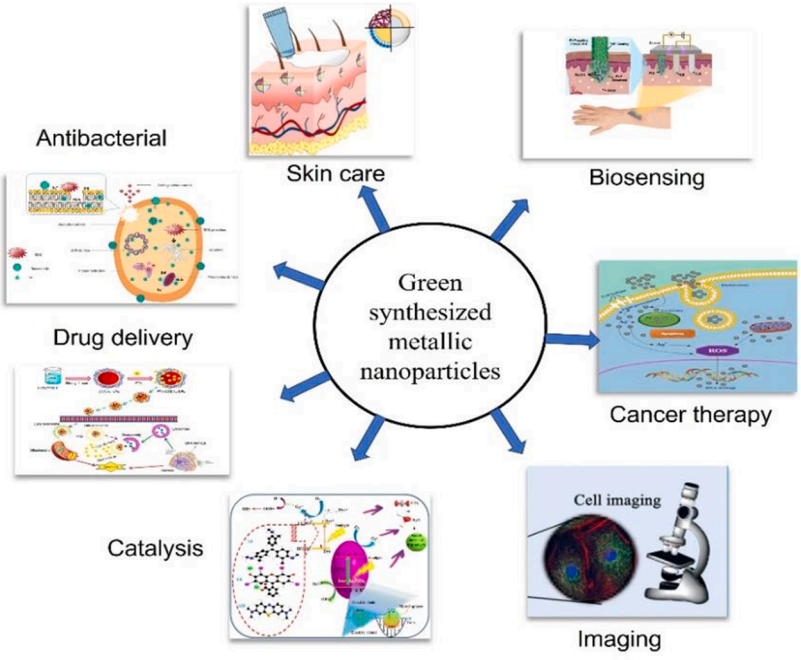

Fig. 1. Applications of green synthesized metallic nanoparticles [22–28].

it is very difficult to maintain the conditions required for microorganisms' culture, and therefore a cheaper and easier synthesis based on plant extracts has received more attention. In recent years, many approaches have already been explored for the preparation of metal nanoparticles (MNPs) using different plant parts such as leaves, fruits, peels, stems, and seeds, etc. Due to their attractive antibacterial property, silver nanoparticles (Ag NPs) are widely used in the field of wound healing applications. Moreover, it has other applications in agriculture, water treatment, air filtration, oxidation catalysis, etc. There are different plants, such as *Ocinum sanctum, Lantana camera, Alovera,* etc., mainly used to prepare AgNPs. These plant extracts contain various phenolic compounds like flavonoids and terpenoids, which can be utilized as reducing and stabilizing agents for the preparation of the AgNPs (Fig. 2a). Various research works in the synthesis of AgNPs using green synthesis routes have already been reported. For example, silver nanoparticles (AgNPs) having an average size in the range of 15–33 nm, were synthesized successfully by Widatalla et al. [33] using green tea extract solution. According to photochemical and FTIR analysis [34], green tea extract contains a variety of compounds, including gallic acid (GA), catechin (CE), gallocatechin (GC), epigallocatechin protein, flavonoids, saponin, and glycosides. Green tea flavonoids contain more hydroxyl groups than epigallocatechin gallate, which acts as a strong reducing agent for AgNP synthesis [35]. Likewise, Farshori et al. [36] also prepared AgNPs where they used *Phoenix dactylifera* seed extract as a reducing agent. *Phoenix dactylifera* seed extract contains various chemical compounds such as flavonoids, alkaloids, saponin, terpenoids, anthraquinones, phenolics, fatty acids, proteins, etc. [37,38]. Amongst them, phenolic compounds mainly act as stabilizing and reducing agents for the synthesis of AgNPs. The average size of the synthesized AgNPs was found to be 15 nm. A flow chart for the extraction and preparation of AgNPs is depicted in Fig. 2b.

Liu and colleagues [39] synthesized AgNPs using rice husk extract as a reducing agent (Fig. 3a). In the presence of rice husk extract (which contains quinones), caffeic acid (CA) was found as the main chemical compound responsible for reducing Ag+ into metallic silver nanoparticles. TEM analysis confirmed that the synthesized AgNPs had an average size of 425 nm. Likewise, Kesharwani et al. [40] prepared AgNPs using *Datura metel* leaf extract as a reducing agent (Fig. 3b). *Datura metel* leaf extract contains different active biomolecules such as polysaccharides, alkaloids, proteins, enzymes, amino acids, vitamins, etc., which can be reduced by the Ag^{+} ion into the metallic silver nanoparticles. The as-synthesized AgNPs were confirmed by UV–Vis spectroscopy, where a sharp absorption peak is depicted at 420 nm, corresponding to the AgNPs. TEM analysis confirmed that AgNPs had an average size of 16–40 nm.

In another study, Kumar and co-workers [41], prepared the Ag NPs using *Pimenta dioica* leaf extract as a reducing and stabilising agent. The synthesised Ag NPs had an average size of 422 nm, as confirmed by UV spectroscopy. Further, gas chromatography-mass spectroscopy (GCMS–) and liquid chromatography-mass spectroscopy (LC-MS) analyses were carried out to identify various bioactive compounds present in the *Pimenta dioica* leaf extract.

Due to the lower cost of copper precursors, researchers have focused on synthesising them using plant extracts [42]. For example, Ghosh et al. [43] prepared Cu NPs using A*tropha curcas* leaf extract. Different polyphenolic compounds such as flavonoids and tannins are present in the *Atropha curcas* leaf extract and these compounds are used as reducing and stabilizing agents during the synthesis of Cu NPs. The size of the as-prepared Cu NPs was found to be 11 nm or 12 nm. Likewise, *Celastrus paniculatus* Willd. leaf extract was also used to prepare Cu NPs by Mali et al. [44], and the authors reported that the size of the nanoparticles was found to be in the range of 2–10 nm. The extract is a rich source of flavonoid compounds which can be transferred from enol to keto form by releasing a reactive hydrogen atom, and that hydrogen can reduce Cu^{2+} ions to CuNPs [45]. Similarly, Nieto-Maldonado and colleagues [46] reported the green synthesis of CuNPs using ascorbic acid and Rosa 'Andeli' double delight fresh petals (RAFE) or *Gardenia jasminoides* Ellis fresh leaves (GJLE) extract as reducing and stabilizing agents, respectively. RAFE or GJLE extract contains different active compounds like salicylic acid, isoquercitrin, quercitin, gallic acid, caffeic acid, geniposide, gardenoside, ixoroside, etc. (Fig. 4a) amongst them, quercetin works as a stabilizing agent for the synthesis of the CuNPs (Fig. 4b). After successful synthesis of the CuNPs, different characterizations were carried example, FTIR for structural, TEM for morphological, and so on. It was found that the synthesized CuNPs had an average size of 11.7 nm and were spherical in shape out, for.

The gold nanoparticles (Au NPs) have also been synthesized well using different plant extracts. For a typical example, Rodríguez-León et al. [47] prepared AuNPs using *Mimosa tenuiflora* extracts. The powder from *Mimosa tenuiflora* was analysed by FTIR to evaluate chemical compounds such as polyphenolic compounds (Mimosa tannin, flavone sakuranetin, triterpenoid saponins, chalcones, and the N, N-dimethyltryptamine alkaloid). The polyphenolic compounds can provide electrons for the reduction of Au^{3+} ions to metallic gold nanoparticles

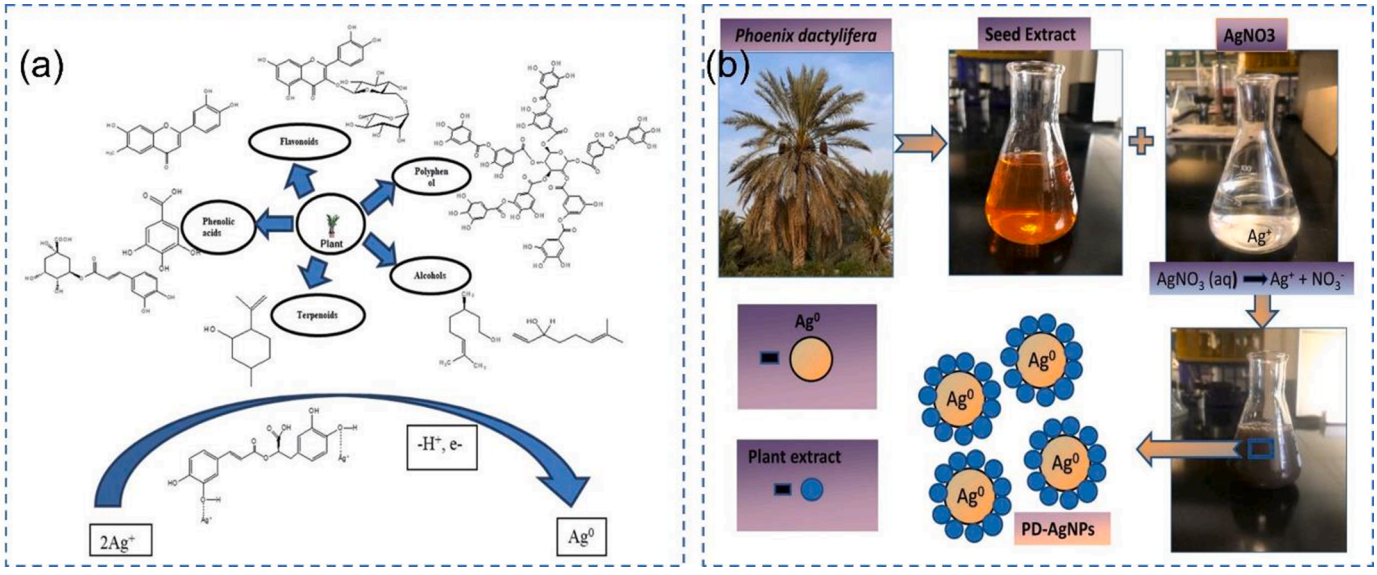

Fig. 2. (a) Mechanism for synthesis of AgNPs using plant extract [33], (b) process flow chart for synthesis of AgNPs using *Phoenix dactylifera* seed extract [36].

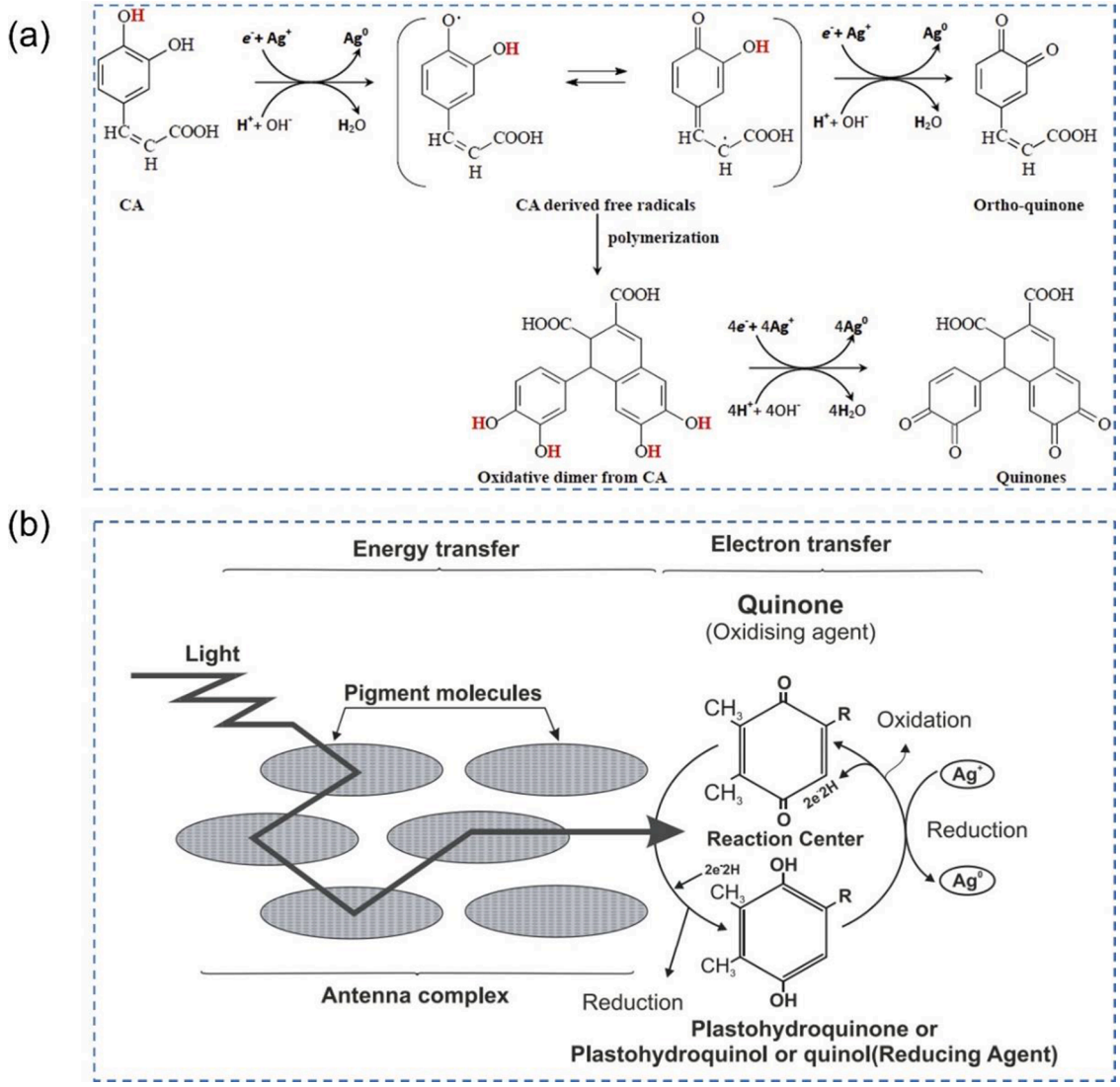

Fig. 3. Synthesis mechanism of AgNPs using (a) rice husk extract [39], and (b) *Datura metel* leaf extract [40].

(AuNPs) [48]. The size of the synthesized AuNPs was found to be in the range of 20 nm to 200 nm, confirmed by TEM analysis. As shown in Fig. 5a, the synthesis of AuNPs uses parsley leaf extract as a reducing agent [49]. An FTIR study of the parsley leaf extract revealed the presence of flavonoids like apigenin, cosmosiin, apiin, quercetin, and oxypeucedanin hydrate. These biomolecules act as reducing agents to convert Au^{3+} ions to the metallic gold nanoparticles (AuNPs). Moreover, the hydroxyl and carboxyl ions of these biomolecules can also be utilized as stabilizing agents in AuNP synthesis [50]. TEM analysis confirmed that the AuNPs had an average size in the range of 20–40 nm. In another study, Singh et al. [51] also reported AuNPs preparation using cardamom extract as a reducing agent. The cardamom extract contains 1,8-cineole (65%), -pinene (0.85%), and -terpineol (7.92%) compounds, which are the main constituents to reduce Au^{3+} ions to the AuNPs [52]. The reduction mechanism of AuNPs synthesis is shown in Fig. 5b. Khandanlou et al. [53] have also synthesized the Au NPs using *Tasmannia lanceolata* leaf extract. The leaf extract contains various phenolic compounds, confirmed by LC-MS analysis. These phenolic compounds were used as a reducing and stabilizing agents during synthesis of Au NPs as stated by the authors. The as synthesized Au NPs had an average size in the range of 6.44 nm to 7.76 nm confirmed by the TEM analysis.

Iron nanoparticles (Fe NPs) are also widely used in different applications, such as waste water treatment, biomedicine, antibacterial activity, and many more. Therefore, the synthesis of the Fe nanoparticles is an important task without hampering environmental balance. In this regard, green synthesis of Fe nanoparticles could be a better option compared to other chemical synthesis methods. Amongst different green synthesis approaches, plant extract mediated synthesis has drawn the most interest because of its easy availability, cost-effectiveness, and non-toxic nature. Many studies are already being conducted in the field of iron nanoparticle synthesis using various plant extracts. For instance, a group of researchers has reported the synthesis of Fe NPs using a plant extract (*Catharanthus roseus*) [54]. The main ingredients in plant extracts are polyphenols, alkaloids, steroids, flavonoids, and terpenoids, which help in reducing as well as stabilizing. The Fe NPs synthesis was further validated by UV–vis spectroscopy, DLS, and FTIR. Likewise, Perveen and colleagues [55] have reported the synthesis of Fe NPs using *Plumeria obtuse* plant extract. The as synthesised NPs were characterised by employing various techniques such as FTIR, SEM, TEM, UV/Vis, and XRD. They further reported that the Fe NPs possessed a spheroidal shape and an average size of 50 nm. Similarly, in another reported work, the authors have utilised peanut skin extract to synthesise Fe NPs. Such a less explored extract was collected from agricultural waste products and was easy to obtain in large quantities. Fig. 6 depicts a schematic representation of the synthesis of Fe NPs using peanut skin extract [56]. In another study, Wu et al. [57] prepared Fe NPs using green tea extract as

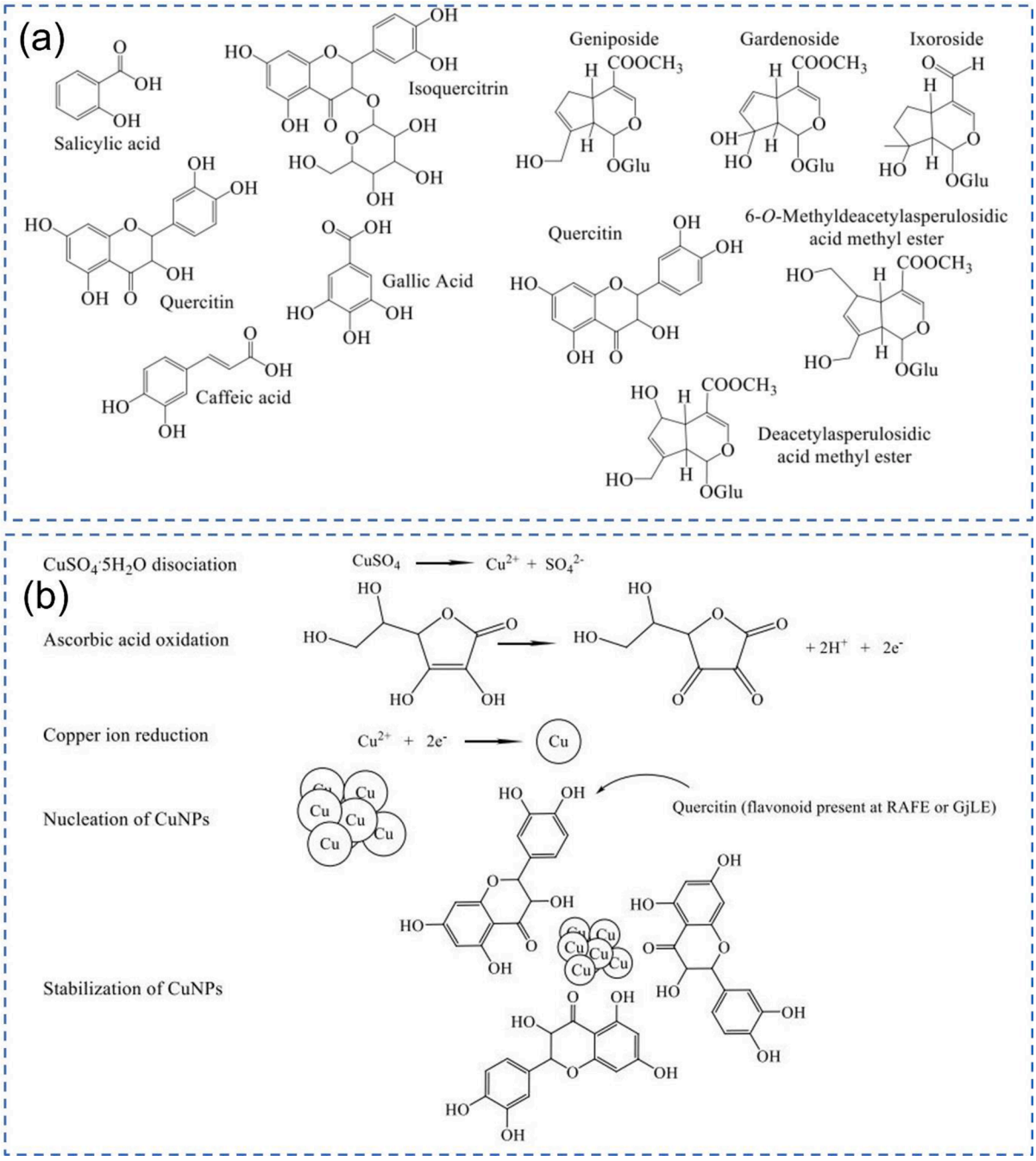

Fig. 4. (a) Different active compounds present in RAFE and GJLE extract, and (b) possible synthesis mechanism of CuNPs using ascorbic acid and RAFE or GJLE extract as reducing and stabilizing agent [46].

a reducing and stabilising agent. Green tea extract contains different bioactive compounds such as polyphenols, L-theanine, caffeine, etc., confirmed by the GC–MS and LC-MS analyses. TEM and SEM analysis shows an average nanoparticle size in the range of 50 nm to 100 nm.

Metal nanoparticles (MNPs) are also widely synthesized using different microorganisms like bacteria, fungi, and algae, etc. Several studies on the green synthesis of silver nanoparticles have already been conducted, with researchers using bacterial cell-free supernatant, intercellular, and extracellular attempts for both gram-positive and gram-negative bacteria. Using Letendraea sp. WZ0 fungus, Qiao et al. [58] prepared silver nanoparticles. Interestingly, the synthesized AgNPs have an average size of 33.8 nm. As per the reported work, *Letendraea* sp. WZ0 fungus extract contains flavonoid and polyphenolic biomolecules. The phenolic compounds can reduce the Ag^{+} ion to the metallic silver nanoparticles (AgNPs). Similarly, Durán and colleagues [59] synthesized AgNPs using *Fusarium oxysporum* strains. The synthesized AgNPs had an average size in the range of 20 nm to 50 nm. Kimber et al. [60] reported the synthesis of copper nanoparticles (CuNPs) using *Shewanella oneidensis* bacteria, and it was found that prepared copper nanoparticles have an average size in the range of 20 nm to 40 nm. In another study, Ahmadi-Nouraldinvand et al. [61] synthesized copper nanoparticles through a green route where they used *Trichoderma harzianum* bacteria fungus extract as a reducing agent. The average size of the Cu nanoparticles was found to be in the range of 10–15 nm, and their shape was found to be spherical as well. Likewise, a marine actinobacterial isolate (extracted from seaweed) was used as a reducing agent for the preparation of the CuNPs [62]. The isolated *Streptomyces* sp. MHM38 strains were inoculated in a medium composed of starch, 20 g/l; K_2HPO_4, 1 g/L;

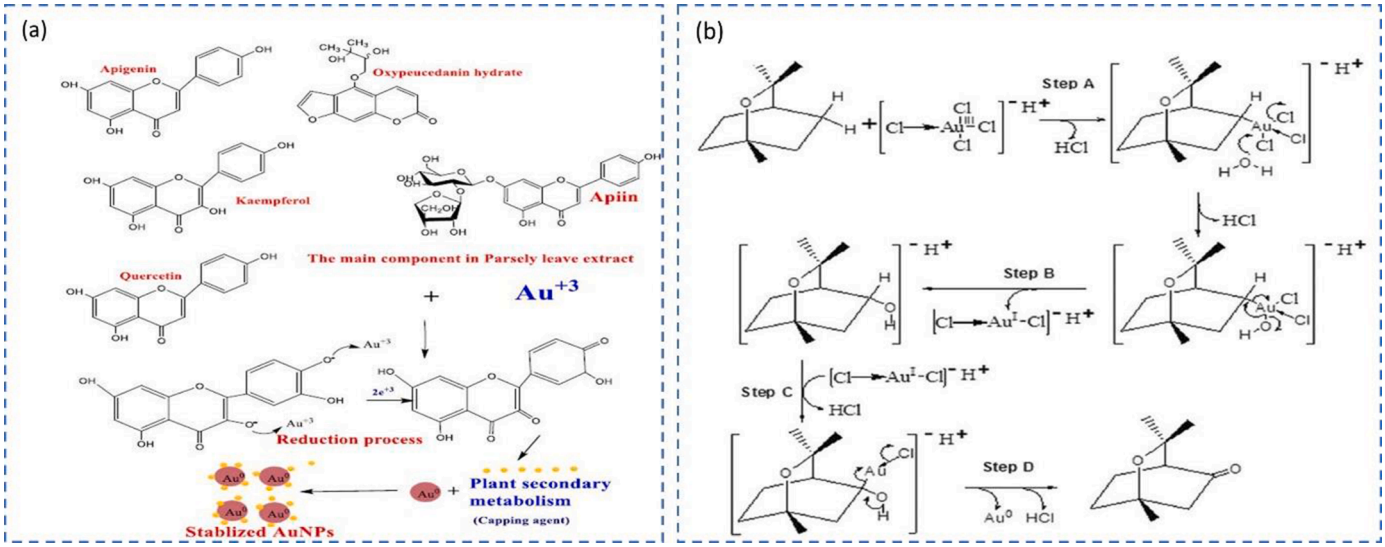

Fig. 5. (a) Reduction mechanism of AuNPs synthesis using Parsely leaves extract [49], and (b) black cardamom extract [51].

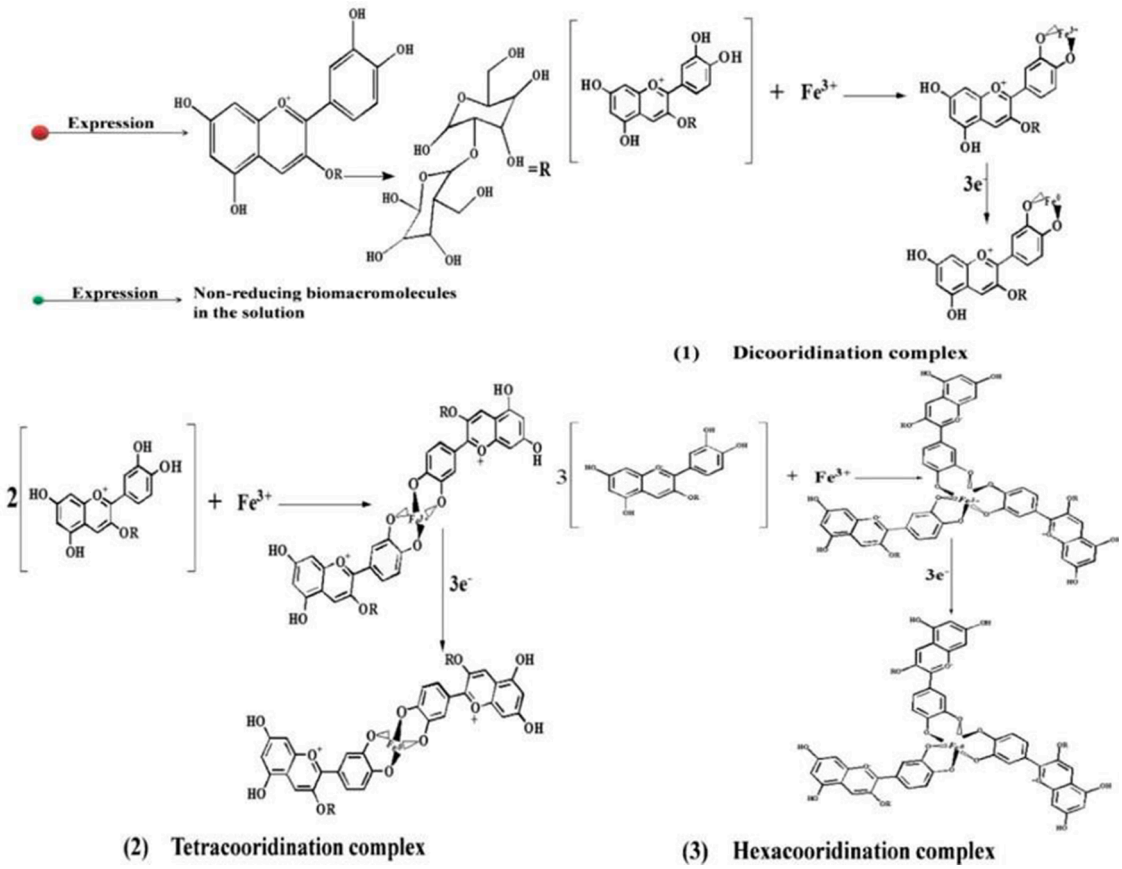

Fig. 6. Synthesis flowchart of Fe NPs using peanut skin extract [56].

KNO_3, 2 g/l; and $MgSO_4$, 0.5 g/l.

Patil et al. [63] prepared gold (Au) nanoparticles using marine-based bacteria, i.e., *Paracoccus haeundaensis* BC74171T (Fig. 7). Indeed, marine-based microorganisms can adapt to harsh environments and can thus be used in the synthesis of metal nanoparticles. Furthermore, marine-based microbes are generally used to develop different biomolecules, and these biomolecules are used in human well-being. *Paracoccus haeundaensis* bacteria produced NPs with a diameter in the range of 20.93 3.46 nm, confirmed by TEM and DLS characterizations. The synthesis of AuNPs using an -NADPH mediated sulfite reductase enzyme extracted from *E. coli* bacteria has also been reported [64]. Table 1 shows a list of microorganisms and plant extracts involved in the synthesis of different monometallic nanoparticles.

The microorganisms (bacteria and fungi) were also used to synthesise Fe NPs by employing bacterial supernatants that contained a complex made up of auxin (indole-3-acetic acid, IAA). The synthesised NPs had a spherical shape with an average size range of 250 to 300 nm, which was confirmed by TEM and UV/Vis analysis. Furthermore, FTIR

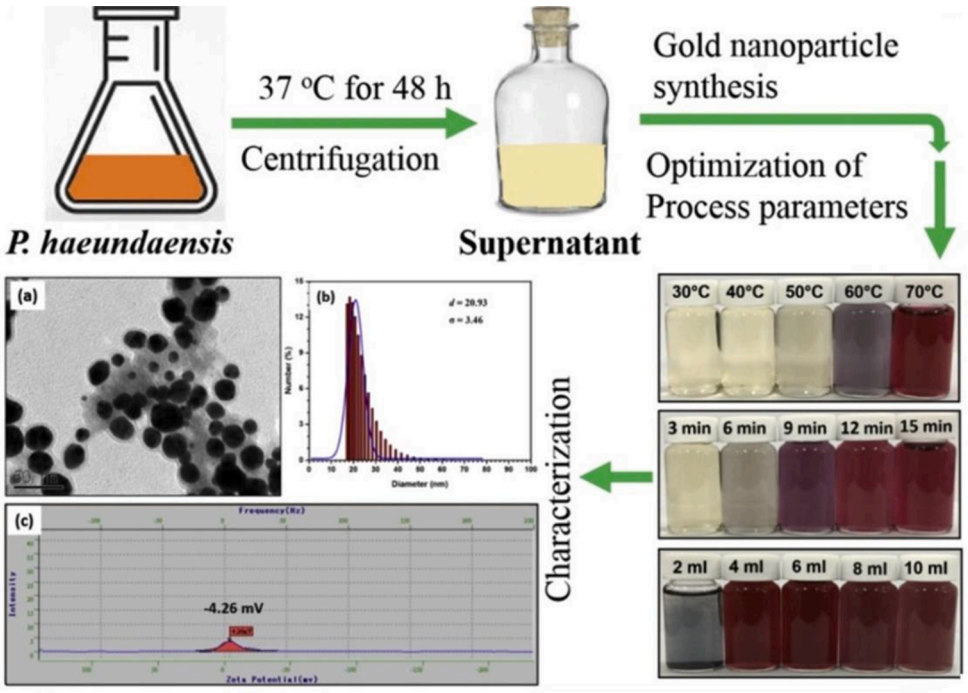

Fig. 7. The synthesis of Au NPs using Paracoccus haeundaensis BC74171^T [63].

spectroscopy discovered corresponding functional groups of auxin [96]. Vitta et al. [97] also reported the synthesis of Fe NPs, where an aqueous extract of *Eucalyptus robusta* was used as a reducing and stabilising agent.

2.2. Green synthesis of metal oxide nanoparticles

Since it is now very well known that polyphenolic compounds from natural products are also suitable for the synthesis of various metal oxide nanoparticles like ZnO, CuO, PdO, TiO_2, etc., Several investigations are underway towards the synthesis of metal oxide nanoparticles from plant derivatives. For example, Naseer and colleagues [98] reported the synthesis of ZnO nanoparticles using *Cassia fistula* and *Melia azedarach* plant extract. *Cassia fistula* and *Melia azedarach* plant extracts contain flavonoids, alkaloids, glycosides, limonoids, fixed oil and other polyphenolic compounds like saponins, tannins, triterpenes, nimbin, melianol, etc. Polyphenolic compounds are primarily responsible for the reduction of Zn ions to ZnO NPs. Demissie and colleagues [99] synthesized ZnO nanoparticles from *Lippia adoensis* leaf extract. The synthesized ZnO nanoparticles were 19.78 in average size and were spherical and hexagonal in shape. Moreover, the synthesized nanoparticles have shown a strong absorption band in the range of 360 nm to 363 nm in the UV-spectroscopy analysis, which confirms the synthesis of ZnO nanoparticles. *Cayratia pedate* leaf extract was also synthesized into ZnO nanoparticles [100]. As shown in Fig. 8a, *Cayratia pedate* leaf extract contains different compounds like aldehydes, terpenoids, flavonoids, phenolic compounds, fatty acids, alkaloids, etc., which can reduce zinc nitrate salt to ZnO nanoparticles. The average size of the ZnO nanoparticles was found to be 52.24 nm, and the nanoparticles also showed a strong absorption peak at 320 nm, which was confirmed by UV-spectroscopy.

CuO nanoparticles also have wide application in different fields, like ZnO nanoparticles. The synthesis of CuO nanoparticles by plant extract has been discussed in detail. Recently, Veisi et al. [101] explored the synthesis of the CuO nanoparticles using *Stachys Lavandulifolia* (herbal tea) flower extract (Fig. 8b). The as-synthesized CuO nanoparticles were 15 nm to 25 nm in size and were spherical in shape, confirmed by TEM analysis. It was also found from the UV-spectrum that synthesized materials can absorb light at 400 nm, which also confirms the synthesis of CuO nanoparticles. Likewise, Sukumar and colleagues [102] prepared CuO nanoparticles using *Caesalpinia bonducella* seed extract. Table 2 shows the list of microorganisms and plant extracts involved in the synthesis of metal oxide nanoparticles.

3. Green synthesis of bimetallic/core-shell and composites

In the above section, green synthesis metal and metal oxide nanoparticles such as Au, Ag, Cu, ZnO, CuO, MgO, nanoparticles etc., using different microorganisms and plant extracts have been elaborated in a systematic way. Synthesis of bimetallic or composite nanoparticles has attracted more attention in recent years as compared to monometallic nanoparticles due to their enhanced physical properties like shape, size, morphology, etc., attractive synergistic effect, enhanced antibacterial property, etc. For a typical example, Bhanja and colleagues [136] prepared Ag@Au bimetallic nanoparticles using *Ramaria botrytis* mushroom extract as a reducing agent, and they studied their catalytic activity against the reduction of 4-nitrophenol, along with antibacterial and antioxidant characteristics. A UV-visible spectroscopy analysis was carried out to confirm Ag@Au NPs and, interestingly, it was found that a sharp peak appears at 507 nm in the UV–vis spectrum. This peak at 507 nm is an intermediate absorption peak between silver (418 nm) and gold (524 nm) (Fig. 9a). The synthesized bimetallic nanoparticles were 150 nm in size and were rectangular in shape. Similarly, in another study, Ag@Fe nanoparticles were synthesized by *Gardenia jasminoides* leaf extract. FTIR and raman spectroscopy revealed that Gardenia jasminoides leaf extract contained chemical compounds such as flavonoids, saponins, alkaloids, tannin, and other polyphenolic compounds. The phenolic compounds can reduce zinc ions to ZnO nanoparticles [137,138]. It was found from the morphological study that, as synthesized (Ag@Fe), bimetallic nanoparticles had a core-shell structure. The synthesized bimetallic NPs were 7–19 nm in average diameter and were spherical in shape [139]. In another study, Ag @Fe nanoparticles were also synthesized using *Salvia officinalis* leaf extract by Malik and colleagues (Fig. 9b) [140]. S. officinalis leaf extract contains flavonoids (methyl rosmarinate, rosmarinic acid, free caffeic acid, flavones, luteolin-7-glucoside, luteolin-7-glucuronide, 6-hydroxyluteolin-7-glucoside, and luteolin-3-glucoside) and

Table 1
List of microorganisms and plant extract involved in the synthesis of mono-metallic nanoparticles.

Nanoparticles	Size and shape	Microorganisms and plant extract	Reference
Plant extract mediated synthesis			
Ag NPs	15 nm to 33 nm and spherical	Green tea extract	[33]
Ag NPs	15 nm and spherical	*Phoenix dactylifera* seed extract	[36]
AgNPs	20.41 nm to 20.93 nm and spherical	*Capsicum chinense* leaf extract	[65]
AgNPs	21 to 173 nm and spherical	*Conocarpus Lancifolius* plant extract	[66]
AgNPs	47 nm and spherical	*Syzygium cumini* fruit extract	[67]
AgNPs	19.401 nm and spherical	*Urtica diocia (UD)* leave extract	[68]
AgNPs	13.85 to 34.30 nm and spherical	*Rubus ellipticus Sm.* Root extract	[69]
AgNPs	11.17 nm to 37.50 nm and cubic structure	*Boswellia sacra* leaf extract	[70]
AgNPs	1o nm to 25 nm and spherical	*Ctenolepis garcini* L. plant extract	[71]
AgNPs	40 nm to 220 nm and spherical	*Citrus medica* plant extract	[72]
CuNPs	11 nm to 12 nm and spherical	*Atropha Curcas* leaf extract	[43]
CuNPs	2 nm to 10 nm and spherical	*Celastrus paniculatus Willd.* Leaf extract	[44]
CuNPs	6.93 nm to 20.70 nm and spherical	*Citrus sinensis* aqueous fruit extract	[73]
CuNPs	7 nm and spherical	*Hyptis suaveolens (L.)* plant extract	[74]
CuNPs	5 nm to 8 nm and spherical	Green coffee bean extract	[75]
CuNPs	20 nm to 30 nm and spherical	*Prunus mahaleb* L. plant extract	[76]
CuNPs	5 nm and spherical	Neem flower extract	[77]
CuNPs	20 nm to 40 nm and spherical	*Angelica keiskei* (Miq.) Koidz. leaves extract	[78]
CuNPs	38.5 nm and spherical	Artemisia plant extract	[79]
CuNPs	54 nm to 80.98 nm and spherical	*Vitis vinifera* L. seed extract	[80]
CuNPs	3.9 nm to 10.9 nm and spherical	*Osmium sanctum* plant extract	[81]
AuNPs	20 nm to 200 nm and spherical	*Mimosa tenuiflora* extracts	[47]
AuNPs	20 nm to 40 nm and spherical	Parsley leaves extract	[49]
AuNPs	13.6 nm and spherical	Citrus peel extract	[82]
AuNPs	57.9 nm to 57.2 nm and spherical	Black tea extract	[83]
AuNPs	16.7 nm and spherical	*Spinacia oleracea* L. Leaf aqueous extract	[84]
AuNPs	28 nm to 43 nm and spherical	*Jatropha integerrima* Jacq. flower extract	[85]
AuNPs	15 nm to 40 nm and spherical	*Bauhinia tomentosa Linn* plant extract	[86]
AuNPs	36.4 nm and spherical	*Mentha Longifolia* leaf extract	[87]
AuNPs	13.20 nm and spherical	*Erythrophyllum* Leaf Extract	[88]
AuNPs	8 nm to 25 nm and spherical	*Curcumae kwangsiensis* leaf aqueous extract	[89]
AuNPs	5 nm to 23 nm and spherical	*Persicaria salicifolia* leaf extract	[90]
AuNPs	5 nm to 20 nm and spherical	*Phragmites australis* root and rhizome extracts	[91]
AuNPs	18 nm to 38 nm and spherical	*Garcinia kola* Pulp Extract	[92]
Microorganisms mediated synthesis			
Ag NPs	10 nm to 30 nm and spherial	*Bacillus methylotrophicus* DC3 bacteria	[93]
Ag NPs	33.8 nm and spherical	*Letendraea* sp. WZ0 fungus	[58]
Cu NPs	20 nm to 40 nm and spherical	*Shewanella oneidensis* bacteria	[60]
Cu NPs	10 nm to 15 nm and spherical	*Trichoderma harzianum* fungus extract	[61]
Cu NPs	1.06 nm to 6.5 nm and spherical	*Streptomyces* sp. MHM38 strains	[62]
Au NPs	20.93 ± 3.46 nm and spherical	*Paracoccus haeundaensis* BC74171^T	[63]
Au NPs	10 nm and spherical	Sephacryl S-300 extracted from *E. coli* bacteria	[64]
Au NPs	30 nm to 60 nm and spherical	*Penicillium brevicompactum* fungus extracts	[94]
Au NPs	12 nm to 15 nm and spherial	*Alternaria chlamydospore* Fungi	[95]

polyphenolic compounds (phenolic acids, salvianolic acids K and I) [141, 142]. It is worth mentioning that flavonoids and polyphenolic compounds are responsible for reducing and stabilizing the Ag-Fe nanoparticles. The UV–vis spectrum has shown three absorption peaks at 450 nm, 350 nm, and 352 nm, respectively, which confirms the formation of Ag-Fe NPs. From morphological (TEM and SEM) analysis, the average diameter of the synthesized Ag@Fe NPs was found to be 30 nm.

Likewise, Riaz and colleagues [138] reported the synthesis of silver-nickel (Ag-Ni) bimetallic nanoparticles using *Salvadora persica* plant extract as a reducing and stabilizing agent. The extract contains many bioactive chemicals such as flavonoids, terpenoids, saponins, steroids, and alkaloids, as confirmed by the FTIR analysis of the extract. These chemical compounds are responsible for the synthesis and stabilizing of the Ag-Ni nanoparticles [145]. Plant extract was mixed with two equimolar solutions of silver nitrate (100 ml) and nickel nitrate (100 ml) salt to make the Ag-Ni bimetallic nanoparticles, and the resulting solution was continuously stirred until a noticeable colour change in the solution was observed. The average diameter of the synthesized Ag-Ni NPs was found to be 23.67 nm. The copper-silver (Cu-Ag) bimetallic nanoparticles synthesized using *Phoenix dactylifera* (Palm tree) leaf extract (Fig. 9c) had an average diameter of 26 nm, confirmed by morphological analysis. [143]. Furthermore, Weng and colleagues [144] prepared Fe-Ni bimetallic nanoparticles using *eucalyptus* leaf extracts as a reducing agent, as shown in Fig. 9d. The *eucalyptus* leaf extract had different compounds like pyrazole-4-carboxaldehyde, 1-methyl, 1-methylethyl)-benzene, hydroquinone, etc., confirmed by GC–MS. These compounds have reducing and stabilizing characteristics. The synthesized Fe-Ni NPs exhibited an average diameter in the range of 20 nm to 50 nm. Olajire et al. [146] prepared palladium-gold (Pd-Au) core-shell bimetallic nanoparticles using *Ananas comosus* leaf extract as a reducing and capping agent. The *Ananas comosus* leaf extract had various polyols like flavones, polysaccharides, terpenoids, etc., confirmed by FTIR analysis. These polyols are mainly responsible for reducing Pd^{2+}-Au^{3+} ions to their respective core-shell structures. The UV–vis spectroscopy analysis of the as synthesized Pd-Au nanoparticles revealed a sharp absorption band at 517 nm, corresponding to the surface plasmon resonance band of Au present on the surface of Pd. The FTIR analysis also revealed the formation of Pd_{Core}-Au_{Shell} nanoparticles. The synthesized Pd_{Core}-Au_{Shell} nanoparticles had an average size in the range of 2.06 nm to 28.59 nm. Similarly, Wicaksono and colleagues [147] also reported the synthesis of gold-palladium (Au-Pd) core-shell bimetallic nanoparticles using orange peel extract as a reducing agent. The orange peel extract contains various biomolecules such as flavonoids and phenolic compounds, which can reduce the Au^{3+}-Pd^{2+} ion to their bimetallic nanoparticles. For synthesis of Au-Pd core-shell structure, first $HAuCl_4$ was reduced by orange peel extract to obtain core Au nanoparticles and then H_2PdCl_4 precursor solution was reduced to form

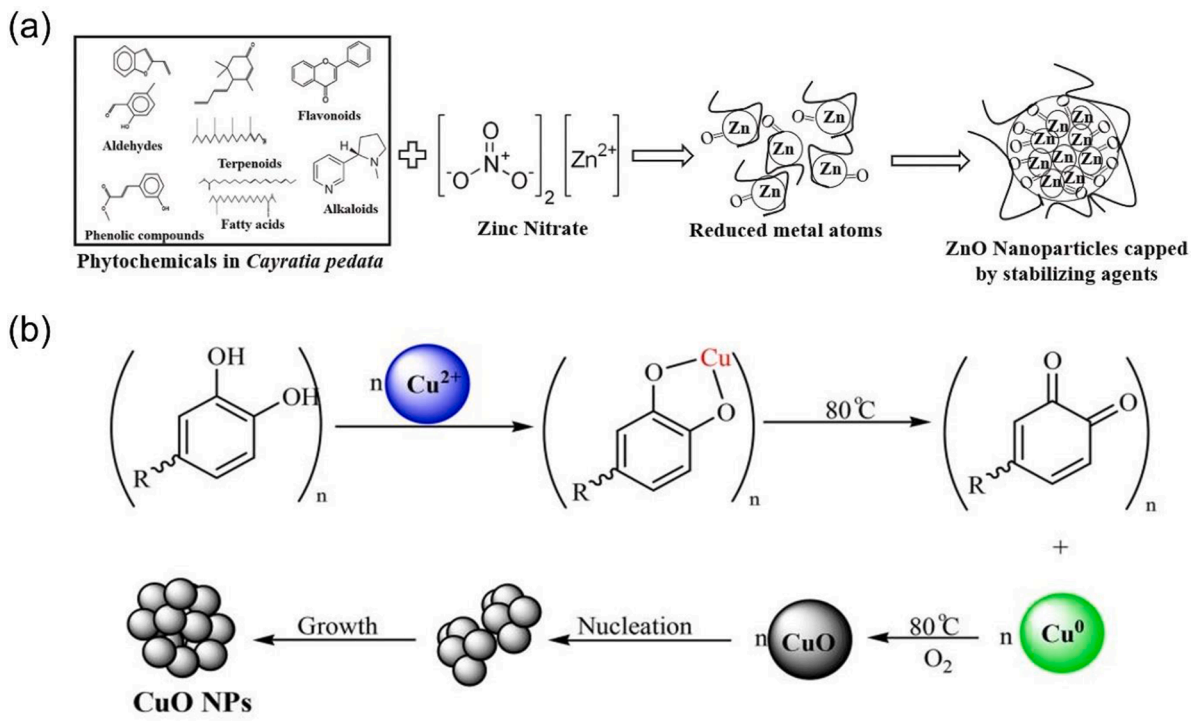

Fig. 8. (a) Mechanism of ZnO NPs synthesis using *Cayratia pedate* leaf extract [100], and (b) CuO NPs synthesis mechanism using *Stachys Lavandulifolia* (herbal tea) flowers extract [101].

a Pd shell on the core Au NPs. The Au-Pd core-shell nanoparticles formation was first confirmed by UV–vis spectroscopy followed by FTIR analysis. An average size of the synthesized Au-Pd NPs was found to be 47 nm.

Nasrollahzadeh and colleagues [148] prepared copper/magnesium oxide composite nanoparticles using *Cassytha filiformis* L. extract as a reducing and stabilizing agent (Fig. 10a and 10b). The average diameter of the synthesized Cu/MgO nanoparticles was found to be 19 nm by TEM analysis. Similarly, Kulkarni and colleagues [149] reported the synthesis of the Au @NiAg composite nanoparticles with a 10 nm size using *A. vasica* leaf extract as a reducing agent (Fig. 10c). Likewise, in another study, Alwhibi and colleagues [150] synthesised Ag @Au nanocomposite nanoparticles using Acacia-nilotica husk extract as a reducing and capping agent. The UV–vis spectrum exhibited a sharp absorption peak at 460 nm to 500 nm, corresponding to the plasmonic absorption of gold nanoparticles. Also, the synthesized Ag/Au nanoparticles have an average size of 223 nm. Furthermore, Tiri et al. [151] prepared Ag@Pt nanocomposite nanoparticles using propolis extract and a strong absorption peak at 300 nm in the UV–vis spectrum confirmed the formation of Ag@Pt nanoparticles (4–19 nm) (Fig. 10d). Table 3 summarizes a list of microorganisms and plant extracts involved in the synthesis of different bimetallic or composite nanoparticles.

4. Removal of dyes from wastewaters

Natural product mediated nanoparticles are widely used in environmental applications, particularly in the dye degradation sector. Dyes are organic compounds that are abundantly used in industries, especially in food, textiles, paper, cosmetics, and pharmaceuticals [152]. The release of these coloured compounds, pesticides, and antibiotics into wastewater is contributing majorly towards increasing pollution levels worldwide [153]. Many of them cause mutagenesis, carcinogenicity, and other birth defects, thus compromising precious human life [154]. Various conventional techniques, including physical, chemical, and biological methods such as flocculation, adsorption, filtration, sedimentation, chemical oxidation and reduction, and coagulation treatment, have been in operation to remove dye effluents, etc. [155]. Since most of the organic contaminants are chemically stable, conventional physiochemical water treatment methods are found to have one or other disadvantage [156]. Recently, nanotechnology is booming in every field and is reported to have a cure for dye pollution as nanoparticles can efficiently degrade a wide range of organic pollutants, including dyes, to harmless by-products through a process called photocatalysis [157,158]. Although different approaches have been used for the synthesis of nanoparticles and their photocatalytic activity, the most efficient approach is green synthesis using different plants. In the past years, several reviews have discussed antimicrobial, biomedical, and photocatalytical applications of synthesised NPs [159–162]. However, recent advances in the use of natural product inspired NPs for dye discoloration have not been reviewed in detail yet.

Metal and metal oxide NPs are one of the most important photocatalysts, and their use in the degradation of organic contaminants to harmless end products has increased dramatically in the past several years [163,164]. Numerous research investigations have shown that the photocatalytic properties of metallic nanoparticles are largely dependant on the reactive oxygen species produced under UV illumination [165,166]. Interestingly, in the photocatalytic reactions, when photons of energy equal to or greater than the energy gap of semi-conducting materials are absorbed, electrons from the valence band get excited to the conduction band, generating electron hole pairs ($\boldsymbol{e^-/h^+}$) [167]. The photogenerated holes (h^+) in the valence band react with water molecules or hydroxyl ions (OH^-) to produce hydroxyl radicals; on the other hand, excited free electrons (e) in the conduction band, react with oxygen molecules present in the solution and convert them to superoxide radicals ($.O_2^-$) anions [168,169]. The superoxide radicals further combine with H^+ ions to produce hydrogen peroxide, which can further be decomposed into OH radicals. During photocatalysis, the generated reactive oxygen species cause oxidation and reduction reactions and potentially attack chromophores of organic pollutants and dyes that are carcinogenic by nature and convert them into less harmful and colourless by-products [170]. The schematic representation of the photocatalytic mechanism by metal NPs is depicted in Fig. 11.

Table 2
List of microorganisms and plant extract involved in the synthesis of metal oxide nanoparticles.

Nanoparticles	Size and shape	Microorganisms and plant extract	Reference
Plant extract mediated synthesis			
ZnO NPs	6 nm to 68 nm and spherical	*Cassia fistula* and *Melia azedarach* plant extract	[98]
ZnO NPs	19.78 nm and spherical	*Lippia adoensis* leaf extract	[99]
ZnO NPs	52.24 nm and spherical	*Cayratia pedate* leaf extract	[100]
ZnO NPs	56 nm to 78 nm and spherical	*Syzygium Cumini* plant extract	[103]
ZnO NPs	11.2 nm to 118.6 nm and hexagonal nanorods	Pomegranate Fruit Peel and Solid Coffee Grounds	[104]
ZnO NPs	100 nm and hexagonal	*Eucalyptus lanceolata* leaf extract	[105]
ZnO NPs	14.4 nm and spherical	*Rivina humilis* leaf extract	[106]
ZnO NPs	69.77 nm to 70.03 nm and rod shape	Gum *Acacia modesta*	[107]
ZnO NPs	209 nm and spherical	*Raphanus sativus* var. *Longipinnatus* leaf extract	[108]
CuO NPs	15 nm to 25 nm and spherical	*Stachys Lavandulifolia* (herbal tea) flowers extract	[101]
CuO NPs	13.07 nm and rice like shape	*Caesalpinia bonducella* seeds extract	[102]
CuO NPs	22 nm to 40 nm and spherical	*Bauhinia tomentosa* leaves extract	[109]
CuO NPs	8 nm to 16 nm and spherical	Bougainvillea Plant Flowers Extract	[110]
CuO NPs	900 nm and spherical	*Capparis decidua* Leaf Extract	[111]
CuO NPs	20 nm to 30 nm and spherical	*Punica granatum* leaf extract	[112]
CuO NPs	33 nm and spherical	*Canthium coromandelicum* leaves extract	[113]
CuO NPs	50.7 nm and spherical	*Rubia cordifolia* bark extract	[114]
CuO NPs	1.7 nm to 15.2 nm and spherical	*Pergularia tomentosa* leaves extract	[115]
FeO NPs	21.59 nm and spherical	*Carica papaya* leaf extract	[116]
FeO NPs	70 nm and spherical	*Bauhinia tomentosa* leaf extract	[117]
MgO NPs	35 nm to 55 nm and polyhedral	*Rosa floribunda* charisma extract	[118]
MgO NPs	36.7 nm and hexagonal	*Manihot esculenta* leaf extract	[119]
MgO NPs	18 nm to 80 nm and spherical	*Amaranthus tricolour, Andrographis paniculata and Amaranthus blitum*	[15]
Microorganisms mediated synthesis			
ZnO NPs	124.2 nm and spherical	*Lactobacillus plantarum* TA4 bacteria strain	[120]
ZnO NPs	34 nm to 55 nm and hexagonal	*Xylaria acuta* fungi extract	[121]
ZnO NPs	16 nm 78 nm and spherical	*Periconium* sp. Fungi extract	[122]
CuO NPs	1.72 nm to 13.49 nm and spherical	*Streptomyces* sp. MHM38	[123]
CuO NPs	30 nm to 75 nm and sphrical	*Lactobacillus casei Subsp. Casei*	[124]
CuO NPs	9.75 nm and spherical	*Penicillium chrysogenum* fungus	[125]
CuO NPs	10 nm to 190 nm and spherical	*Trichoderma* sp. Fungi extract	[126]
FeO NPs	19 nm to 30 nm and spherical	*Proteus vulgaris* ATCC-29,905 bacteria extract	[127]
FeO NPs	30 nm to 45 nm and spherical	*Pseudomonas aeruginosa* bacteria extract	[128]
FeO NPs	40 nm and spherical	*Aspergillus niger* BSC-1fungus extract	[129]
MgO NPs	8 nm to 38 nm and spherical	*Aspergillus terreus* S1fungus strain	[130]
MgO NPs	26.70 nm and spherical	*Burkholderia rinojensis* fungus cell filtrate	[131]
MgO NPs	68.06 nm and spherical	Algae (*Sargassum wightii*) extract	[132]
TiO_2 NPs	20 nm and spherical	*Staphylococcus aureus* bacteria	[133]
TiO_2 NPs	30 nm to 70 nm and spherical	*Streptomyces* sp. HC1bacteria strain	[134]
TiO_2 NPs	70 nm to 130 nm and spherical	*Halomonas elongata* IBRC-M 10,214	[135]

Extensive research work has been done on the photocatalytic degradation of different organic pollutants, particularly methyl orange, rhodamine B, methylene blue etc. Additionally, through a green protocol, a number of renewable and sustainable materials have been introduced to produce efficient nano photocatalysts discussed in subsequent sections.

4.1. Silver nanoparticles in environmental remediation

Silver NPs are versatile mainly due to their low toxicity, chemical stability, and biological activities. Their ease of production, morphology, and excellent dye degradation properties make them favourable candidates for environmental applications [171,172]. Several green chemistry approaches are being explored to synthesize Ag nanoparticles with different morphologies using polyphenolic compounds present in plant extracts. The characterization methods confirmed the synthesis and biogenic formation of Ag nanoparticles using gallic acid and flavanols present in *Terminalia bellerica* kernels [173]. The prepared NPs were spherical and proved strong, fast, and cost-effective toward the reduction of four different potential environmental pollutants. Isoimperatorin, a natural compound isolated from Prangos ferulacea roots, has been used to produce AgNPs for the degradation of different textile dyes. AgNPs were produced when isoimperatorin ethanolic solution was mixed with 12 mL of 1 mM aqueous solution of $AgNO_3$ and the synthesis reaction was allowed to take place under sunlight. The produced NPs (spherical and 79–200 nm) were evaluated for the degradation of new fuchsine, Methylene blue, Erythrosine B, and 4-chlorophenol pollutants under sunlight conditions. It was shown by UV–vis study that almost 96.5% of methylene blue, 92% of erythrosine B, and 96.0% of new fuchsine were degraded after 60 min [174]. In addition, AgNPs have been immobilised onto graphene oxide through in-situ rapid reduction using green tea extract (Fig. 12). The produced composite has demonstrated 633 mg g-1 degradation of methylene blue [175]. Alex and colleagues [176] have shown the ability of leaf extracts of neem, aloe vera, Indian mint, and guava to produce stable, spherical-shaped AgNPs. Diterpenoid-based chemical compounds present in these extracts were reported to be responsible for the reduction of silver nitrate salt. These NPs were employed to understand the photocatalysis of an agricultural fungicide, mancozeb. The authors believed that reactive oxygen species produced during photocatalysis were responsible for damaging or degrading mancozeb pollutants. Li et al. [177] also reported excellent photoactivity of AgNPs synthesised by rhizome extract of Alpinia officinarum on methylene blue and malachite green dyes. Muthu et al. [178] synthesised AgNPs using a seed extract of *Punica granatum*. The TEM analysis showed the AgNPs were spherical in shape and 10–35 nm in size, while XRD showed that the AgNPs were face-centred cubic. These NPs showed effective degradation of methylene orange and 4-nitro phenol. Rani et al. [179] have used kidney bean (*Phaseolus vulgaris)* extract to synthesise AgNPs and examined their degradation ability towards reactive red-141 RR. The

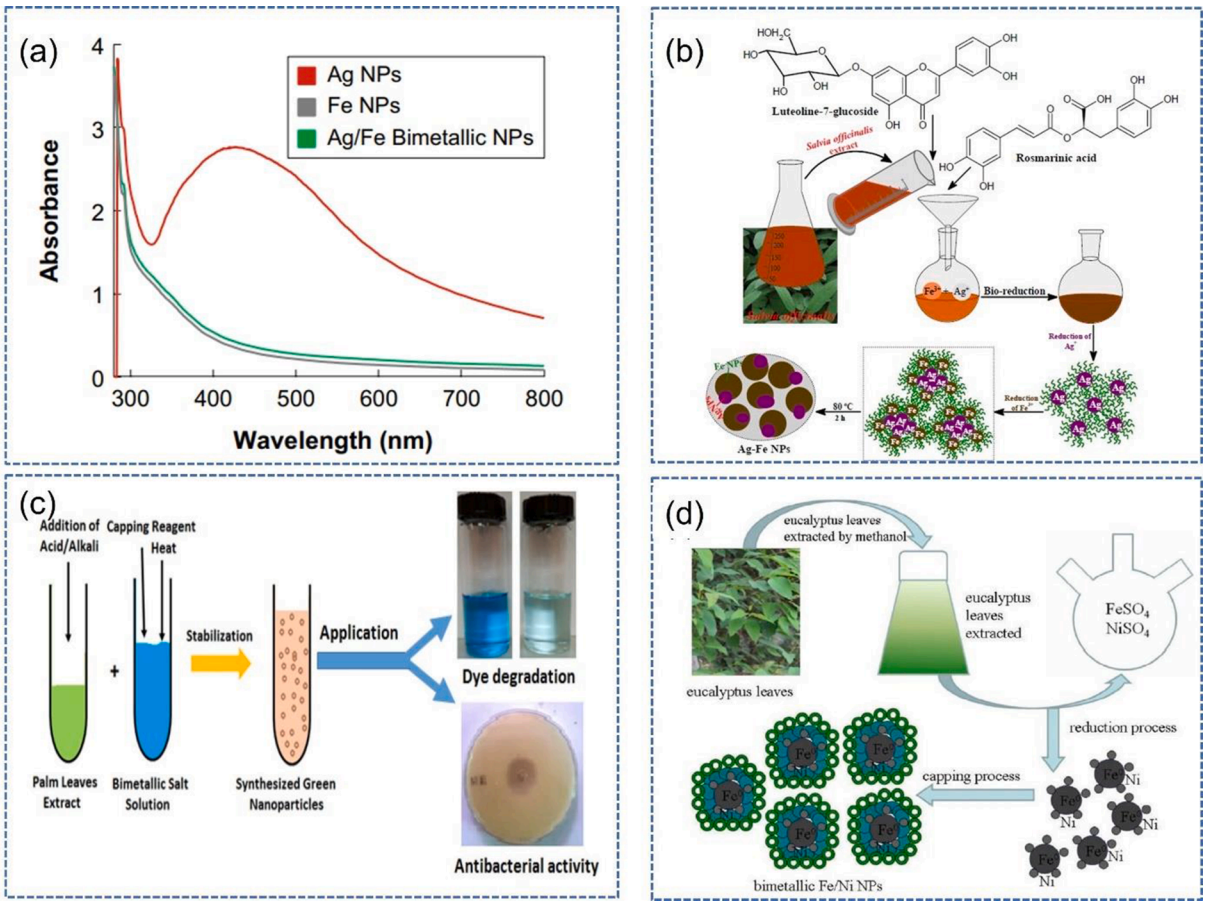

Fig. 9. (a) UV–vis spectrum of synthesised Ag @Fe bimetallic NPs [139], (b) synthesis of Ag @Fe bimetallic nanoparticles using *Salvia officinalis* leaves extract [143], (c) synthesis of Cu @ Ag bimetallic NPs [131], and (d) Fe-Ni bimetallic nanoparticles using *eucalyptus* leaf extracts [144].

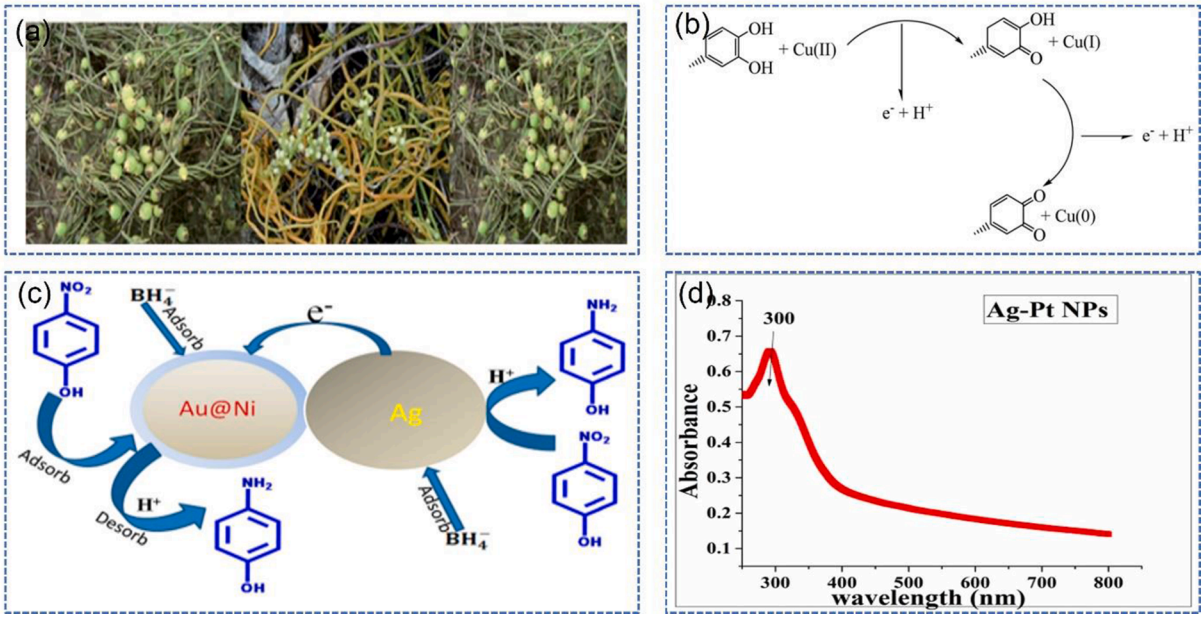

Fig. 10. (a) Image of *Cassytha filiformis* L. plant [148], (b) synthesis mechanism of CuO NPs [148], (c) synthesis of Au@NiAg Core−Shell NPs [149], and (d) UV–vis spectrum of Ag-Pt bimetallic NPs [151].

UV–vis peaks at 332 and 534 nm were monitored and a decrease in peak absorption was noticed within 150 h of incubation time under solar light. They introduced the formation of highly reactive active ROS as a possible degradation agent. Awad et al. [180] have studied the biogenic synthesis of AgNPs by seed extract of *Trigonella foenum-graecum* and calculated their dye degradation and antibacterial activities. They found

Table 3
List of microorganisms and plant extract involved in the synthesis of bimetallic or composite nanoparticles.

Nanoparticles	Size and shape	Microorganisms or plant extract	Reference
Ag @Au	150 nm and were rectangular	*Ramaria botrytis* mushroom extract	[136]
Ag @ Fe	7 nm to 19 nm and spherical	*Gardenia jasminoides* leaves extract	[139]
Ag @Fe	30 nm and spherical	*Salvia officinalis* leaves extract	[140]
Ag-Ni	23.67 nm and spherical	*Salvadora persica* plant extract	[138]
Au @NiAg	10 nm and core-shell	*A. vasica* leaf extract	[149]
Ag @Au	223 nm and spherical	Acacia-nilotica husk extract	[150]
Ag @Pt	4 nm to 19 nm and spherical	Propolis extract	[151]
Cu-Ag	26 nm and spherical	*Phoenix dactylifera* (Palm tree) leaves extract	[143]
Cu/MgO	19 nm and core-shell	*Cassytha filiformis* L. extract	[148]
Au-Pd	47 nm and core-shell	Orange peel extract	[147]
Fe-Ni	20 nm to 50 nm and spherical	*Eucalyptus* leaf extracts	[144]
Pd-Au	2.06 nm to 28.59 nm and spherical	*Ananas comosus* leaf extract	[146]

that with these spherical shaped NPs, rhodamine B was 93% degraded after 216 h.

Also, facile synthesis of AgNPs using extract of Cnicus benedictus for the degradation of methylene blue could be achieved [181]. Ravichandran et al. [182] have utilized aqueous leaf extract of *Parkia speciosa* for the production of Ag NPs with an average size of 35 nm and recorded their antimicrobial and dye discoloration properties. The produced AgNPs showed significant photoactivity for methylene blue under solar irradiation and were found active against a range of microorganisms. Ekennia et al. [183] fabricated AgNPs using *Euphorbia sanguinea* leaf extract. SEM and XRD results showed that these particles have well defined crystallinity and are spherical in shape with an average size of 20–28.8 nm. These NPs also displayed 86% and 90% efficiency of Congo red dye degradation within 5 and 60 min of solar irradiation. *Nypa fruticans* (NF) fruit husk have been used to produce spherical shaped Ag NPs that displayed excellent catalytic conversion of *o*-, *m*-, *p*-nitrophenol to amines compounds. The successful reduction and formation of aminophenols was noticed from the appearance of new peaks in UV–vis spectrum upon addition of $NaBH_4$ [184].

Chand and colleagues [185] have elucidated that methyl orange, methyl red, and Congo red dyes could be effectively degraded with AgNPs having an average size of 5–100 nm, produced by onion, tomato, and acacia catechu plant extracts. Khan et al. [186] have used an extract of *Petroselinum crispum to produce AgNPs with an average size of 25–90 nm. T*hey also demonstrated that alcoholic and polyphenolic compounds present in the extract are responsible for the formation of AgNPs, which were subsequently tested as photocatalysts to remove brilliant green dye from waste waters. In another study, *Ruellia tuberosa* leaf extract was used to synthesize AgNPs. Different characterization techniques such as UV–vis, TEM, FE-SEM, EDX, and DLS analysis showed the formation of stable spherical AgNPs with an average size of 55.65 nm. These AgNPs were used to evaluate the photocatalytic degradation of crystal violet and Coomassie brilliant blue [187]. Rajivgandhi et al. [188] reported that antibacterial and photocatalytic AgNPs were biosynthesised by using leaf extract of *M. citrifolia*. It was investigated that the methylene blue absorption peak at 660 nm shows a gradual decrease with an increase in reaction time, and a complete degradation was observed after 140 mins. In another study conducted by Yazdi et al., 82.50% of methylene blue degradation was reported using AgNPs fabricated by *B. integerrima* fruit extract biomolecules [189]. Kadam et al. [190] synthesised AgNPs employing *Brassica oleracea* extract and studied their role in the removal of methylene blue from waste waters. The effects of extract concentration, silver salt, and pH were also examined to optimize the best conditions for the formation of stable AgNPs. They characterized the AgNPs and found that when 3 mL of plant extract is reacted with 0.5 mM $AgNO_3$ at pH 8.5, it results in the formation of stable NPs. These AgNPs when treated with methylene blue displayed excellent results, with 97.57% dye degradation within 150 min. Mehwish et al. [191] produced green AgNPs using seed extract of *Moringa oleifera* and reported their photocatalytic activity towards methylene blue, orange red, and 4-nitro phenol. The seed extract when exposed to silver nitrate at an alkaline pH resulted in crystalline and spherical AgNPs with an average size of 4 nm. These NPs resulted in > 81% degradation towards methylene blue, > 82% orange red, and > 75% for 4-nitro phenol. Manikandan et al. [192] reported the production of spherical AgNP with an average size of 48.25 nm using leaf extract of *Ocimum americanum*. These NPs were photocatalytic and showed dye degradation efficiencies of 75.41% and 91.17% against eosin yellow dye under UV-irradiation and sunlight, respectively. Furthermore, waste banana peduncles were employed by Desousky and co-workers to fabricate AgNPs which were able to fully degrade methylene blue dye [193]. For the photocatalytic

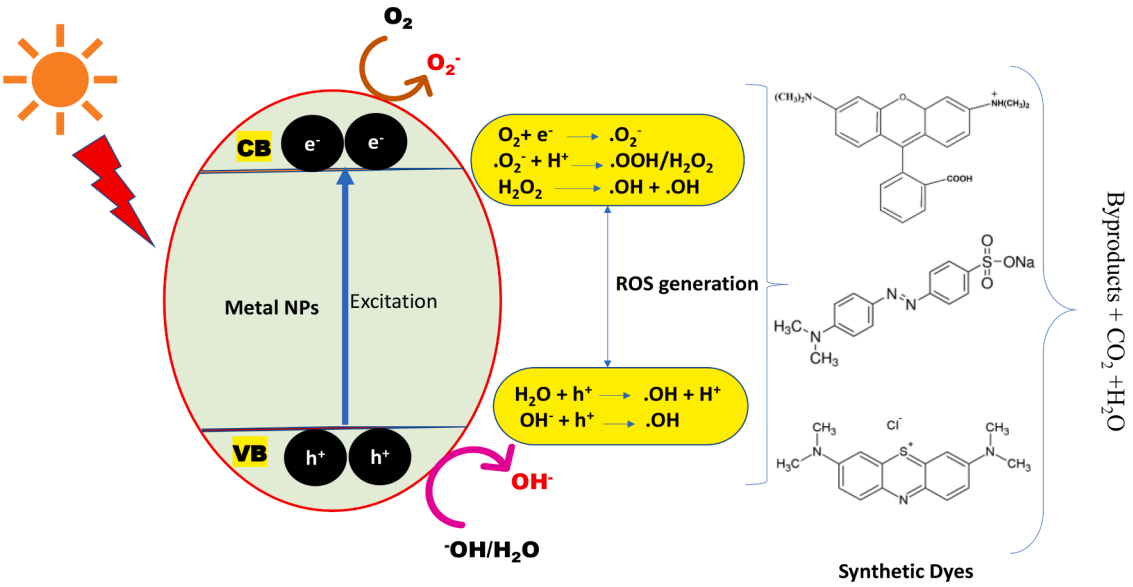

Fig. 11. General mechanism of photocatalysis displayed by inorganic nanoparticles.

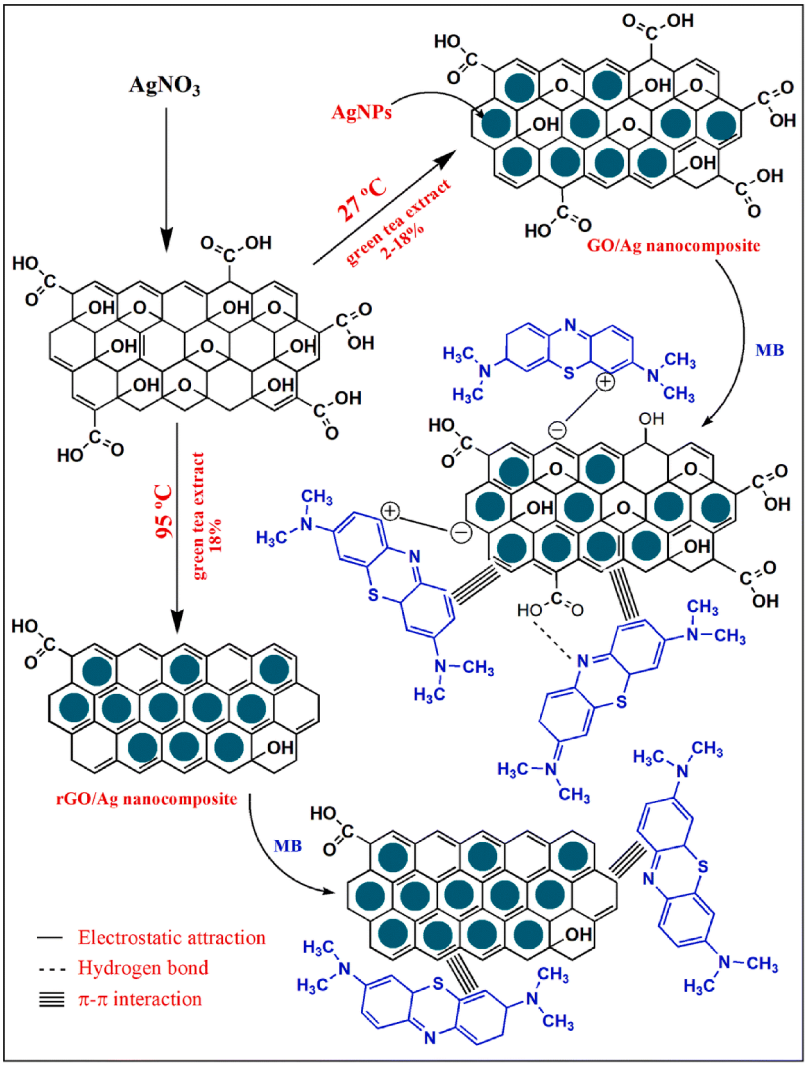

Fig. 12. In situ immobilization of green synthesized AgNPs onto GO and rGO (**a**) and the proposed adsorption mechanism of MB (**b**) [175].

discoloration of Congo red, Chand et al. [194] have examined the rapid green synthesis of AgNPs using seed extract of Nigella sativa. The produced particles were spherical and polydisperse and had an average size of 10–12 nm. They found that 15 mg ml−1 of the produced NPs resulted in the highest degradation of Congo red dye. Chandhru et al. [195] reported the facile formation of AgNPs using the latex of Calotropis procera within 80 min and reported their resultant photocatalytic activity. The produced NPs with their method were found to be stable for more than 5 months and displaced encouraging discoloration results against methyl orange. A potential pollutant, 4-nitro phenol, has been efficiently degraded by bacterial nanocellulose fibers loaded with green Ag and Au NPs synthesised by pomegranate peel extract tannins. It is worth noting that bacterial nanocellulose fibers have a rich number of hydroxyl functional sites available for linking tannin biomolecules of pomegranate peel extract that act as reducing sites for in-situ generation of Ag and Au NPs. The schematic mechanism of formation is displayed in Fig. 13 [196].

4.2. Iron and iron oxide nanoparticles

Because of their low toxicity, high stability, and the presence of active surface functional groups, Fe NPs are an attractive choice for photocatalysis and in the removal of toxic pollutants from bodies of water [197]. In recent years, sustainable methods of preparation for their role in photocatalysis technology have been preferred. Beheshtkhoo et al. [198] used an aqueous flower extract of *Daphne mezereum* to produce iron NPs. The NPs formed using biomolecules extracted from this plant material had a mean diameter of 6.5–14.9 nm with an average size of 9.2 nm. These nanoparticles were applied to remove methyl orange dye from wastewater and were seen to have an efficient dye degradation ability of 81% after 6 h. Taha and co-workers [199] investigated the use of pod extract of *Acacia nilotica* plant to produce iron NPs for the photo degradation of methyl orange dye. Rather et al. [200] used an aqueous leaf extract of Wedelia urticifolia to produce rod shaped iron oxide NPs with a size of 15–20 nm. These NPs exhibited strong dye degradation towards methylene blue from wastewater. Zulfikar et al. [201] reported the photocatalytic ability of iron NPs synthesised by using leaf extract of Mangifera *indica* (mango plant). They observed 80.87% of Congo Red and 82% of Brilliant Green dyes were degraded with these iron NPs. Khunjan et al. [202] used leaf extract of *Ruellia tuberosa* as a green reducing and stabilizing agent to synthesize iron NPs and simultaneously studied their use for photocatalytic degradation of reactive black 5. These NPs exhibited high discoloration performance, with more than 92.1–99.8% degradation. Raman et al. [203] reported the ability of grape leaf extract to produce iron NPs and studied their photocatalytic activity against a range of reactive dyes. Their results showed that 95–98% of dye discoloration was achieved for all the tested dyes with 1.4–2 g/L of produced NPs. Xiao et al. [204] reported the photocatalytic activity of iron NPs produced by a green method employing tea leaf extract. As shown by

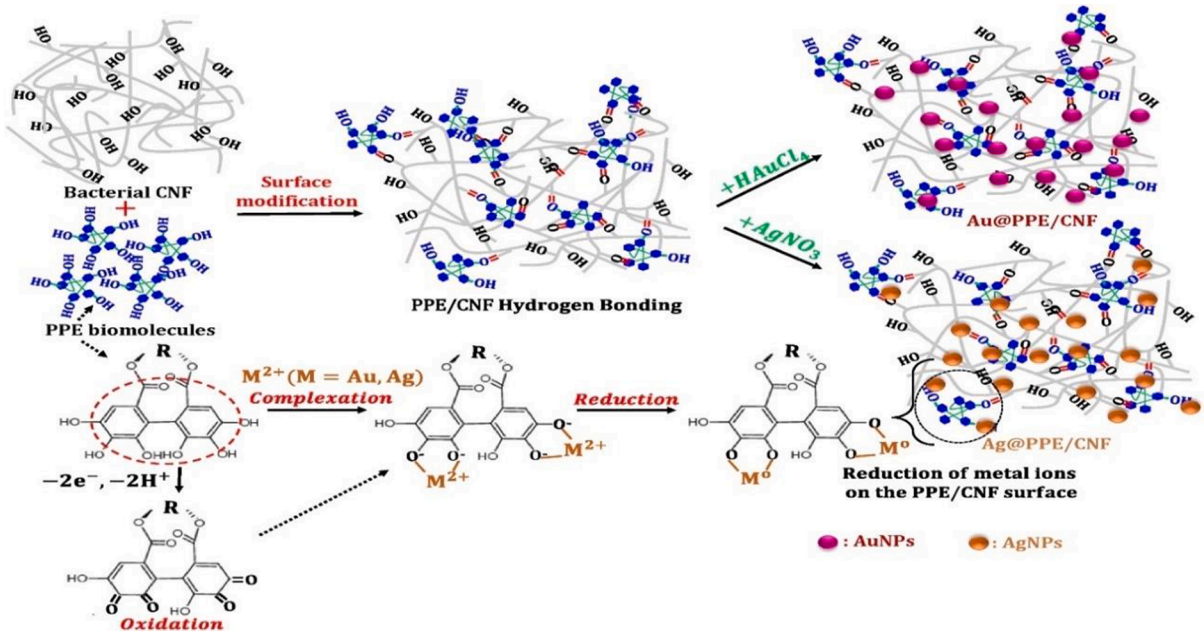

Fig. 13. Dye degradation mechanism of in-situ produced Au and Ag NPs using pomegranate peel extract and bacterial nanocellulose as support for the formation [196].

several characterization methods, the produced NPs having a spherical or ellipsoidal shape with an average size of 75–100 nm were able to degrade cationic dyes malachite green, rhodamine B, and methylene blue effectively by following pseudo-first order kinetics. Yaun and co-workers [205] reported a facile synthesis of iron NPs using an aqueous extract of *Dimocarpus longa* leaves and a precursor salt, $FeCl_3$. These NPs were highly stable for 28 days and were used in Fenton-like reactions to catalyse degradation of methyl orange and several other different dyes. The degradation followed pseudo first-order kinetics and the acidic nature to catalyse the reaction was maintained by the presence of biomolecules in the leaf extract. Dhas and Dhar, [206] likewise, produced spherical and quasi spherical shaped iron NPs (74 nm) using young shoots of *Camellia sinensis* and found them highly effective to degrade Rhodamine B within 1 hour. Likewise, tea leaves were also used by Wang et al. to produce iron NPs on hydrochar in order to decolorize methylene blue, and it was observed that almost 97.77% of the dye was absorbed within 60 min of catalysis [207]. Ting and Chin [208] reported on the use of apple peel extract as an effective reductant and stabilizing agent for making elliptical and spherical shaped iron NPs with an average size of 50 nm. These NPs showed 71.51% discoloration on the degradation of malachite green within the first minute.

Synthesis of FeO NPs using an aqueous leaf extract of *Ruellia tuberosa* has successfully been reported by Vasantharaj et al. [209]. These NPs showed a peak at 405 nm in the UV–vis spectrum and were further characterized by FT-IR, SEM, TEM, DLS, and DSC techniques. The authors proved that FeO NPs were able to decolorize crystal violet synthetic dye with 80% efficiency under solar light irradiation. The XPS spectra displaying the surface chemistry of Fe-O NPs produced by *C. citratus* extract further confirms the presence of hydroxyl and carbonyl groups in the spectrum [210]. Qasim et al. [211] reported a one-step synthesis of FeO NPs using berry extract of *Withania coagulans*. The extract resulted in the production of FeO nanorods with an average size of 16 nm. These nanorods displayed efficient degradation of safranin dye. They proved that iron oxide NPs synthesised by green methods display better photocatalytic efficiency than chemical methods.

The dye degradation potential of FeO—NPs synthesised in a green way by using Avicennia marina flower extract has been carried out by Karpagavinayagam et al. [212]. Shalaby and co-workers [213] reported the natural-product mediated synthesis of iron oxide NPs using Pirulina platensis microalgae and their photocatalytic activity to remove synthetic crystal violet and methyl orange dyes. The synthesised NPs displayed good degradation of both the dyes following pseudo-second order kinetics. Prakash et al. [214] prepared iron oxide NPs by using aqueous neem leaf extract and used them to degrade acid blue dye. They used Fenton and ultrasound assisted Fenton processes and found ultrasound more efficient as the degradation was completed in 20 mins. Arasu et al. [215] synthesised iron oxide NPs in one step using *Acorus calamus* rhizome extract and showed them to be effective photocatalysts to reduce two azo dyes, methylene blue and Congo red. The formation mechanism and catalytic degradation of methylene blue dye with zero valent iron NPs produced by *Cymbopogon citratus* and *R. communis* extracts, respectively, are shown in Fig. 14 [216,217].

Iron hexacyanoferrate *NPs with* hexagonal, rod, and spherical shapes and having a size range of 10–60 nm could be easily produced using *Sapindus-mukorossi* as a natural surfactant. The produced NPs were found to degrade toxic organic pollutants such as anthracene and phenanthrene with 80–90% efficiency, whereas chrysene, fluorene, and benzopyrene degraded 70–80% in water and soils [218]. Sharma et al. [219] reported the use of biosurfactant extracted from the bacterium Alcaligenes sp. for the synthesis of iron oxide NPs. The TEM analysis revealed a size of 176.69 ± 5 nm, and the photocatalytic studies demonstrated that these NPs could remove 93.77 ± 0.12% of malachite green within 1.5 min.

Bhuiyan et al. [220] prepared (α-Fe_2O_3) NPs from precursor hexahydrate ferric chloride salt using *Carica papaya* leaf extract and used them for the degradation of remazol yellow RR from wastewater. These NPs showed efficient dye degradation activity for remazol, whereby 76.6% was effectively degraded in the presence of a 0.8 g/L catalyst dose after 6 h at pH 2. Bini et al. [221] studied the feasibility of using *Punica granatum* seeds to extract biomolecules to synthesize spherical shaped Fe_2O_3 NPs for photodegradation of a reactive blue 4 dye. As identified by LC/MS, the pomegranate extracts are rich in polyphenols, which resulted in the fast generation of iron oxide nanoparticles with a size in the range of 25–30 nm. Under UV irradiation, they observed more than 95% of the dye was degraded in less than 56 min.

In another work, extracts of *K. alvarezii* plants have been used to produce Fe_3O_4–NPs by Arularasu and coworkers [222]. These NPs displaced antibacterial activity against S. aureus and E. coli and showed

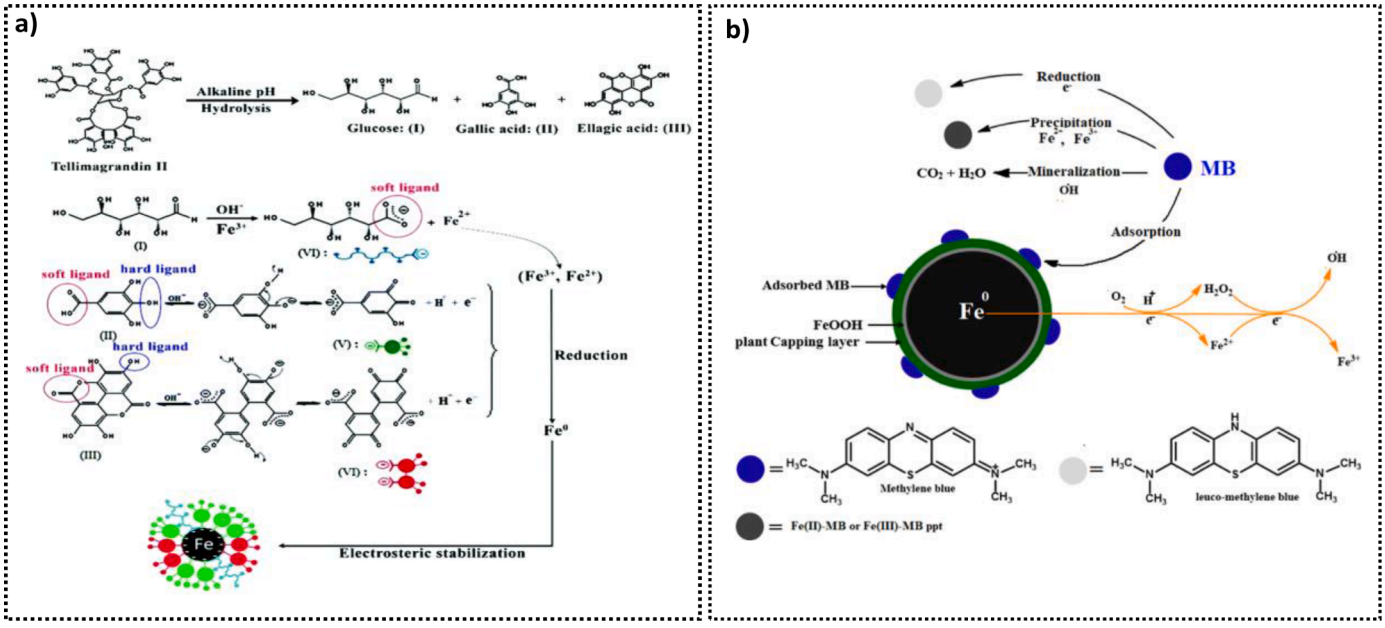

Fig. 14. a. Probable reaction mechanism of hydrolysable tannin-based reduction of iron salt. The phenolic groups in the tannins get oxidized to quinines with the subsequent release of electrons which reduce the iron ions and b. Proposed mechanism for the removal of MB onto RC-nZVI [216,217].

excellent dye degradation activity towards removing cationic textile dye wastes. Pai et al. [223] reported the Thunbergia grandiflora leaf extract mediated one-step synthesis of Fe3O4 NPs and investigated their photocatalytic activity against acid blue 115 dye. The synthesised NPs were predominantly spherical in shape (25 nm) and had a degradation rate of 95% at pH 2 in less than 3.5 h. A plausible mechanism for the formation of α-Fe_2O_3 and Fe_3O_4 using C*amellia sinensis* and *Zanthoxylum armatum* leaf extracts is shown in Figs. 15a and b [224,225].

4.3. Copper and CuO NPs as photocatalysts

Copper is a low-cost metal and the most widely used, with numerous potential applications in almost every sector [226]. In the medical field, as an antimicrobial agent and disinfectant, as a coating material for drugs in pharmaceuticals, a conducting material in electronics, and for sensing in environmental applications [227,228]. Nowadays, attempts are made to develop advanced Cu and CuO NPs using biological and renewable materials for their application in water purification technology [229]. An aqueous leaf extract of Celastrus paniculatus has been used for the rapid synthesis of CuNPs in the 2–10 nm size range. The NPs were produced when 50 mL of 5 mM copper sulphate solution was mixed with 5 mL of plant extract at pH value 7. These CuNPs displayed excellent photocatalytic activity towards converting methylene blue to less harmful by-products under solar irradiation for 120 min [44]. The degradation spectra of Nile blue (93%) and reactive yellow 160 (81%) in 120 min with CuO NPs produced from *Psidium guajava* leaf extract is shown in Fig. 16 [230].

CuNPs with a size range of 9–11 nm were produced using *Jatropha*

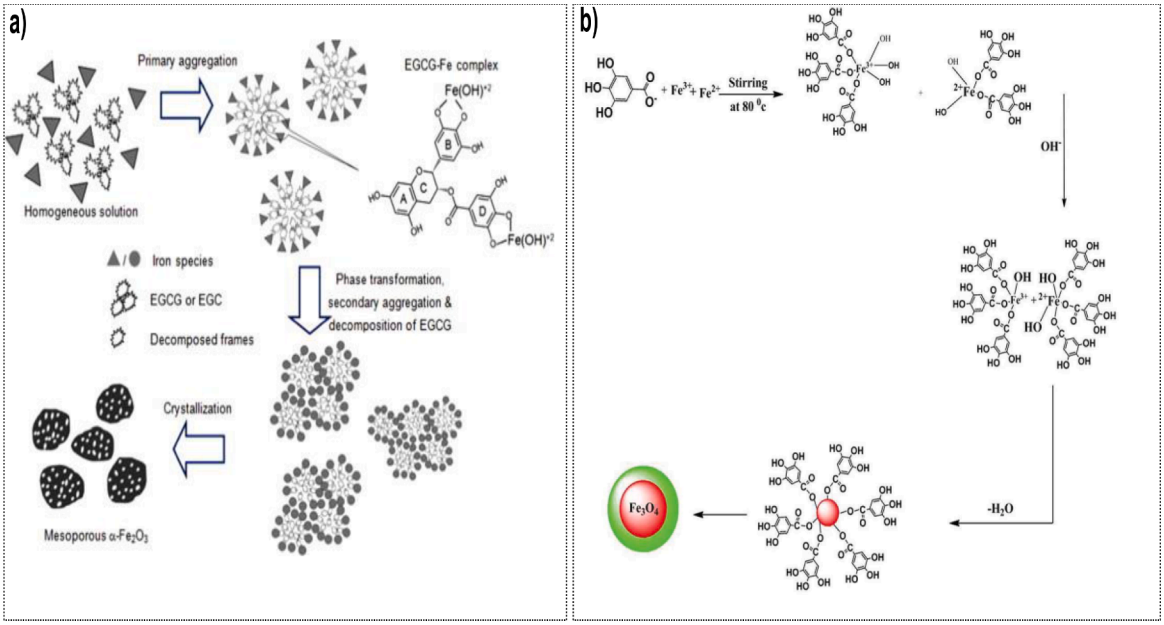

Fig. 15. Schematic illustration for the green formation-mechanism of αFe_2O_3 and Fe_3O_4 NPs using *C. sinensis* and Z. *armatum* leaf extracts [224,225].

curcas leaf extract, and were found to efficiently degrade the methylene blue dye under solar light. Reduction of copper salt to CuNPs using leaf extract of *Jatropha curcas* was attributed to the presence of flavonoids, tannins, glycosides, and alkaloid compounds [43]. In a study, an extract of *Ageratum houstonianum* leaves was reported to reduce copper salt to CuNPs, and the particles were characterized viz. UV–vis, XRD, SEM, FT-IR, TEM, and zeta particle size analyser. The CuNPs synthesised using *Ageratum houstonianum* extract were cubic, hexagonal, and rectangular with an average size of 80 nm. These NPs were able to completely degrade Congo red dye within 2 h of light illumination [231]. An extract of Manilkara zapota leaves has been used to generate spherical shaped CuNPs (18.9–42.5 nm). Methyl violet (92.2%), Malachite green (94.9%), and Coomassie brilliant blue (78.8%) were found to degrade in 50, 40, and 60 min, respectively [232]. A green method was described by Karuppannan et al. [233] to synthesis and characterize CuNPs by treating copper ions with *Cardiospermum halicacabum* extract. They mixed 10 mM $CuSO_4$ with 20 mL of leaf extract and reported the formation of stable spherical shaped CuNPs within 2 h of reaction time. These NPs were observed to cause 93% methylene blue degradation under sunlight. Synthesis of CuNPs using an aqueous coffee bean extract was described by Wang et al. [75]. The CuNPs were stable and synthesised rapidly with an average size of 5–8 nm. These NPs proved as potential catalysts in the degradation of amido black, methylene blue and xylenol orange. Chawla et al. [234] synthesised green CuNPs capped with gum arabic and showed them photoactive to degrade 95% methylene blue and crystal violet within 40 and 20 min of reaction time, respectively. Sarwar and colleagues [235] synthesised highly stable CuNPs using extract of cinnamon bark. Cinnamon bark is rich in terpenoids mainly eugenol and this compound was described as responsible for the biogenic reduction of Cu ions to NPs (Fig. 17). These NPs were spherical and catalysed or degraded more than 80% of two textile dyes namely methylene blue and methyl orange. Raina et al. [236] observed the photocatalytic degradation behaviour of three textile dyes in UV–vis spectrum using spherical CuNPs produced by leaf extract of *Centella asiatica.* They noticed that CuNPs were able to produce 98.49% degradation in methyl red, 98.84% methyl orange and 99.62% in phenyl red under optimal treatment conditions. Extract of O. americanum leaves has been used by Manikandan et al. [237] to produce spherical CuO NPs with a size of 68 nm. These NPs caused efficient discoloration of eosin yellow, rhodamine, and methylene blue azo based dyes. Sharma et al. [238] reported the green synthesis of CuO NPs using aloe-vera extract biomolecules as reducing and capping agents. The formed NPs were 5–20 nm in size and exhibited excellent photocatalytic activity against methyl orange with 96% of degradation within 24 min under UV light illumination. Rafique et al. [239] reported a study for the degradation of Rhodamine B dye using CuO NPs produced using *Citrofortunella macrocarpa* leaves extract. More than 98% dye was degraded under UV irradiation. The mechanism of photocatalysis was proposed based on generation of ROS which attack on the dye molecule and covert it to less harmful by-products. Sharma et al. [240] described the synthesis and photocatalysis of CuO NPs from leaves extract of *Ocimum tenuiflorum*. The formation of CuO NPs was first confirmed by the peaks at 360 and 368 nm in UV–vis spectrum. Other characterization techniques showed that the produced CuO NPs are elliptical, spherical or rice shaped (6–18 nm). These CuO NPs demonstrated excellent degradation activity, with 96.4 ± 0.83% methyl orange discoloration within 24 min. Zaman et al. [241] likewise, produced CuO NPs using leaf and fruit extracts of *Tamarindus indica* and evaluated their photocatalytic activity. The NPs produced by fruit extract (5- 10 nm) were smaller in size than leaf extract (50–100 nm). The photocatalytic results on Rhodamine B under UV–vis illumination showed that leaf mediated NPs degraded 65% while as 77% was noticed using fruit produced CuO NPs. In another study, photocatalytic activity of CuO NPs produced by chemical and a green method using aqueous leaf extract of *Solanum nigrum* was described by Muthuvel et al. [242] They compared the photocatalytic activity of chemically produced CuO NPs with biogenic and found that methylene blue was more efficiently discolourised by plant extract mediated CuO NPs. Sukumar et al. [243] employed leaf extract of *Annona muricata* to fabricate CuO NPs which were characterized by UV–vis, XRD, Bio-TEM, SEM-EDX, FT-IR techniques. The results showed CuO NPs to be spherical with an average pure crystalline size of 30–40 nm. These NPs were utilized for discoloration of reactive red and methyl orange. The results from their study revealed that these NPs exhibited dye degradation efficacy of 90% (reactive red), and 95% (methyl orange) after 60 min under solar radiations.

4.4. Zinc oxide NPs in catalysis

A wide variety of plant and microbe products have been utilized over the last few decades to synthesise ZnNPs by various research groups worldwide [244,245]. Apart from being biocidal, ZnO NPs are proven photocatalysts and have been used extensively to convert toxic azo dyes into less harmful by-products [246]. In recent years, the photocatalytic activity of ZnNPs synthesised via biological routes has attracted more and more interest of researchers. The digital photographs of green fabricated ZnO NPs under normal and UV-light are shown in Fig. 18 [247]. *Calliandra haematocephala* leaf extract mediated synthesis of nano-flower shaped and hexagonal-formed wurtzite structures for the degradation of methylene blue was reported by Vinayagam et al. [248]. In their work they examined degradation efficiency of the dye molecule at different time intervals using UV–vis spectroscopy and found 88% dye discoloration within 270 min under solar light. Methyl orange and Methyl blue were degraded viz photo catalytically by Mirgane et al. [249] using ZnO NPs produced by *Abelmoschus esculentus* leaf extract.

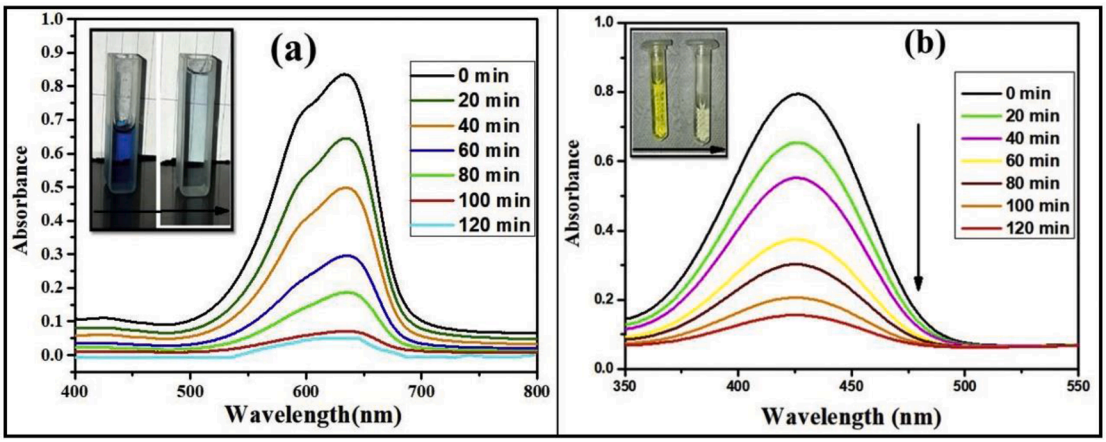

Fig. 16. UV–visible spectra during degradation: (a) NB dye and (b) RY160 dye catalysed by CuO NPs under direct sunlight [230].

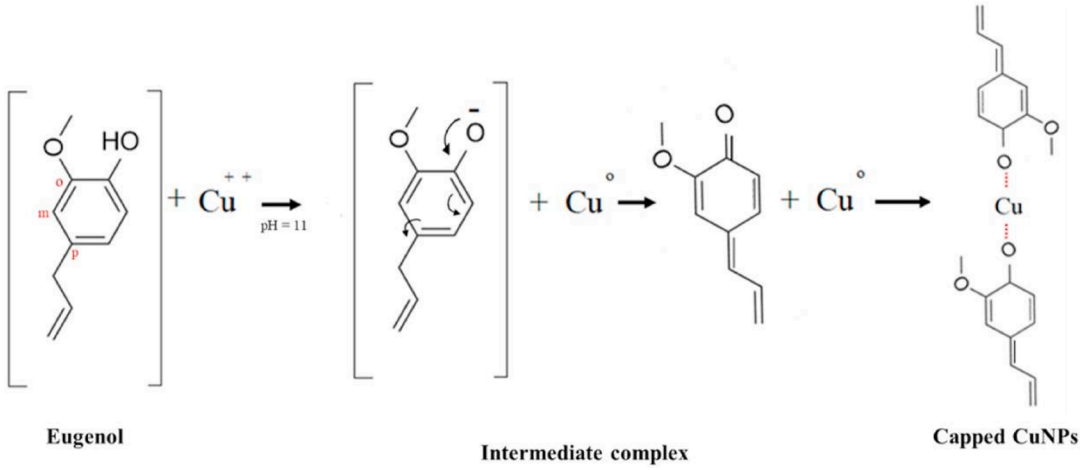

Fig. 17. Reduction mechanism of eugenol and subsequent capping [235].

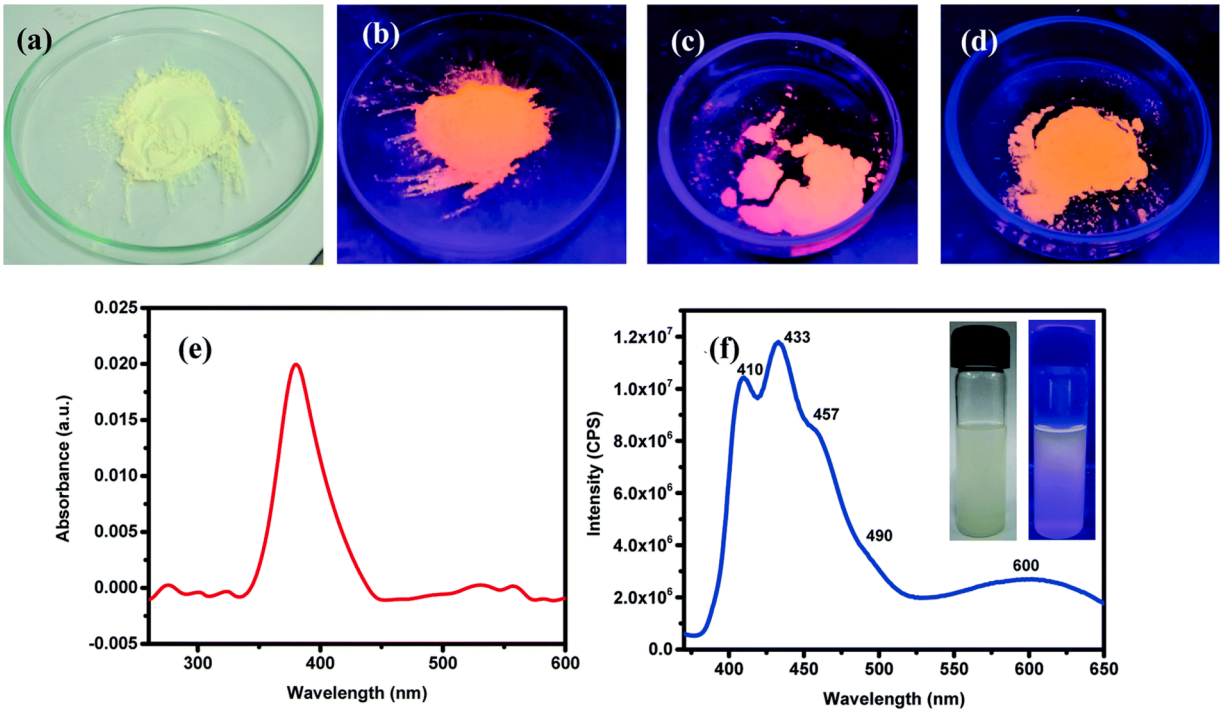

Fig. 18. Digital photographs of the green-synthesized ZnO NPs by *Nelumbo nucifera* leaves extract [247].

Charkarborty et al. [250] reported synthesis and congo red dye degradation of ZnO produced by Averrhoe carambola fruit extract. They found that appearance of a peak at around 350 nm in UV–vis spectrum confirmed the formation of stable ZnO NPs. The ZnO NPs had significant photocatalytic efficiency of 93% under UV light. Also, leaf extracts of Hibiscus *rosa-sinensis* have produced ZnO NPs (spherical and 100 nm) for the removal of Congo red from waste waters [251]. In another study conducted by Liu and colleagues, [252] highly active ZnO NPs were produced using *Amomum longiligulare* fruit extract for the degradation of methylene blue. *Moghaddas* et al. [253] used zinc nitrate hexahydrate as a precursor and Quince seed mucilage as source of bio reducing and stabilizing agents to produce highly stable ZnO NPs with photocatalytic applications. They tested the produced ZnO NPs (25 nm) towards methylene blue and observed more than 80% degradation efficiency with 2 h. Park et al. [254] reported synthesis of ZnO NPs using *Gynostemma pentaphyllum* extract biomolecules as reducing agents and examined their Malachite Green dye degradation activity. The results revealed that the malachite green absorption peak decreases with an increase in exposure time and finally exhibits 89% removal after 180 min under UV illumination.

Aegle marmelos juice has also produced ZnO NPs for degradation of methylene blue. It was shown that Aegle marmelos synthesised NPs could bring more than 96% discoloration in methylene blue within 30 min of UV irradiation [255]. Rambabu et al. [256] studied the use of date pulp/Phoenix dactylifera waste for green synthesis of ZnO NPs. They characterized ZnO NPs produced by treating 5 g of Zn precursor with 50 mL of plant extract using various analytical methods. It was concluded that date palm extract mediated NPs were spherical, crystalline with a mean diameter of 30 nm. By using these ZnO NPs as catalysts for methylene blue and eosin yellow, they noticed the calculated dye degradations were more than 95%. Methylene blue was effectively also degraded by *Eriobutria japonica* seed extract produced ZnO NPs [257]. ZnO NPs reported to be produced by Euphorbia sanguinea extract showed strong photoactivity towards malachite green dye [258].

SEM/EDX demonstrated that these NPs are flower shaped and XRD showed their hexagonal crystalline structure. The formed NPs demonstrated 92% degradation of Malachite green after 60 min under solar irradiation. Also, *Asperagus racemosus* root extract produced spherical and hexagonal ZnO NPs with an average size of 30–70 nm has displayed 93.20% discoloration of Malachite green after 3 h of illumination. They proposed shatavarins based compounds present in root extract were able to bind zinc ion and convert them to NPs (Fig. 19) [259].

Rafique et al. [260] fabricated hexagonal crystalline and spherical shaped ZnO NPs by treating aqueous leaf extract of Syzygium cumini with zinc ions and subsequently evaluated their photocatalytic activity. The synthesis was quick and the presence of flavonoids, phenolic acids, enzymes and steroids in the leaves extract demonstrated by FT-IR were proposed mainly responsible for reduction and stabilization. In their work more than 98% Rhodamine B dye was catalysed and it was concluded that irradiation time, temperature and pH were crucial parameters controlling the Rhodamine B dye degradation efficiency.

4.5. TiO_2/SnO_2 and other NPs

A one-pot method has been used for the synthesis of crystalline and tetragonal TiO_2 NPs using *A. indica* twigs, *F. benghalensis,* and *S. aromaticum* plant extracts. The produced NPs were stable and exhibited 70% photocatalytic activity on the degradation of methylene blue [261]. *Phyllanthus emblica* leaf extract has demonstrated its use for the synthesis of 20–30 nm crystalline TiO_2 NPs which showed effective degradation of Coralline Red dye under solar light (rate constant 0.005 min−1 and efficiency~93%) [262]. Anatase TiO_2 NPs with an 80–100 nm size range and a band gap of 3.22 eV have been successfully synthesised using citric acid present in the leaf extract of *Citrus limetta*. The photocatalytic activity of these NPs was examined on Rh-B, and the results showed that the degradation efficiency was 90% under UV irradiation for 80 min [263].

A novel green method for the synthesis of TiO_2 NPs using aqueous extract of lemon peels is described by Nabi et al. [264]. Spherical shaped particles containing anatase TiO_2 with an average size of 80 −140 nm were produced by the hesperidin flavanol compound present in lemon extract. The UV–vis calculations showed a band gap energy of 3.08 eV. These NPs were found to degrade Rhd-B dye and showed 70% activity, much higher than commercially available TiO_2 NPs (60%) under UV-irradiation. Likewise, in another study, the effect of Lagenaria siceraria leaf extract on the synthesis of TiO_2 NPs was investigated to compare its photocatalytic performance with chemically produced TiO_2 on Reactive Green 19 dye. Under similar acidic pH conditions, it was found that green fabricated TiO_2 NPs achieved 98.88%, whereby only 88.55% of dye removal was exhibited by chemically produced TiO_2. The improvement in catalytic efficiency of the green method was attributed to the generation of a greater number of electron hole pairs due to its smaller size, higher surface area, and increased pore diameter compared to chemically synthesised TiO_2 [265]. More recently, Helmy et al. [266] presented biological synthesis of S-doped TiO_2 NPs using *Malva parviflora* as a source of green reductants and compared their results with a chemically synthesised counterpart. By using BET analysis, they noticed that green synthesised NPs had a 135.5 m^2/g surface area, much higher than chemically produced and could effectively degrade methyl orange under solar illumination (Fig. 20). The photocatalytic results of their study provide new insights for green mediated S-doped TiO_2 NPs in environmental applications.

Apart from TiO_2, the green fabricated semiconductor materials SnO_2 have demonstrated excellent dye degradation results. Likewise, the synthesis of spherical shaped SnO_2 NPs has been carried out by using chitosan as a stabilizer. The synthesised NPs were characterized by different analytical techniques and evaluated for photocatalytic activity on Eriochrome Black T under mercury lamp (500 W) irradiation. The photocatalytic efficiency was optimised by examining the effect of

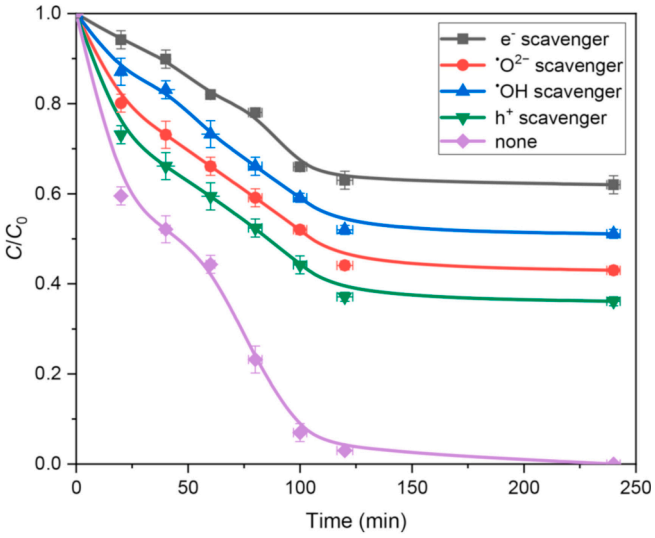

Fig. 20. Effects of different radicals on the photocatalytic bleaching efficiencies of MO dye over GST NPs under visible light irradiations [266].

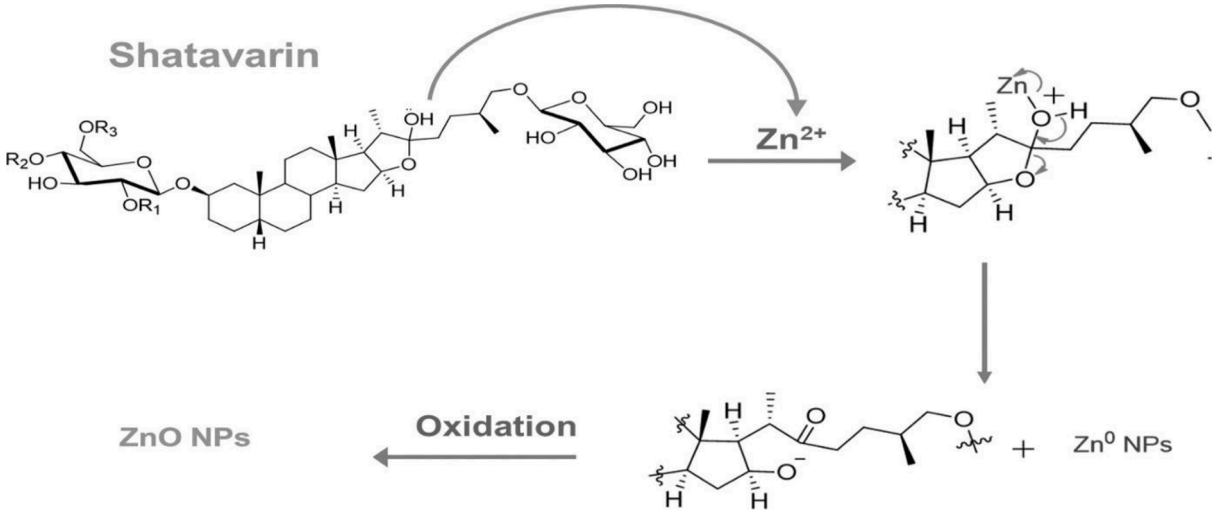

Fig. 19. Schematic representation of the possible mechanism for the green synthesis of ZnO NPs using aqueous *Asperagus racemosus* root extract [259].

different reaction conditions, and it was concluded that 21.1 mg/L of the photocatalyst at pH 5 effectively degraded 77% of the tested dye in 4 h [267]. A reusable SnO_2 photocatalyst for the removal of methylene blue and eriochrome black-T from wastewaters has been synthesised using reducing and stabilizing power of flavonoid compounds isolated from jujube fruit extract. These NPs were able to remove both the dyes under

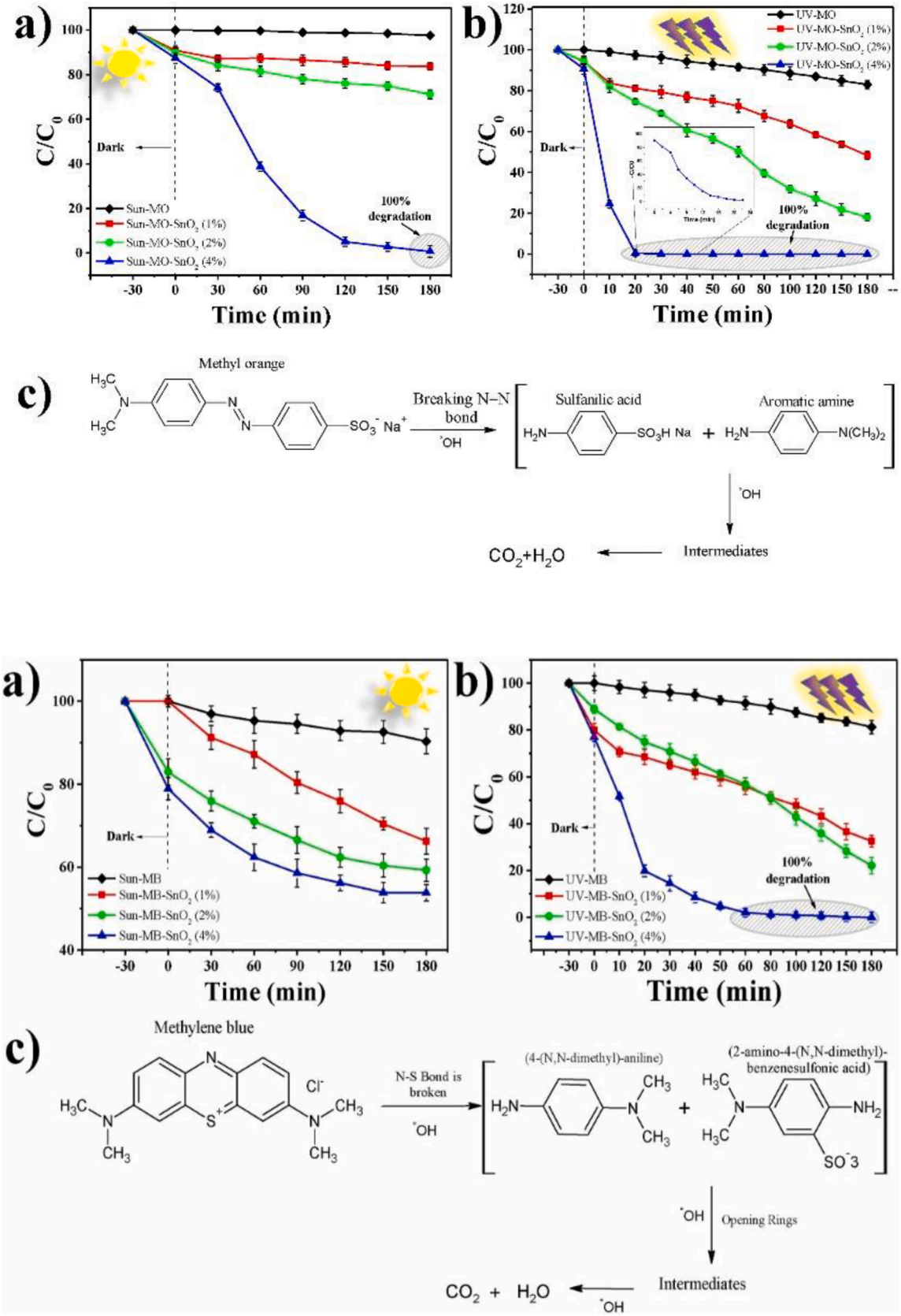

Fig. 21. Photocatalytic activity of green synthesised SnO_2 NPs in the degradation of MO, MB, and RhB [272].

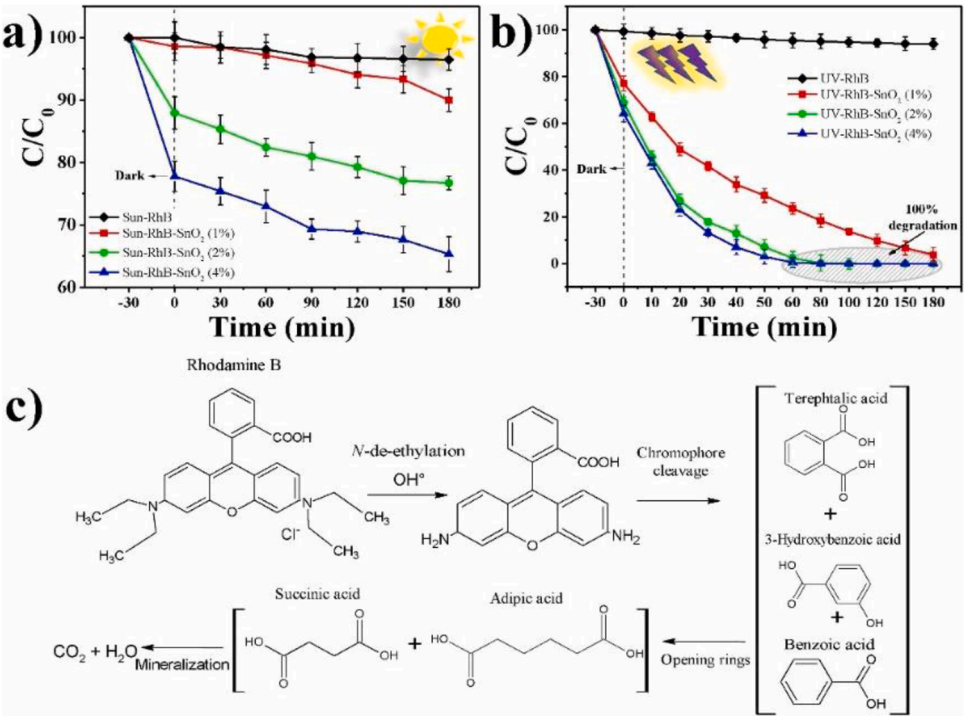

Fig. 21. (*continued*).

solar light illumination with degradation percentage of 90% and 83% towards methylene blue and eriochrome black-T, respectively [268]. Spherical and crystalline SnO_2 NPs were also produced using leaf extract of *Piper betle*. As synthesised NPs exhibited 92.17% discoloration of RY-186 dye under solar light following pseudo-second order kinetics with a rate constant of 1.3×10^{-2} min^{-1} [269]. A green process was reported for the synthesis of SnO_2 NPs using fruit extract of *Vitex agnus-castus*. The characterizations showed 8 nm size and spherical shape and further analysis by UV–vis confirmed their use in photocatalytic dye degradation of Rh-B under UV irradiation. The discoloration of 91.7% at 298 K was achieved within 190 min [270]. SnO_2 NPs with spherical shape (5–10 nm) were also prepared for the first time using *Actinidia deliciosa* (Kiwi) peel extract and characterized by UV–vis, FT-IR, TEM, SEM and EDX techniques. These SnO_2 NPs displayed good photodegradation performance towards discoloration of methylene blue (89% in 8 min), methyl orange (87% in 8 min), and rhodamine B (97% in 6 min) [271]. In another interesting work, the photocatalytic degradation of *Citrus paradisi* grapefruit peel extract mediated *(*flavonoid and polyphenols*)* SnO_2 was investigated on methyl orange, methylene blue and Rhodamine B under both solar light and UV irradiation. SnO_2 NPs prepared by this cleaner route had quasi-spherical morphology with 4- 8 nm size range. The photocatalytic degradation under sunlight and UV and also possible degradation patterns of all the three dyes is shown in Fig. 21. As can be seen clearly from the results, 100% decomposition was achieved on all the tested dyes under sunlight and UV by using 4% extract concentration in the formation of SnO_2. It was concluded that UV irradiations cause degradations in shorter duration (20 min for MO, and 60 min for MB and RhB) compared to solar light (180 min) [272].

Nowadays, newer NPs are also explored via green routes for water purification applications. In this direction, Pd NPs have been formed by the reduction of Pd $(NO_3)_2$ salt using kernel shell extract of apricots. The reduction of Pd^{+2} to Pd NPs was quick and this was attributed mainly to the presence of hydroxyl and polyphenolics in apricot, as evidenced by FTIR Results. The photocatalytic results showed these NPs can be used to degrade Methyl Orange, Methylene Blue, Rhodamine B, and Congo Red dyes [273]. Nickel (Ni) and nickel oxide (NiO) NPs were synthesized using Hordeum vulgare extract. The results showed that 1 M precursor salt, pH 12 at 60 °C for 60 min were optimum reaction conditions for the formation of stable NPs. These NPs showed good photocatalytic degradation of methylene blue dye by following first order kinetics [274].

5. Green bimetallic/tri/core-shell NPs as next generation photocatalysts

As disused in this review nanoparticles are attractive choice for the environmental cleaning applications. Catalysis by NPs is highly influenced by surface area which can be altered or tuned by using bimetals and changing their compositions [275]. . Increased stability, higher surface area, catalytic activity, synergy phenomenon, and improved electronic conductivity of bimetallic NPs has sparkled significant interest and made them attractive candidates for a promising research interest in environmental remediation treatments [276,277]. Most importantly, synthesising bimetallic NPs based on sustainable and renewable materials is considered a new and exciting research area and therefore, the catalytic ability of core shell or bimetallic NPs to degrade coloured synthetic dyes via this emerging route has recently been explored. Ag/Au bimetallic NPs have been produced in a single-step reaction by aqueous extract of clove buds and used as photocatalysts for the degradation of methyl orange, and methylene blue. As expected, excellent photocatalytic activity is reported by Ag/Au bimetallic NPs towards both the dyes compared to AuNPs and AgNPs when used separately. This enhancement was assigned to synergistic effect of both the metals and capping of NPs with extract biomolecules. From FT-IR results, it was concluded that eugenol present in clove extract provides required 4 electrons necessary for the formation of bimetallic NPs. Ghosh et al. also observed highest catalytic activity for Ag-Au formed by plant extract [278]. The UV–vis spectrum of bimetallic Ag-Au synthesised with *Polyalthia longifolia* leaf extract compounds is shown in Fig. 22 [278]. The synthesis mechanism of bioactive Ag–TiO_2 bimetallic by bio-reductants such as carnosol, ursolic acid, carsonic acid, lithospermic acid isolated from *Origanum majoana* is shown in Fig. 23 [279]. Al-Asfar et al. [280] synthesised silver-iron bimetallic NPs using fruit extract of date palm as a reducing agent in the presence of $AgNO_3$ and Fe $(NO_3)_3$ as precursor salts. These core-shell NPs were reported to display

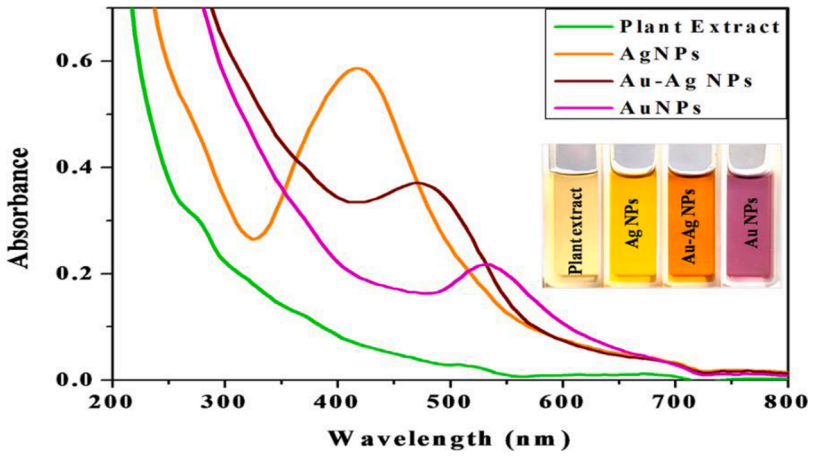

Fig. 22. UV–vis diagram for the reduction of metal ions; and formation of Au-Ag BMNPs [278]

photocatalytic degradation of bromothymol blue. This catalytic activity was attributed to the generation of active holes leading to the formation of hydroxyl radicals which are responsible for actual degradation phenomenon.

In another work CuO/ZnO nanocomposites for excellent photocatalytic activity were synthesised using eggshell membranes (ESM). The SEM and EDX showing uniform distribution of particles (100 nm) of the formed composite is shown in Fig. 24 [281]. Date palm (*Phoenix dactylifera*) leaves extract has also been employed to prepare 26 nm Cu-Ag NPs. These bimetallic NPs were formed by reacting equal volume 80 mL silver nitrate and copper nitrate salts and to this mixture 40 mL of extract solution was added after heating at 95 °C for 10 min. Photocatalytic tests revealed bimetallic NPs when treated with 5.0 mg/L methylene blue solution produced 82% degradation after 24 h of incubation [282]. Spherical shaped Ag-Pt BM NPs with 30 nm diameter were prepared using green method based on ethanolic leaf extract of *Crocus sativus* plant. In the presence of synthesised Ag/Pt NPs and $NaBH_4$ as reducing agent, photocatalytic degradation of methyl orange was examined and it was noticed that these BMNPs cause 96.68% methyl orange discoloration much higher than by monometallic Ag NPs (70.5%). These BMNPs catalysed reaction by reducing the activation energy and kinetic barrier between donor and acceptor by facilitating a

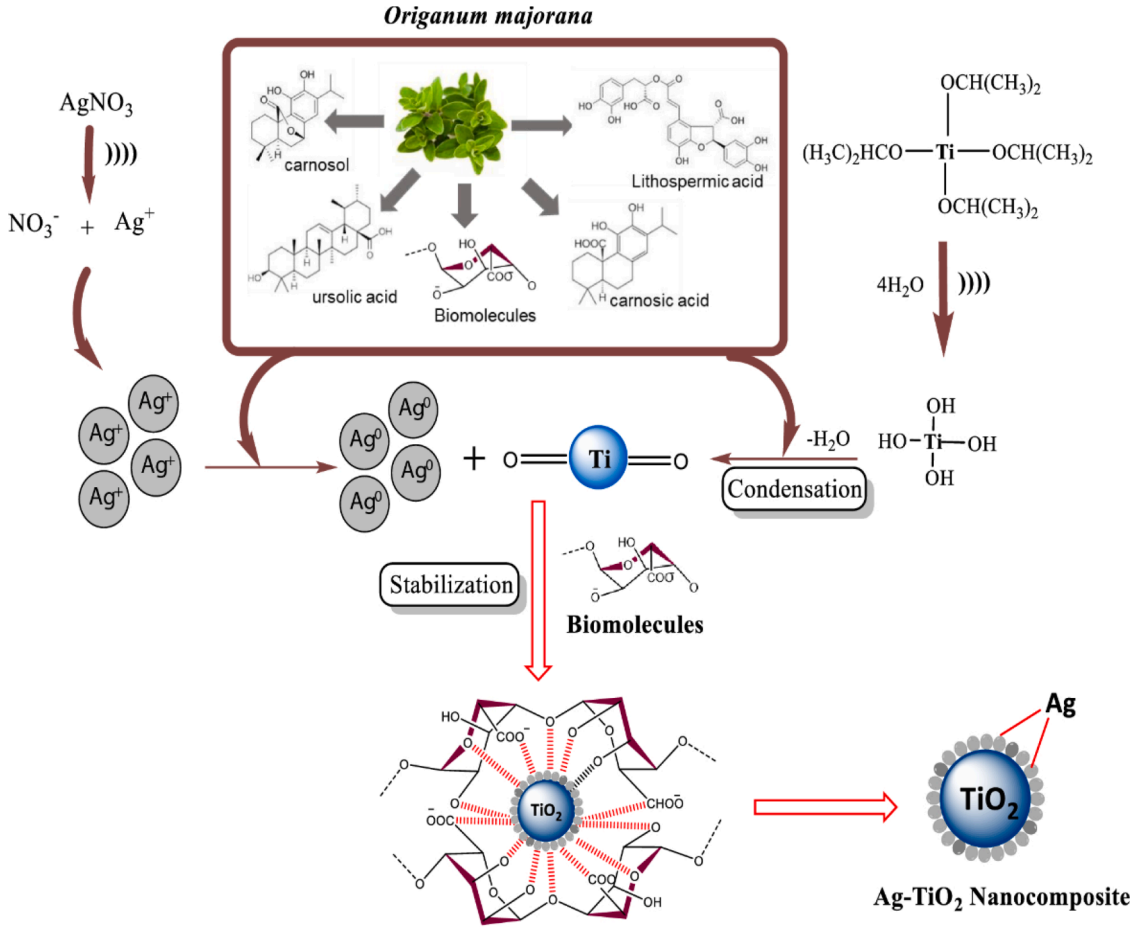

Fig. 23. Schematic representation for the synthesis of bimetallic Ag–TiO_2 NCs using *Origanum majorana* leaf extract [279].

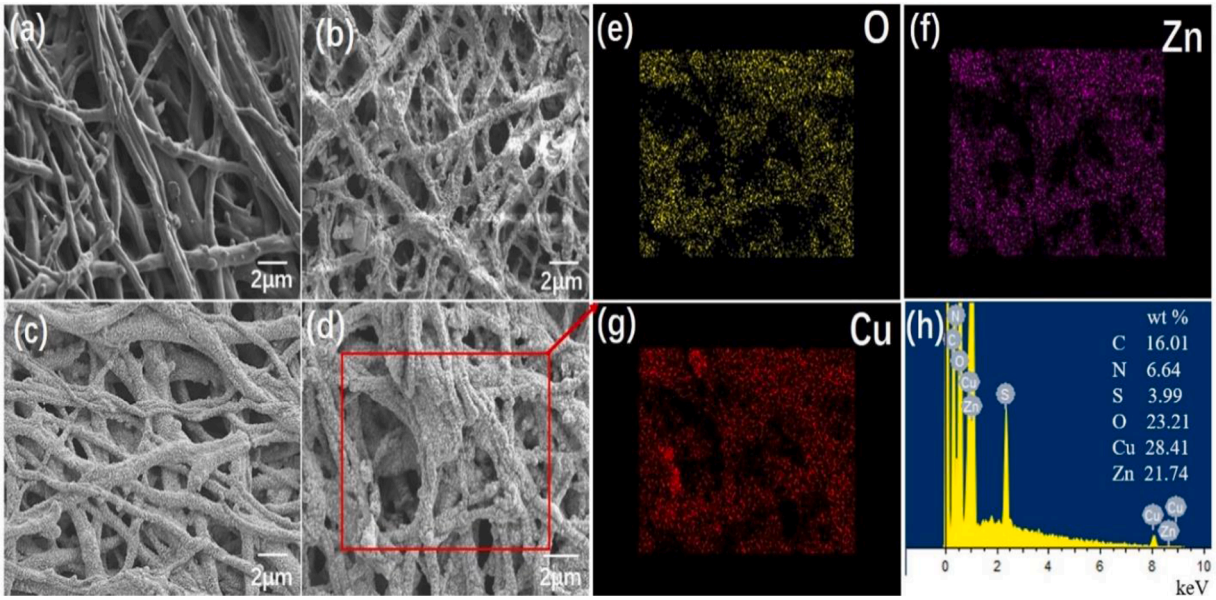

Fig. 24. FE-SEM images of (a) the natural ESM; (b) the CuO-ESM nanomaterials, (c) the ZnO-ESM nanomaterials, and (d) CZ-ESM nanocomposites, and (e-g) corresponding elemental mapping images of Cu, O, and Zn in (d), (h) the EDX spectrum of CZ-ESM nanocomposites [281].

movement in electrons generated by BH_4^- ions to dye structures [283]. Synergistic photocatalytic activity of *A. muricata* leaves extract mediated Ag–Cu and Ag–Zn BNPs in the presence of sodium borohydride was also studied on Methylene orange and rhodamine B dyes. The percentage degradation of 96% in 40 min for rhod-B and 94% in 25 min for MO displayed by Ag-Cu was higher than Ag–Zn BNPs combination where 95% in 80 min for rh-B and 96% in 45 min for MO was observed. As summarized in Fig. 25, they proposed BM NPs helped in the generation of hydroxyl and oxygen radicals by the transfer of electrons from borohydride ions to MO and rhod-B dye molecules and turn these dyes into less harmful by-products [284].

Besides, a few papers have been published on the formation of CuO/ZnO and CuO/ZnO carbon composites for wastewater purification applications using biological chemicals. The presence of CuO and ZnO peaks in the structure of XRD displayed in Fig. 26a shows the useful formation of these composites by the biomass filtrate of *P. corylophilum.* The CuO/ZnO displays good dye adsorption results and by inception of carbon in the composites, excellent removal of Cr metal and Congo red dye have been obtained that are ascribed to different interactions operating as shown in Fig. 26b. [285,286].

The adsorption of Congo red and other dye molecules onto ZnO based composites is mainly a pH-dependant reaction. The ZnO nanoparticles produced by Tulsi leaf extract could interact with the dye molecules via electrostatic and hydrogen bonding [287]. ZnO–$CdWO_4$ nanoparticles have also been formed by lemon grass extract to effectively degrade organic congo red dye. The maximum adsorption capacity of 5 mg/g was observed. Different modes of interaction between ZnO and ZnO based composites with negatively charged dye molecule

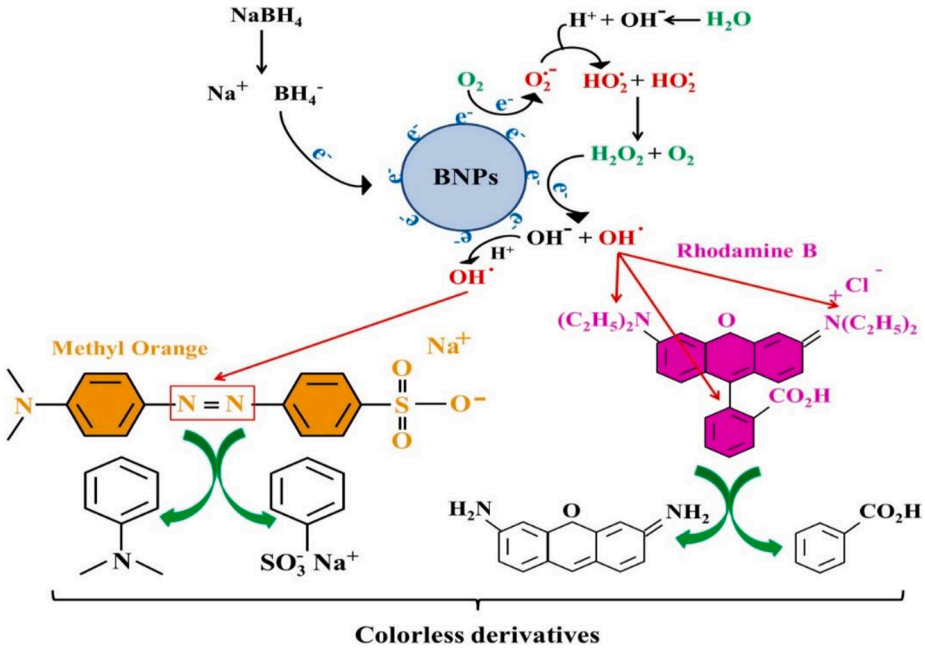

Fig. 25. Possible mechanism involved in the reduction of rh-B and MO textile dyes by BNPs as catalyst in the presence of $NaBH_4$ [284].

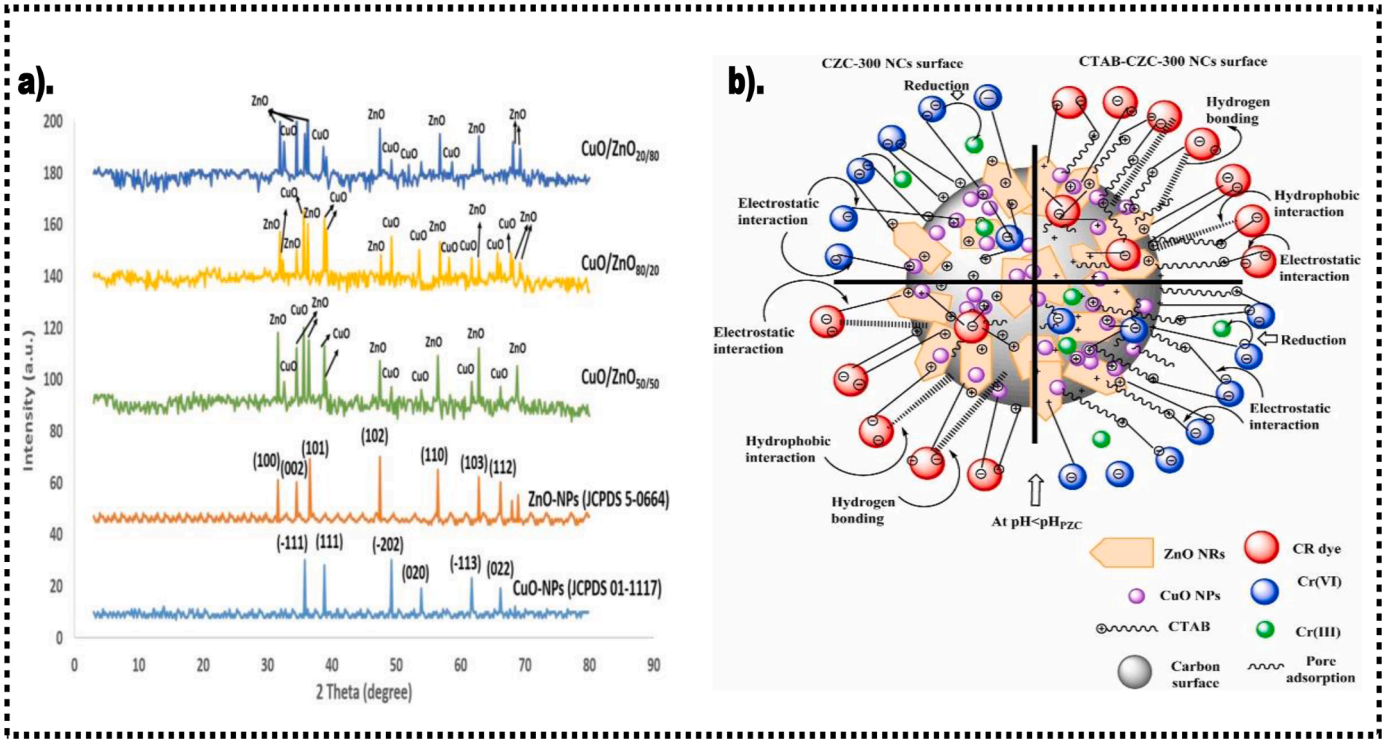

Fig. 26. a. XRD analysis of CuO/ZnO and b. mechanism of dye adsorption by CuO/ZnO and carbon composite materials fabricated by green reducing agents [285,286].

surfaces are shown in Fig. 27 [288].

To prevent the electron-hole combinations and therefore enhance the photocatalytic activity of ZnO, it was also coupled with SnO_2 by different research groups. *Viscum album* L extract was used by Sayadi et al. to synthesise ZnO- SnO_2 for the degradation of three organic pollutants, including Congo red dye. The formation of this composite was proved by XRD, FT-IR and UV results, and the photocatalytic mechanism of a similar composite produced by orange peel extract is shown in Fig. 28a-d [289,290]. Using *Salvia officinalis* extract as a green source of reducing and stabilizing agent, the pollutant 4 nitro-phenol is converted to 4-amiphenol within 45 min of treatment [291]. Devan et al. used aqueous leaf extract of the Catharanthus plant for the green synthesis of Ag/Pd NPs (15–30 nm) and tested their photocatalytic activity on Safranin O dye [292]. These NPs exhibited excellent discoloration activity and showed more than 98% Safranin dye degradation within 40 min under UV irradiation. Younas et al. [293] reported the formation and photocatalytic activity of Fe-Cu core-shell bimetallic NPs using an aqueous extract of *Ixora finlaysoniana*. These synthesised bimetallic NPs had a 50–200 nm size and showed efficiency in the degradation of methylene blue within 17 min of reaction time. Recently, Suvarna et al. [294] also reported a green, facile, and one-step synthesis of Fe-Cu core shell NPs using Cyclea peltata leaf extract. The core-shell NPs were detected by a UV–vis peak at around 250 nm with iron at the core and copper as the shell. These bimetallic NPs exhibited 82% of methylene green dye degradation within 105 min. Deng et al. reported the bimetallic NP synthesis of Ni/Fe_2O_3 by leaf extract of *Moringa oleifera*. Deng

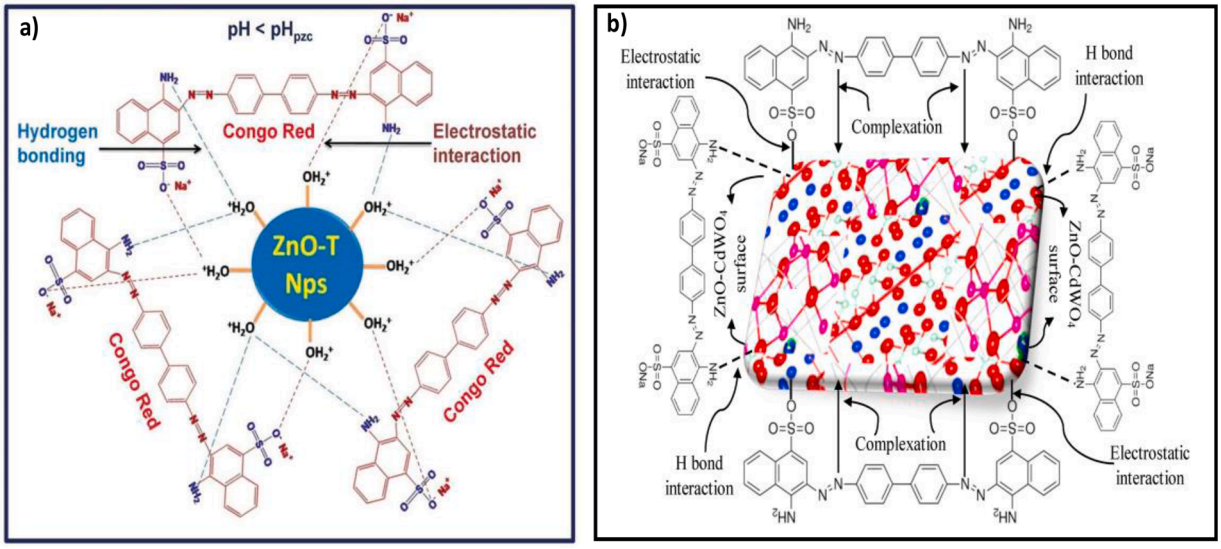

Fig. 27. Mechanism of congo red dye degradation using ZnO and ZnO–$CdWO_4$ composites produced by green chemistry methods [287,288]>.

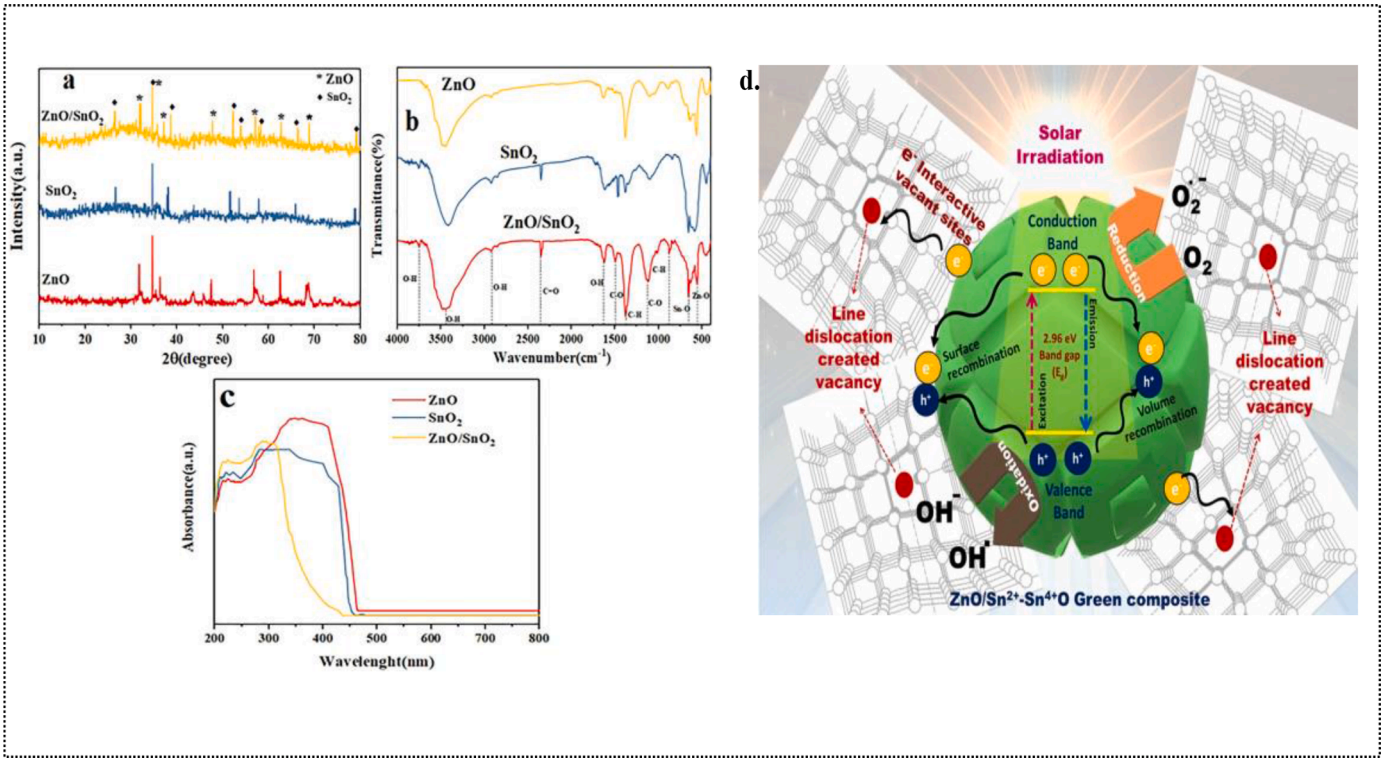

Fig. 28. XRD, b) FTIR, and c) UV–vis spectra of green synthesised ZnO, SnO_2, and ZnO/SnO_2 and d). Photocatalytic illustration of green ZnO/SnO_2 nanocomposite [289,290].

and colleagues [295] reported the potential of proanthocyanins, a natural chemical compound found in fruits, bark, leaves, and seed extracts of several plants, to produce Au/Ag bimetallic NPs. The proanthocyanins were able to reduce Au^{3+} and Ag^{+} ions to NPs when a mixture of precursor salts, 2% of $AuCl_3$ HCl_4H_2O and 1% of $AgNO_3$ were reacted with it. XRD and TEM techniques showed that synthesised particles have a uniform core-shell structure with a spherical shape. The photocatalytic activity data of these NPs demonstrated they were successful in degrading methylene blue and Rhodamine B by 96% and 92.70% when exposed to light for 30 min, respectively. Nasrollahzadeh et al. [296] reported the production of Cu/MgO NPs from aqueous fruit extract of *Cassytha filiformis* L. for the reduction of 4-nitrophenol, methylene blue, 2,4-dinitrophenylhydrazine, and congo red. They have noticed a colour change from whitish to dark and have used several other characterizations such as UV–vis spectroscopy, FT-IR, FE-SEM, EDX, and TEM to confirm the synthesis of Cu/MgO NPs. It was interesting to see that methylene blue and Congo red were reduced after 1 s and 190 s, respectively, suggesting the efficient nature of the catalytic reaction. Recently, a few research papers have used bacteria to prepare bimetallic NPs.

In this direction, the use of the bacterium *Deinococcus radiodurans* protein extract mediated synthesis of Au-AgNPs has been reported by Weng et al. [297]. These NPs caused 83.68% methylene green degradation. They have observed that as the pH increases from acidic to alkaline, the degradation capability of synthesised NPs towards methylene green also increases. This showed that pH 9.6 is the optimum pH for methylene green discoloration and was attributed to the reason that electrostatic forces operate between positively charged dye molecules and bimetallic NPs in addition to the leuco form conservation of methylene green dye in alkaline conditions. Furthermore, GC–MS analysis revealed that a less toxic product, 4-(dimethylamine) benzophenone, and other by-products were produced after the degradation reaction was completed.

6. Removal of heavy metals and antibiotics

Heavy metals and antibiotics are reported as priority and emerging contaminants; both of them remain an unprecedented global issue due to their mobility in water ecosystems and their acute toxicity to human health [298,299]. Heavy metal pollution occurs in wastewaters produced by the discharges from the mining industry, from vehicle emissions, and through the paper, dye, surfactant, and paint industries [300]. Most heavy metals such as Pb, Cr, Cd, and Hg, as well as other antibiotics such as levofloxacin, tetracycline etc., produced by the pharmaceutical and above-described sectors, are non-biodegradable and have a high toxicity potential even at trace ppm levels due to their bioaccumulation in the environment [301,302]. As a result, different physiochemical and biological methods for the removal of toxic heavy metal ions from industrial wastewaters have been widely applied in recent years. Amongst these methods, green nanoparticles and composites produced by the use of biomass are relatively new and environmentally green adsorbents that have demonstrated great potential for removing many kinds of pollutants [303]. Leaf biomass of *S. ravannae, S. officinarum,* and *O. sativa* has been successfully used to fabricate silica nanoparticles for the adsorption of Pb^{2+} and Cu^{2+}ions from aqueous solutions. Different parameters such as pH, adsorbent dose, contact time, initial metal ion concentration, and temperature were varied, and more than 95 percent of both metal ions were removed [304]. In another study conducted by Primo et al., a green method based on the synthesis of ZnO using aloe vera extract for the removal of Cu (II) was reported. The adsorption results showed that ZnO nanoparticles could efficiently remove heavy metal pollution from wastewaters [305]. Ebrahimian et al. studied the adsorption capacity of *Vitex agnus-castus*-mediated SnO_2 NPs against Co^{+2} from wastewaters. More than 94% of heavy cobalt ions were removed at 298 K after 60 min [306]. A detailed list of emerging pollutants along with the removal capacities of different biomass-synthesised NPs is summarized in Table 4. Several researchers have also attempted to remove antibiotics from polluted waters. Altaf and co-workers showed the feasibility of using greenly fabricated Fe_3O_4

Table 4
A list of some emerging pollutants along with the removal capacities of different biomass-synthesised NPs

Biomass/Green agent	Nanomaterial	Shape	Heavy metal/ Antibiotic/ pollutant	Efficiency/adsorption capacity	Ref.
Peanut skin	Fe	Spherical	Cr (VI)	100%	[56]
Abutilon indicum	MnO	Spherical	Cr (VI)	11.50%	[310]
Sphagneticola trilobata	ZnO	Irregular	Cr (VI)	80%	[311]
Catharanthus roseus	AgNPs and CuO—NPs	–	Cr and Cd	47.84% (Ag) and 5.68% (CuO)	[312]
Hevea brasiliensis	magnetite	–	Cd	37.03 mg g^{-1})	[313]
Aspergillus tubingensis	Fe_2O_3	Spherical	Pb, Ni, Cu, Zn	98.0037% of Pb (II), 96.4502% of Ni (II), 92.1984% of Cu (II), and 93.9913% of Zn (II)	[314]
Tridax plant	γ-Fe_2O_3	–	Pb, Cd	96% (Pb)	[315]
Punica granatum	Fe_3O_4	Rod shape	Pb (II)	46.18 mg/g	[316]
Pine tree leaves	ZnO/SnO_2	Spherical	Cu^{2+}, Pb^{2+} and Zn^{2+} ions	Cu^{2+} (38.92 mg g^{-1}), Pb^{2+} (117.16 mg g^{-1}) and Zn^{2+} (29.12 mg g^{-1})	[317]
Lemon extract	Au	Spherical, trigonal, hexagonal, trapezoidal, pentagonal, rectangular, small rod, and oval	Ni (II)	–	[318]
Trianthema portulacastrum and *Chenopodium quinoa*	TiO_2	–	Cd (II)	–	[319]
Ficus benjamina	Ag	–	Cd^{2+}	0.845 mg/g	[320]
S. oneidensis	Pd	Spherical	Cr (VI)	200 mg/L	[321]
Syzygium cumini	TiO_2	Spherical	Pb (II)	82.53%	[322]
Citrus limon	Fe_3O_4	–	Pb (II), Cd (II), and As (III)	98.8 ± 5.6, 46.0 ± 1.3, and 48.2 ± 2.6%	[323]
Mint leaves and orange peels	CuO	Spherical	Pb (II), Ni (II), and Cd (II)	88.80, 54.90, and 15.60 mg g^{-1} for Pb (II), Ni (II), and Cd (II).	[324]
Bamboo	SiO_2	Spherical	Cu^{2+}	121.95 mg/g	[325]
Phoenix dactylifera	FeS	Spherical	Ciprofloxacin and Cr (VI)	7.69 mg g^{-1} and 8.50 mg g^{-1}	[326]
Punica granatum	NiFe	–	Tetracycline	77 ± 1.12	[327]
Green tea	Fe	–	Pb (II) and rifampicin	100% and 91.6%	[328]
Pseudomonas aeruginosa	ZrO_2	Spherical	Tetracycline	526.32 mg/g	[329]
Excoecaria cochinchinensis	Fe_3O_4	Spherical	Rifampicin	98.4%	[330]
Moringa olifera	Fe_3O_4	Irregular, polyhedral and spherical	Levofloxacin	86.15%	[307]
Monsonia burkeana	$ZnFe_2O_4$	Spherical and rod	Sulfisoxazole	67%	[331]
banana peels	ZnO	Spherical	Amoxicillin	90%	[332]
Euphorbia polygonifolia	Fe_3O_4@CuO	–	Metronidazole, ciprofloxacin and cephalexin	89%, 94%, and 96%	[333]

nanoparticles from *Moringa olifera* extract for the removal of the antibiotic levofloxacin from wastewater [307]. The green synthesised Fe_3O_4 nanoparticles displayed better results than chemically synthesized ones, with a maximum adsorption capacity of 22.47 mg/g. *Ari et al.* [308] published a study on the degradation of tetracycline using -Fe_2O_3 synthesized from *Azadirachta indica* leaf extract. Their results showed that the catalyst can be used over a wide pH range with a reusability up to five cycles. Gopal et al. [309] discovered that bimetallic Fe/Pd nanocomposite synthesised by biomolecules from pomegranate peel extract removed more than 80% of tetracycline antibiotic. It can be concluded that exploring more cost-effective sources and with a deeper understanding of the green synthesis of NPs, it is anticipated that this technology could be operated at a pilot scale for the removal of emerging pollutants in the near future.

7. Conclusion and future prospects

The presence of various organic and inorganic pollutants, including dyes and heavy metals, in the effluents from industrial activities has been considered an important environmental issue with numerous ecotoxicological and health implications. Most biological wastewater treatment systems are not capable of treating such effluents, and hence there has been a trend in the literature for the development of feasible physico-chemical treatment technologies such as advanced oxidation processes (AOPs). Photocatalysis has received enormous attention but is still suffering from technical, environmental, and economic issues preventing its rapid commercialization. Green synthesis of nanomaterials, including metal oxides, has been an approach to minimising the possible environmental impacts of the precursors and methods used for the fabrication of nanostructured materials. In this regard, biosynthesis has been considered a means of meeting such needs, and several natural sources, such as plant components (leaves, roots, seeds, fruits, etc.) and microorganisms (bacteria, fungi, algae, etc.), have been extensively used for the synthesis of various metal (Ag, Cu, Au, Fe, etc.) and metal oxide (ZnO, CuO, MgO, FeO, etc.) nanoparticles. Amongst all biological sources, plant extracts are mostly used for the synthesis owing to their excellent reducing and stabilising activities towards the precise control of the size, shape, crystallinity, and other specific features of the nanomaterials. These nanomaterials are nowadays excellent candidates to protect aquatic systems from different unwanted wastes like heavy metals, organic compounds, fertilizers, industrial effluents, etc. Greenly synthesised nanoparticles have a higher surface-to-volume ratio, higher surface energy, greater biocompatibility, and higher chemical reactivity, which make them suitable for different applications. Biosynthesis can considerably help in the fabrication of sustainable materials. However, there are research gaps that need more attention. Economic analysis is required to identify key areas that can help reduce the fabrication costs of nanomaterials. Furthermore, the potential advantages of such an approach to preventing the release of dangerous substances into the environment need to be investigated in future studies. There is also a need to study the applicability of such methods for the synthesis of structures capable of efficient separation of the photogenerated electrons and holes and the development of visible-light active materials. Other important areas that require the scientific community's attention include the standardisation of protocols for the green synthesis of photocatalytic materials and discovering the actual mechanism behind the green synthesis of nanoparticles.

Funding

This research received no specific grant from any funding agency in the public, commercial, or not-for-profit sectors.

Declaration of Competing Interest

The authors declare that they have no known competing financial interests or personal relationships that could have appeared to influence the work reported in this paper.

Data availability

No data was used for the research described in the article.

References

[1] P. Rani, V. Kumar, P.P. Singh, A.S. Matharu, W. Zhang, K.H. Kim, J. Singh, M. Rawat, Highly stable AgNPs prepared via a novel green approach for catalytic and photocatalytic removal of biological and non-biological pollutants, Environ. Int. 143 (2020), 105924, https://doi.org/10.1016/j.envint.2020.105924.
[2] R.T. Kapoor, M.R. Salvadori, M. Rafatullah, M.R. Siddiqui, M.A. Khan, S. A. Alshareef, Exploration of microbial factories for synthesis of nanoparticles – a sustainable approach for bioremediation of environmental contaminants, Front. Microbiol. (2021) 12, https://doi.org/10.3389/fmicb.2021.658294.
[3] G. Sharma, N.D. Jasuja, M. Kumar, M.I. Ali, Biological synthesis of silver nanoparticles by cell-free extract of spirulina platensis, J. Nanotechnol. 2015 (2015), https://doi.org/10.1155/2015/132675.
[4] F. Ahmed, N. Arshi, M.S. Anwar, R. Danish, B.H. Koo, Quantum-confinement induced enhancement in photocatalytic properties of iron oxide nanoparticles prepared by Ionic liquid, Ceram. Int. 40 (2014) 15743–15751, https://doi.org/10.1016/j.ceramint.2014.07.098.
[5] T. Ahmed, S. Imdad, K. Yaldram, N.M. Butt, A. Pervez, Emerging nanotechnology-based methods for water purification: a review, Desalin. Water Treat. 52 (2014) 4089–4101, https://doi.org/10.1080/19443994.2013.801789.
[6] S.C. Kumari, V. Dhand, P.N. Padma, Green synthesis of metallic nanoparticles: a review, Nanomaterials (2021) 259–281, https://doi.org/10.1016/b978-0-12-822401-4.00022-2.
[7] O.P. Bolade, A.B. Williams, N.U. Benson, Green synthesis of iron-based nanomaterials for environmental remediation: a review, Environ. Nanotechnol. Monit. Manag. (2020) 13, https://doi.org/10.1016/j.enmm.2019.100279.
[8] L. Fang, C. Xu, W. Zhang, L.Z. Huang, The important role of polyvinylpyrrolidone and Cu on enhancing dechlorination of 2,4-dichlorophenol by Cu/Fe nanoparticles: performance and mechanism study, Appl. Surf. Sci. 435 (2018) 55–64, https://doi.org/10.1016/j.apsusc.2017.11.084.
[9] D.C. Manatunga, R.M. de Silva, K.M.N. de Silva, N. de Silva, S. Bhandari, Y. K. Yap, N.P. Costha, pH responsive controlled release of anti-cancer hydrophobic drugs from sodium alginate and hydroxyapatite bi-coated iron oxide nanoparticles, Eur. J. Pharm. Biopharm. 117 (2017) 29–38, https://doi.org/10.1016/j.ejpb.2017.03.014.
[10] V. Arumugam, P. Sriram, T.J. Yen, G.G. Redhi, R.M. Gengan, Nano-material as an excellent catalyst for reducing a series of nitroanilines and dyes: triphosphonated ionic liquid- CuFe2O4-modified boron nitride, Appl. Catal. B Environ. 222 (2018) 99–114, https://doi.org/10.1016/j.apcatb.2017.08.059.
[11] E. Allard-Vannier, K. Hervé-Aubert, K. Kaaki, T. Blondy, A. Shebanova, K. V. Shaitan, A.A. Ignatova, M.L. Saboungi, A.V. Feofanov, I. Chourpa, Folic acid-capped PEGylated magnetic nanoparticles enter cancer cells mostly via clathrin-dependent endocytosis, Biochim. Biophys. Acta - Gen. Subj. 1861 (2017) 1578–1586, https://doi.org/10.1016/j.bbagen.2016.11.045.
[12] G. Kania, M. Sternak, A. Jasztal, S. Chlopicki, A. Błażejczyk, A. Nasulewicz-Goldeman, J. Wietrzyk, K. Jasiński, T. Skórka, S. Zapotoczny, M. Nowakowska, Uptake and bioreactivity of charged chitosan-coated superparamagnetic nanoparticles as promising contrast agents for magnetic resonance imaging, Nanomed. Nanotechnol. Biol. Med. 14 (2018) 131–140, https://doi.org/10.1016/j.nano.2017.09.004.
[13] L. Pereira, F. Mehboob, A.J.M. Stams, M.M. Mota, H.H.M. Rijnaarts, M.M. Alves, Metallic nanoparticles: microbial synthesis and unique properties for biotechnological applications, bioavailability and biotransformation, Crit. Rev. Biotechnol. 35 (2015) 114–128, https://doi.org/10.3109/07388551.2013.819484.
[14] J.R. Peralta-Videa, Y. Huang, J.G. Parsons, L. Zhao, L. Lopez-Moreno, J. A. Hernandez-Viezcas, J.L. Gardea-Torresdey, Plant-based green synthesis of metallic nanoparticles: scientific curiosity or a realistic alternative to chemical synthesis? Nanotechnol. Environ. Eng. 1 (2016) 1–29, https://doi.org/10.1007/s41204-016-0004-5.
[15] J. Jeevanandam, S.F. Kiew, S. Boakye-Ansah, S.Y. Lau, A. Barhoum, M. K. Danquah, J. Rodrigues, Green approaches for the synthesis of metal and metal oxide nanoparticles using microbial and plant extracts, Nanoscale 14 (2022) 2534–2571, https://doi.org/10.1039/d1nr08144f.
[16] A. Mohamed, E. Shafey, Shafey2020.Pdf, (2020) 304–339.
[17] S. Iravani, Green synthesis of metal nanoparticles using plants, Green Chem. 13 (2011) 2638–2650, https://doi.org/10.1039/c1gc15386b.
[18] K.M. Metz, S.E. Sanders, J.P. Pender, M.R. Dix, D.T. Hinds, S.J. Quinn, A.D. Ward, P. Duffy, R.J. Cullen, P.E. Colavita, Green synthesis of metal nanoparticles via natural extracts: the biogenic nanoparticle corona and its effects on reactivity, ACS Sustain. Chem. Eng. 3 (2015) 1610–1617, https://doi.org/10.1021/acssuschemeng.5b00304.
[19] A. Muthuvinothini, S. Stella, Green synthesis of metal oxide nanoparticles and their catalytic activity for the reduction of aldehydes, Process Biochem. 77 (2019) 48–56, https://doi.org/10.1016/j.procbio.2018.12.001.
[20] A.J. Kora, L. Rastogi, Green synthesis of palladium nanoparticles using gum ghatti (Anogeissus latifolia) and its application as an antioxidant and catalyst, Arab. J. Chem. 11 (2018) 1097–1106, https://doi.org/10.1016/j.arabjc.2015.06.024.
[21] J. Singh, T. Dutta, K.H. Kim, M. Rawat, P. Samddar, P. Kumar, Green" synthesis of metals and their oxide nanoparticles: applications for environmental remediation, J. Nanobiotechnol. 16 (2018) 1–24, https://doi.org/10.1186/s12951-018-0408-4.
[22] L. Salvioni, L. Morelli, E. Ochoa, M. Labra, L. Fiandra, L. Palugan, D. Prosperi, M. Colombo, The emerging role of nanotechnology in skincare, Adv. Colloid Interface Sci. 293 (2021), 102437, https://doi.org/10.1016/j.cis.2021.102437.
[23] A.C. Paiva-Santos, A.M. Herdade, C. Guerra, D. Peixoto, M. Pereira-Silva, M. Zeinali, F. Mascarenhas-Melo, A. Paranhos, F. Veiga, Plant-mediated green synthesis of metal-based nanoparticles for dermopharmaceutical and cosmetic applications, Int. J. Pharm. (2021) 597, https://doi.org/10.1016/j.ijpharm.2021.120311.
[24] S. Yesilot, C. Aydin, Silver nanoparticles; a new hope in cancer therapy? East. J. Med. 24 (2019) 111–116, https://doi.org/10.5505/ejm.2019.66487.
[25] S.D. Anderson, V.V. Gwenin, C.D. Gwenin, Magnetic functionalized nanoparticles for biomedical, drug delivery and imaging applications, Nanoscale Res. Lett. 14 (2019), https://doi.org/10.1186/s11671-019-3019-6.
[26] M. Mavaei, A. Chahardoli, Y. Shokoohinia, A. Khoshroo, A. Fattahi, One-step synthesized silver nanoparticles using isoimperatorin: evaluation of photocatalytic, and electrochemical activities, Sci. Rep. 10 (2020) 1–12, https://doi.org/10.1038/s41598-020-58697-x.
[27] H. Jahangirian, K. Kalantari, Z. Izadiyan, R. Rafiee-Moghaddam, K. Shameli, T. J. Webster, A review of small molecules and drug delivery applications using gold and iron nanoparticles, Int. J. Nanomed. 14 (2019) 1633–1657, https://doi.org/10.2147/IJN.S184723.
[28] J.A. Hernández-Díaz, J.J.O. Garza-García, A. Zamudio-Ojeda, J.M. León-Morales, J.C. López-Velázquez, S. García-Morales, Plant-mediated synthesis of nanoparticles and their antimicrobial activity against phytopathogens, J. Sci. Food Agric. 101 (2021) 1270–1287, https://doi.org/10.1002/jsfa.10767.
[29] M. Parmar, M. Sanyal, Extensive study on plant mediated green synthesis of metal nanoparticles and their application for degradation of cationic and anionic dyes, Environ. Nanotechnology, Monit. Manag. 17 (2022), 100624, https://doi.org/10.1016/j.enmm.2021.100624.
[30] A. Mukherjee, D. Sarkar, S. Sasmal, A review of green synthesis of metal nanoparticles using algae, Front. Microbiol. 12 (2021) 1–7, https://doi.org/10.3389/fmicb.2021.693899.
[31] E.R. Protima Rauwel, Siim Küünal, Stanislav Ferdov, a review on green synthesis of silver, Adv. Mater. Sci. Eng. 2015 (2014) 1–9.
[32] K.X. Lee, K. Shameli, Y.P. Yew, S.Y. Teow, H. Jahangirian, R. Rafiee-Moghaddam, T.J. Webster, Recent developments in the facile bio-synthesis of gold nanoparticles (AuNPs) and their biomedical applications, Int. J. Nanomed. 15 (2020) 275–300, https://doi.org/10.2147/IJN.S233789.
[33] H.A. Widatalla, L.F. Yassin, A.A. Alrasheid, S.A. Rahman Ahmed, M. O. Widdatallah, S.H. Eltilib, A.A. Mohamed, Green synthesis of silver nanoparticles using green tea leaf extract, characterization and evaluation of antimicrobial activity, Nanoscale Adv. 4 (2022) 911–915, https://doi.org/10.1039/d1na00509j.
[34] L. Xing, H. Zhang, R. Qi, R. Tsao, Y. Mine, Recent advances in the understanding of the health benefits and molecular mechanisms associated with green tea polyphenols, J. Agric. Food Chem. 67 (2019) 1029–1043, https://doi.org/10.1021/acs.jafc.8b06146.
[35] S. Sen, R. Chakraborty, Herbal medicine in India: indigenous knowledge, practice, innovation and its value, Herb. Med. India Indig. Knowledge, Pract. Innov. Its Value. (2019) 1–620, https://doi.org/10.1007/978-981-13-7248-3.
[36] Farshori, (n.d.).
[37] A.M. Adeosun, S.O. Oni, O.M. Ighodaro, O.H. Durosinlorun, O.M. Oyedele, Phytochemical, minerals and free radical scavenging profiles of Phoenix dactilyfera L. seed extract, J. Taibah Univ. Med. Sci. 11 (2016) 1–6, https://doi.org/10.1016/j.jtumed.2015.11.006.
[38] E. dine T. Bouhlali, C. Alem, J. Ennassir, M. Benlyas, A.N. Mbark, Y.F. Zegzouti, Phytochemical compositions and antioxidant capacity of three date (Phoenix dactylifera L.) seeds varieties grown in the South East Morocco, J. Saudi Soc. Agric. Sci. 16 (2017) 350–357, https://doi.org/10.1016/j.jssas.2015.11.002.
[39] Y.S. Liu, Y.C. Chang, H.H. Chen, Silver nanoparticle biosynthesis by using phenolic acids in rice husk extract as reducing agents and dispersants, J. Food Drug Anal. 26 (2018) 649–656, https://doi.org/10.1016/j.jfda.2017.07.005.
[40] J. Kesharwani, K.Y. Yoon, J. Hwang, M. Rai, Phytofabrication of silver nanoparticles by leaf extract of Datura metel: hypothetical mechanism involved in synthesis, J. Bionanosci. 3 (2009) 39–44, https://doi.org/10.1166/jbns.2009.1008.
[41] D. Kumar, P. Kumar, K. Vikram, H. Singh, Fabrication and characterization of noble crystalline silver nanoparticles from Pimenta dioica leave extract and

analysis of chemical constituents for larvicidal applications, Saudi J. Biol. Sci. 29 (2022) 1134–1146, https://doi.org/10.1016/j.sjbs.2021.09.052.
[42] S. Küünal, P. Rauwel, E. Rauwel, Plant Extract Mediated Synthesis of Nanoparticles, Elsevier Inc., 2018, https://doi.org/10.1016/B978-0-323-51254-1.00014-2.
[43] M.K. Ghosh, S. Sahu, I. Gupta, T.K. Ghorai, Green synthesis of copper nanoparticles from an extract ofJatropha curcasleaves: characterization, optical properties, CT-DNA binding and photocatalytic activity, RSC Adv. 10 (2020) 22027–22035, https://doi.org/10.1039/d0ra03186k.
[44] S.C. Mali, A. Dhaka, C.K. Githala, R. Trivedi, Green synthesis of copper nanoparticles using Celastrus paniculatus Willd. leaf extract and their photocatalytic and antifungal properties, Biotechnol. Reports. 27 (2020) e00518, https://doi.org/10.1016/j.btre.2020.e00518.
[45] A. Akturk, F.K. Güler, M.E. Taygun, G. Goller, S. Küçükbayrak, Synthesis and antifungal activity of soluble starch and sodium alginate capped copper nanoparticles, Mater. Res. Express. 6 (2019), https://doi.org/10.1088/2053-1591/ab677e.
[46] A. Nieto-Maldonado, S. Bustos-Guadarrama, H. Espinoza-Gomez, L.Z. Flores-López, K. Ramirez-Acosta, G. Alonso-Nuñez, R.D. Cadena-Nava, Green synthesis of copper nanoparticles using different plant extracts and their antibacterial activity, J. Environ. Chem. Eng. (2022) 10, https://doi.org/10.1016/j.jece.2022.107130.
[47] E. Rodríguez-León, B.E. Rodríguez-Vázquez, A. Martínez-Higuera, C. Rodríguez-Beas, E. Larios-Rodríguez, R.E. Navarro, R. López-Esparza, R.A. Iñiguez-Palomares, Synthesis of gold nanoparticles using mimosa tenuiflora extract, assessments of cytotoxicity, cellular uptake, and catalysis, Nanoscale Res. Lett. 14 (2019), https://doi.org/10.1186/s11671-019-3158-9.
[48] G. Erkan, K. Şengül, S. Kaya, Dyeing of white and indigo dyed cotton fabrics with Mimosa tenuiflora extract, J. Saudi Chem. Soc. 18 (2014) 139–148, https://doi.org/10.1016/j.jscs.2011.06.001.
[49] O.M. El-Borady, M.S. Ayat, M.A. Shabrawy, P. Millet, Green synthesis of gold nanoparticles using Parsley leaves extract and their applications as an alternative catalytic, antioxidant, anticancer, and antibacterial agents, Adv. Powder Technol. 31 (2020) 4390–4400, https://doi.org/10.1016/j.apt.2020.09.017.
[50] M.H. Farzaei, Z. Abbasabadi, M.R.S. Ardekani, R. Rahimi, F. Farzaei, Parsley: a review of ethnopharmacology, phytochemistry and biological activities, J. Tradit. Chinese Med. 33 (2013) 815–826, https://doi.org/10.1016/s0254-6272(14)60018-2.
[51] A.K. Singh, O.N. Srivastava, One-step green synthesis of gold nanoparticles using black cardamom and effect of pH on its synthesis, Nanoscale Res. Lett. (2015) 10, https://doi.org/10.1186/s11671-015-1055-4.
[52] K.N. Gurudutt, J.P. Naik, P. Srinivas, B. Ravindranath, Volatile constituents of large cardamom (Amomum subulatum Roxb, Flavour Fragr. J. 11 (1996) 7–9, https://doi.org/10.1002/(SICI)1099-1026(199601)11:1<7::AID−FFJ542>3.0.CO;2-9.
[53] R. Khandanlou, V. Murthy, H. Wang, Gold nanoparticle-assisted enhancement in bioactive properties of Australian native plant extracts, Tasmannia lanceolata and Backhousia citriodora, Mater. Sci. Eng. C. 112 (2020), 110922, https://doi.org/10.1016/j.msec.2020.110922.
[54] A. Roy, V. Singh, S. Sharma, D. Ali, A.K. Azad, G. Kumar, T. Bin Emran, Antibacterial and dye degradation activity of green synthesized iron nanoparticles, J. Nanomater. 2022 (2022), https://doi.org/10.1155/2022/3636481.
[55] S. Perveen, R. Nadeem, S. ur Rehman, N. Afzal, S. Anjum, S. Noreen, R. Saeed, M. Amami, S.H. Al-Mijalli, M. Iqbal, Green synthesis of iron (Fe) nanoparticles using Plumeria obtusa extract as a reducing and stabilizing agent: antimicrobial, antioxidant and biocompatibility studies, Arab. J. Chem. 15 (2022), 103764, https://doi.org/10.1016/j.arabjc.2022.103764.
[56] Z. Pan, Y. Lin, B. Sarkar, G. Owens, Z. Chen, Green synthesis of iron nanoparticles using red peanut skin extract: synthesis mechanism, characterization and effect of conditions on chromium removal, J. Colloid Interface Sci. 558 (2019) 106–114, https://doi.org/10.1016/j.jcis.2019.09.106.
[57] Z. Wu, X. Su, Z. Lin, N.I. Khan, G. Owens, Z. Chen, Removal of As(V) by iron-based nanoparticles synthesized via the complexation of biomolecules in green tea extracts and an iron salt, Sci. Total Environ. 764 (2021), 142883, https://doi.org/10.1016/j.scitotenv.2020.142883.
[58] Z.P. Qiao, M.Y. Wang, J.F. Liu, Q.Z. Wang, Green synthesis of silver nanoparticles using a novel endophytic fungus Letendraea sp. WZ07: characterization and evaluation of antioxidant, antibacterial and catalytic activities (3-in-1 system), Inorg. Chem. Commun. 138 (2022), 109301, https://doi.org/10.1016/j.inoche.2022.109301.
[59] N. Durán, P.D. Marcato, O.L. Alves, G.I.H. De Souza, E. Esposito, Mechanistic aspects of biosynthesis of silver nanoparticles by several Fusarium oxysporum strains, J. Nanobiotechnol. 3 (2005) 1–7, https://doi.org/10.1186/1477-3155-3-8.
[60] R.L. Kimber, E.A. Lewis, F. Parmeggiani, K. Smith, H. Bagshaw, T. Starborg, N. Joshi, A.I. Figueroa, G. van der Laan, G. Cibin, D. Gianolio, S.J. Haigh, R.A. D. Pattrick, N.J. Turner, J.R. Lloyd, Biosynthesis and characterization of copper nanoparticles using shewanella oneidensis: application for click chemistry, Small 14 (2018) 1–8, https://doi.org/10.1002/smll.201703145.
[61] F. Ahmadi-Nouraldinvand, M. Afrouz, S.G. Elias, S. Eslamian, Green synthesis of copper nanoparticles extracted from guar seedling under Cu heavy-metal stress by Trichoderma harzianum and their bio-efficacy evaluation against Staphylococcus aureus and Escherichia coli, Environ. Earth Sci. 81 (2022) 1–10, https://doi.org/10.1007/s12665-022-10184-4.
[62] M.H. Moaz-microhotmailcom, Biosynthesis of copper oxide nanoparticles by marine streptomyces MHM38 and their preventive E cacy against paracetamol-inducing hepatic damage of albino rats, (2021) 1–16.
[63] M.P. Patil, M. jae Kang, I. Niyonizigiye, A. Singh, J.O. Kim, Y.B. Seo, G. Do Kim, Extracellular synthesis of gold nanoparticles using the marine bacterium Paracoccus haeundaensis BC74171T and evaluation of their antioxidant activity and antiproliferative effect on normal and cancer cell lines, Colloids Surfaces B Biointerfaces 183 (2019), 110455, https://doi.org/10.1016/j.colsurfb.2019.110455.
[64] M. Gholami-Shabani, M. Shams-Ghahfarokhi, Z. Gholami-Shabani, A. Akbarzadeh, G. Riazi, S. Ajdari, A. Amani, M. Razzaghi-Abyaneh, Enzymatic synthesis of gold nanoparticles using sulfite reductase purified from Escherichia coli: a green eco-friendly approach, Process Biochem. 50 (2015) 1076–1085, https://doi.org/10.1016/j.procbio.2015.04.004.
[65] D.A. Lomelí-Rosales, A. Zamudio-Ojeda, O.K. Reyes-Maldonado, M.E. López-Reyes, G.C. Basulto-Padilla, E.J. Lopez-Naranjo, V.M. Zuñiga-Mayo, G. Velázquez-Juárez, Green synthesis of gold and silver nanoparticles using leaf extract of capsicum Chinense plant, Molecules (2022) 27, https://doi.org/10.3390/molecules27051692.
[66] M. Oves, M. Ahmar Rauf, M. Aslam, H.A. Qari, H. Sonbol, I. Ahmad, G. Sarwar Zaman, M. Saeed, Green synthesis of silver nanoparticles by Conocarpus Lancifolius plant extract and their antimicrobial and anticancer activities, Saudi J. Biol. Sci. 29 (2022) 460–471, https://doi.org/10.1016/j.sjbs.2021.09.007.
[67] A. Chakravarty, I. Ahmad, P. Singh, M. Ud Din Sheikh, G. Aalam, S. Sagadevan, S. Ikram, Green synthesis of silver nanoparticles using fruits extracts of Syzygium cumini and their bioactivity, Chem. Phys. Lett. 795 (2022), 139493, https://doi.org/10.1016/j.cplett.2022.139493.
[68] M. Binsalah, S. Devanesan, M.S. Alsalhi, A. Nooh, O. Alghamdi, N. Nooh, Biomimetic Synthesis of Silver Nanoparticles Using Ethyl Acetate Extract of Urtica diocia Leaves, Characterizations and Emerging Antimicrobial Activity (2022).
[69] L.N. Khanal, K.R. Sharma, H. Paudyal, K. Parajuli, B. Dahal, G.C. Ganga, Y. R. Pokharel, S.K. Kalauni, Green synthesis of silver nanoparticles from root extracts of rubus ellipticus sm. and comparison of antioxidant and antibacterial activity, J. Nanomater. 2022 (2022) 1–11, https://doi.org/10.1155/2022/1832587.
[70] S.N.H. Azmi, B.M.H. Al-Jassasi, H.M.S. Al-Sawafi, S.H.G. Al-Shukaili, N. Rahman, M. Nasir, Optimization for synthesis of silver nanoparticles through response surface methodology using leaf extract of Boswellia sacra and its application in antimicrobial activity, Environ. Monit. Assess. 193 (2021), https://doi.org/10.1007/s10661-021-09301-w.
[71] M. Narayanan, S. Divya, D. Natarajan, S. Senthil-Nathan, S. Kandasamy, A. Chinnathambi, T.A. Alahmadi, A. Pugazhendhi, Green synthesis of silver nanoparticles from aqueous extract of Ctenolepis garcini L. and assess their possible biological applications, Process Biochem. 107 (2021) 91–99, https://doi.org/10.1016/j.procbio.2021.05.008.
[72] K. Chandhirasekar, A. Thendralmanikandan, P. Thangavelu, B.S. Nguyen, T. A. Nguyen, K. Sivashanmugan, A. Nareshkumar, V.H. Nguyen, Plant-extract-assisted green synthesis and its larvicidal activities of silver nanoparticles using leaf extract of Citrus medica, Tagetes lemmonii, and Tarenna asiatica, Mater. Lett. 287 (2021), 129265, https://doi.org/10.1016/j.matlet.2020.129265.
[73] I. Jahan, F. Erci, I. Isildak, Facile microwave-mediated green synthesis of non-toxic copper nanoparticles using Citrus sinensis aqueous fruit extract and their antibacterial potentials, J. Drug Deliv. Sci. Technol. 61 (2021), 102172, https://doi.org/10.1016/j.jddst.2020.102172.
[74] K.R. Shubhashree, R. Reddy, A.K. Gangula, G.S. Nagananda, P.K. Badiya, S. S. Ramamurthy, P. Aramwit, N. Reddy, Green synthesis of copper nanoparticles using aqueous extracts from Hyptis suaveolens (L.), Mater. Chem. Phys. 280 (2022), 125795, https://doi.org/10.1016/j.matchemphys.2022.125795.
[75] G. Wang, K. Zhao, C. Gao, J. Wang, Y. Mei, X. Zheng, P. Zhu, Green synthesis of copper nanoparticles using green coffee bean and their applications for efficient reduction of organic dyes, J. Environ. Chem. Eng. 9 (2021), 105331, https://doi.org/10.1016/j.jece.2021.105331.
[76] Z. Dashtizadeh, F. Jookar Kashi, M. Ashrafi, Phytosynthesis of copper nanoparticles using Prunus mahaleb L. and its biological activity, Mater. Today Commun. 27 (2021), 102456, https://doi.org/10.1016/j.mtcomm.2021.102456.
[77] V. Gopalakrishnan, S. Muniraj, Neem flower extract assisted green synthesis of copper nanoparticles - Optimisation, characterisation and anti-bacterial study, Mater. Today Proc. 36 (2019) 832–836, https://doi.org/10.1016/j.matpr.2020.07.013.
[78] C. Krishnaraj, G.M. Young, S. Il Yun, In vitro embryotoxicity and mode of antibacterial mechanistic study of gold and copper nanoparticles synthesized from Angelica keiskei (Miq.) Koidz. leaves extract, Saudi J. Biol. Sci. 29 (2022) 2552–2563, https://doi.org/10.1016/j.sjbs.2021.12.039.
[79] M.A.A. Al-Khafaji, R.A.K. Al-Refai'a, O.M.Y. Al-Zamely, Green synthesis of copper nanoparticles using artemisia plant extract, Mater, Today Proc. 49 (2021) 2831–2835, https://doi.org/10.1016/j.matpr.2021.10.067.
[80] J. Vardhana, R. Sivasankaran, T.R. Ramkumar, J. Anitha, Biogenic synthesis of copper nanoparticles using Vitis vinifera L. seed extract, and its in-vitro biological applications, J. Plant Biochem. Biotechnol. 5 (2022), https://doi.org/10.1007/s13562-022-00766-5.
[81] N. Li, P.Thakur Saruchi, J. Pandey, V. Kumar, Controlled release of antibiotic cobex by biosynthesize copper nanoparticles using Osmium sanctum and its antibacterial activity, Mater. Lett. 312 (2022), 131666, https://doi.org/10.1016/j.matlet.2022.131666.

[82] L. Gao, S. Mei, H. Ma, X. Chen, Ultrasound-assisted green synthesis of gold nanoparticles using citrus peel extract and their enhanced anti-inflammatory activity, Ultrason. Sonochem. 83 (2022), 105940, https://doi.org/10.1016/j.ultsonch.2022.105940.
[83] T. Das, S. Mishra, S. Nag, K.Das Saha, Green-synthesized gold nanoparticles from black tea extract enhance the chemosensitivity of doxorubicin in HCT116 cells via a ROS-dependent pathway, RSC Adv. 12 (2022) 8996–9007, https://doi.org/10.1039/d1ra08374k.
[84] B. Zhu, N. Xie, L. Yue, K. Wang, M.Z. Bani-Fwaz, H.E. Hussein Osman, A.F. El-kott, X. Bai, Formulation and characterization of a novel anti-human endometrial cancer supplement by gold nanoparticles green-synthesized using Spinacia oleracea L. Leaf aqueous extract, Arab. J. Chem. 15 (2022), 103576, https://doi.org/10.1016/j.arabjc.2021.103576.
[85] G. Suriyakala, S. Sathiyaraj, R. Babujanarthanam, K.M. Alarjani, D.S. Hussein, R. A. Rasheed, K. Kanimozhi, Green synthesis of gold nanoparticles using Jatropha integerrima Jacq. flower extract and their antibacterial activity, J. King Saud Univ. - Sci. 34 (2022), 101830, https://doi.org/10.1016/j.jksus.2022.101830.
[86] G. Gnanamoorthy, K. Ramar, D. Ali, V.K. Yadav, A. Jafar ahamed, G. Kumar, Synthesis and effective performance of Photocatalytic and Antimicrobial activities of Bauhinia tomentosa Linn plants using of gold nanoparticles, Opt. Mater. (Amst). 123 (2022), 111945, https://doi.org/10.1016/j.optmat.2021.111945.
[87] S. Li, F.A. Al-Misned, H.A. El-Serehy, L. Yang, Green synthesis of gold nanoparticles using aqueous extract of Mentha Longifolia leaf and investigation of its anti-human breast carcinoma properties in the in vitro condition, Arab. J. Chem. 14 (2021), 102931, https://doi.org/10.1016/j.arabjc.2020.102931.
[88] O.T. Fanoro, S. Parani, R. Maluleke, T.C. Lebepe, J.R. Varghese, V. Mavumengwana, O.S. Oluwafemi, Facile green, room-temperature synthesis of gold nanoparticles using Combretum erythrophyllum leaf extract: antibacterial and cell viability studies against normal and cancerous cells, Antibiotics 10 (2021), https://doi.org/10.3390/antibiotics10080893.
[89] J. Chen, Y. Li, G. Fang, Z. Cao, Y. Shang, S. Alfarraj, S.Ali Alharbi, X. Duan, S. Yang, J. Li, Green synthesis, characterization, cytotoxicity, antioxidant, and anti-human ovarian cancer activities of Curcumae kwangsiensis leaf aqueous extract green-synthesized gold nanoparticles, Arab. J. Chem. 14 (2021), 103000, https://doi.org/10.1016/j.arabjc.2021.103000.
[90] M. Hosny, M. Fawzy, Instantaneous phytosynthesis of gold nanoparticles via Persicaria salicifolia leaf extract, and their medical applications, Adv. Powder Technol. 32 (2021) 2891–2904, https://doi.org/10.1016/j.apt.2021.06.004.
[91] M. Hosny, M. Fawzy, O.M. El-Borady, A.E.D. Mahmoud, Comparative study between Phragmites australis root and rhizome extracts for mediating gold nanoparticles synthesis and their medical and environmental applications, Adv. Powder Technol. 32 (7) (2021) 2268–2279.
[92] S.A. Akintelu, S.C. Olugbeko, A.S. Folorunso, Green synthesis, characterization, and antifungal activity of synthesized silver nanoparticles (AgNPS) from Garcinia Kola Pulp extract, Bionanoscience 12 (2022) 105–115, https://doi.org/10.1007/s12668-021-00925-3.
[93] M. Wang, Y. Meng, H. Zhu, Y. Hu, C.P. Xu, X. Chao, W. Li, C. Li, C. Pan, Green synthesized gold nanoparticles using viola betonicifolia leaves extract: characterization, antimicrobial, antioxidant, and cytobiocompatible activities, Int. J. Nanomed. 16 (2021) 7319–7337, https://doi.org/10.2147/IJN.S323524.
[94] A. Mishra, S.K. Tripathy, R. Wahab, S.H. Jeong, I. Hwang, Y.B. Yang, Y.S. Kim, H. S. Shin, S. Il Yun, Microbial synthesis of gold nanoparticles using the fungus Penicillium brevicompactum and their cytotoxic effects against mouse mayo blast cancer C 2C 12 cells, Appl. Microbiol. Biotechnol. 92 (2011) 617–630, https://doi.org/10.1007/s00253-011-3556-0.
[95] F. Ameen, K.S. Al-Maary, A. Almansob, S. AlNadhari, Antioxidant, antibacterial and anticancer efficacy of Alternaria chlamydospora-mediated gold nanoparticles, Appl. Nanosci. (2022), https://doi.org/10.1007/s13204-021-02047-4.
[96] G.M. de França Bettencourt, J. Degenhardt, L.A. Zevallos Torres, V.O. de Andrade Tanobe, C.R. Soccol, Green biosynthesis of single and bimetallic nanoparticles of iron and manganese using bacterial auxin complex to act as plant bio-fertilizer, Biocatal. Agric. Biotechnol. 30 (2020), 101822, https://doi.org/10.1016/j.bcab.2020.101822.
[97] Y. Vitta, M. Figueroa, M. Calderon, C. Ciangherotti, Synthesis of iron nanoparticles from aqueous extract of Eucalyptus robusta Sm and evaluation of antioxidant and antimicrobial activity, Mater. Sci. Energy Technol. 3 (2020) 97–103, https://doi.org/10.1016/j.mset.2019.10.014.
[98] M. Naseer, U. Aslam, B. Khalid, B. Chen, Green route to synthesize zinc oxide nanoparticles using leaf extracts of Cassia fistula and Melia azadarach and their antibacterial potential, Sci. Rep. 10 (2020) 1–10, https://doi.org/10.1038/s41598-020-65949-3.
[99] M.G. Demissie, F.K. Sabir, G.D. Edossa, B.A. Gonfa, Synthesis of zinc oxide nanoparticles using leaf extract of lippia adoensis (Koseret) and evaluation of its antibacterial activity, J. Chem. (2020) 2020, https://doi.org/10.1155/2020/7459042.
[100] A. Jayachandran, T.R. Aswathy, A.S. Nair, Green synthesis and characterization of zinc oxide nanoparticles using Cayratia pedata leaf extract, Biochem. Biophys. Reports. 26 (2021), 100995, https://doi.org/10.1016/j.bbrep.2021.100995.
[101] H. Veisi, B. Karmakar, T. Tamoradi, S. Hemmati, M. Hekmati, M. Hamelian, Biosynthesis of CuO nanoparticles using aqueous extract of herbal tea (Stachys Lavandulifolia) flowers and evaluation of its catalytic activity, Sci. Rep. 11 (2021) 1–13, https://doi.org/10.1038/s41598-021-81320-6.
[102] S. Sukumar, A. Rudrasenan, D.Padmanabhan Nambiar, Green-synthesized rice-shaped copper oxide nanoparticles using caesalpinia bonducella seed extract and their applications, ACS Omega 5 (2020) 1040–1051, https://doi.org/10.1021/acsomega.9b02857.
[103] M. Rafique, R. Tahir, S.S.A. Gillani, M.B. Tahir, M. Shakil, T. Iqbal, M. O. Abdellahi, Plant-mediated green synthesis of zinc oxide nanoparticles from Syzygium Cumini for seed germination and wastewater purification, Int. J. Environ. Anal. Chem. 102 (2022) 23–38, https://doi.org/10.1080/03067319.2020.1715379.
[104] H.M. Abdelmigid, N.A. Hussien, A.A. Alyamani, M.M. Morsi, N.M. Alsufyani, H. A. Kadi, Green synthesis of zinc oxide nanoparticles using pomegranate fruit peel and solid coffee grounds vs. chemical method of synthesis, with their biocompatibility and antibacterial properties investigation, Molecules 27 (2022), https://doi.org/10.3390/molecules27041236.
[105] P. Sharma, M. Urfan, R. Anand, M. Sangral, H.R. Hakla, S. Sharma, R. Das, S. Pal, M. Bhagat, Green synthesis of zinc oxide nanoparticles using Eucalyptus lanceolata leaf litter: characterization, antimicrobial and agricultural efficacy in maize, Physiol. Mol. Biol. Plants. 28 (2022) 363–381, https://doi.org/10.1007/s12298-022-01136-0.
[106] A. Annapoorani, A. Koodalingam, M. Beulaja, G. Saiprasad, P. Chitra, A. Stephen, S. Palanisamy, N.M. Prabhu, S.G. You, S. Janarthanan, R. Manikandan, Eco-friendly synthesis of zinc oxide nanoparticles using Rivina humilis leaf extract and their biomedical applications, Process Biochem 112 (2022) 192–202, https://doi.org/10.1016/j.procbio.2021.11.022.
[107] M. Irfan, H. Munir, H. Ismail, Characterization and fabrication of zinc oxide nanoparticles by gum Acacia modesta through green chemistry and impregnation on surgical sutures to boost up the wound healing process, Int. J. Biol. Macromol. 204 (2022) 466–475, https://doi.org/10.1016/j.ijbiomac.2022.02.043.
[108] A. Umamaheswari, S.L. Prabu, S.A. John, A. Puratchikody, Green synthesis of zinc oxide nanoparticles using leaf extracts of Raphanus sativus var. Longipinnatus and evaluation of their anticancer property in A549 cell lines, Biotechnol. Reports. 29 (2021) e00595, https://doi.org/10.1016/j.btre.2021.e00595.
[109] G. Sharmila, R. Sakthi Pradeep, K. Sandiya, S. Santhiya, C. Muthukumaran, J. Jeyanthi, N. Manoj Kumar, M. Thirumarimurugan, Biogenic synthesis of CuO nanoparticles using Bauhinia tomentosa leaves extract: characterization and its antibacterial application, J. Mol. Struct. 1165 (2018) 288–292, https://doi.org/10.1016/j.molstruc.2018.04.011.
[110] M.W. Shammout, A.M. Awwad, SSRN-id3865991, (2021) 71–78.
[111] A. Iqbal, A.U. Haq, G.A. Cerrón-Calle, S.A.R. Naqvi, P. Westerhoff, S. Garcia-Segura, Green synthesis of flower-shaped copper oxide and nickel oxide nanoparticles via capparis decidua leaf extract for synergic adsorption-photocatalytic degradation of pesticides, Catalysts 11 (2021), https://doi.org/10.3390/catal11070806.
[112] T.B. Vidovix, H.B. Quesada, R. Bergamasco, M.F. Vieira, A.M.S. Vieira, Adsorption of Safranin-O dye by copper oxide nanoparticles synthesized from Punica granatum leaf extract, Environ. Technol. (United Kingdom) 0 (2021) 1–17, https://doi.org/10.1080/09593330.2021.1914180.
[113] K. Selvam, G. Albasher, O. Alamri, C. Sudhakar, T. Selvankumar, S. Vijayalakshmi, L. Vennila, Enhanced photocatalytic activity of novel Canthium coromandelicum leaves based copper oxide nanoparticles for the degradation of textile dyes, Environ. Res. 211 (2022), 113046, https://doi.org/10.1016/j.envres.2022.113046.
[114] A. Vinothkanna, K. Mathivanan, S. Ananth, Y. Ma, S. Sekar, Biosynthesis of copper oxide nanoparticles using Rubia cordifolia bark extract: characterization, antibacterial, antioxidant, larvicidal and photocatalytic activities, Environ. Sci. Pollut. Res. (2022), https://doi.org/10.1007/s11356-022-18996-4.
[115] Y.O. Al-Ghamdi, M. Jabli, R. Soury, S.A. Khan, Synthesis of copper oxide nanoparticles using Pergularia tomentosa leaves and decolorization studies, Int. J. Phytoremediation. 24 (2022) 118–130, https://doi.org/10.1080/15226514.2021.1926914.
[116] M.S.H. Bhuiyan, M.Y. Miah, S.C. Paul, T. Das Aka, O. Saha, M.M. Rahaman, M.J. I. Sharif, O. Habiba, M. Ashaduzzaman, Green synthesis of iron oxide nanoparticle using Carica papaya leaf extract: application for photocatalytic degradation of remazol yellow RR dye and antibacterial activity, Heliyon 6 (2020) e04603, https://doi.org/10.1016/j.heliyon.2020.e04603.
[117] S. Lakshmnarayanan, M.F. Shereen, K.L. Niraimathi, P. Brindha, A. Arumugam, One-pot green synthesis of iron oxide nanoparticles from Bauhinia tomentosa: characterization and application towards synthesis of 1, 3 diolein, Sci. Rep. 11 (2021) 1–13, https://doi.org/10.1038/s41598-021-87960-y.
[118] I.Y. Younis, S.S. El-Hawary, O.A. Eldahshan, M.M. Abdel-Aziz, Z.Y. Ali, Green synthesis of magnesium nanoparticles mediated from Rosa floribunda charisma extract and its antioxidant, antiaging and antibiofilm activities, Sci. Rep. 11 (2021) 1–15, https://doi.org/10.1038/s41598-021-96377-6.
[119] E.R. Essien, V.N. Atasie, A.O. Okeafor, D.O. Nwude, Biogenic synthesis of magnesium oxide nanoparticles using Manihot esculenta (Crantz) leaf extract, Int, Nano Lett 10 (2020) 43–48, https://doi.org/10.1007/s40089-019-00290-w.
[120] H. Mohd Yusof, R. Mohamad, U.H. Zaidan, N.A. Rahman, Sustainable microbial cell nanofactory for zinc oxide nanoparticles production by zinc-tolerant probiotic Lactobacillus plantarum strain TA4, Microb. Cell Fact. 19 (2020) 1–17, https://doi.org/10.1186/s12934-020-1279-6.
[121] B. Sumanth, T.R. Lakshmeesha, M.A. Ansari, M.A. Alzohairy, A.C. Udayashankar, B. Shobha, S.R. Niranjana, C. Srinivas, A. Almatroudi, Mycogenic synthesis of extracellular zinc oxide nanoparticles from xylaria acuta and its nanoantibiotic potential, Int. J. Nanomedicine. 15 (2020) 8519–8536, https://doi.org/10.2147/IJN.S271743.
[122] V. Ganesan, M. Hariram, S. Vivekanandhan, S. Muthuramkumar, Periconium sp. (endophytic fungi) extract mediated sol-gel synthesis of ZnO nanoparticles for

antimicrobial and antioxidant applications, Mater. Sci. Semicond. Process. 105 (2020), 104739, https://doi.org/10.1016/j.mssp.2019.104739.
[123] S.I. Bukhari, M.M. Hamed, M.H. Al-Agamy, H.S.S. Gazwi, H.H. Radwan, A. M. Youssif, Biosynthesis of copper oxide nanoparticles using streptomyces MHM38 and its biological applications, J. Nanomater. (2021) 2021, https://doi.org/10.1155/2021/6693302.
[124] M. Kouhkan, P. Ahangar, L.A. Babaganjeh, M. Allahyari-Devin, Biosynthesis of copper oxide nanoparticles using lactobacillus casei subsp. Casei and its anticancer and antibacterial activities, Curr. Nanosci. 16 (2019) 101–111, https://doi.org/10.2174/1573413715666190318155801.
[125] A.I. El-Batal, G.S. El-Sayyad, F.M. Mosallam, R.M. Fathy, Penicillium chrysogenum-mediated mycogenic synthesis of copper oxide nanoparticles using gamma rays for in vitro antimicrobial activity against some plant pathogens, J. Clust. Sci. 31 (2020) 79–90, https://doi.org/10.1007/s10876-019-01619-3.
[126] K. Saravanakumar, S. Shanmugam, N.B. Varukattu, D. MubarakAli, K. Kathiresan, M.H. Wang, Biosynthesis and characterization of copper oxide nanoparticles from indigenous fungi and its effect of photothermolysis on human lung carcinoma, J. Photochem. Photobiol. B Biol. 190 (2019) 103–109, https://doi.org/10.1016/j.jphotobiol.2018.11.017.
[127] S. Majeed, M. Danish, M.N. Mohamad Ibrahim, S.H. Sekeri, M.T. Ansari, A. Nanda, G. Ahmad, Bacteria mediated synthesis of iron oxide nanoparticles and their antibacterial, antioxidant, cytocompatibility properties, J. Clust. Sci. 32 (2021) 1083–1094, https://doi.org/10.1007/s10876-020-01876-7.
[128] A.A. Khan, S. Khan, S. Khan, S. Rentschler, S. Laufer, H.P. Deigner, Biosynthesis of iron oxide magnetic nanoparticles using clinically isolated Pseudomonas aeruginosa, Sci. Rep. 11 (2021) 1–10, https://doi.org/10.1038/s41598-021-99814-8.
[129] S. Chatterjee, D. Lee, S.W. Lee, MW, Enhanced adsorption of congo red from aqueous solutions by chitosan hydrogel beads impregnated with cetyl trimethyl ammonium bromide, Bioresour. Technol. J. 100 (2009) 2803–2809. https://www.sciencedirect.com/science/article/pii/S0960852408010936 (accessed December 12, 2020).
[130] M.S. Enayati, T. Behzad, P. Sajkiewicz, M. Rafienia, R. Bagheri, L. Ghasemi-Mobarakeh, D. Kolbuk, Z. Pahlevanneshan, S.H. Bonakdar, Development of electrospun poly (vinyl alcohol)-based bionanocomposite scaffolds for bone tissue engineering, J. Biomed. Mater. Res. - Part A. 106 (2018) 1111–1120, https://doi.org/10.1002/jbm.a.36309.
[131] M.M. Abdel-Aziz, T.M. Emam, E.A. Elsherbiny, Bioactivity of magnesium oxide nanoparticles synthesized from cell filtrate of endobacterium Burkholderia rinojensis against Fusarium oxysporum, Mater. Sci. Eng. C. 109 (2020), 110617, https://doi.org/10.1016/j.msec.2019.110617.
[132] A. Pugazhendhi, R. Prabhu, K. Muruganantham, R. Shanmuganathan, S. Natarajan, Anticancer, antimicrobial and photocatalytic activities of green synthesized magnesium oxide nanoparticles (MgONPs) using aqueous extract of Sargassum wightii, J. Photochem. Photobiol. B Biol. 190 (2019) 86–97, https://doi.org/10.1016/j.jphotobiol.2018.11.014.
[133] K.S. Landage, C.J.B. Gajanan K Arbade, Pawan Khanna, Biological approach to synthesize TiO2 nanoparticles using Staphylococcus aureus for antibacterial and anti- biofilm applications, J. Microbiol. Exp. Res. 8 (2020) 36–43, https://doi.org/10.15406/jmen.2020.08.00283.
[134] G.K. Ağçeli, H. Hammachi, S.P. Kodal, N. Cihangir, Z. Aksu, A novel approach to synthesize tio2 nanoparticles: biosynthesis by using streptomyces sp. HC1, J. Inorg. Organomet. Polym. Mater. 30 (2020) 3221–3229, https://doi.org/10.1007/s10904-020-01486-w.
[135] M. Taran, M. Rad, M. Alavi, Biosynthesis of TiO2 and ZnO nanoparticles by Halomonas elongata IBRC-M 10214 in different conditions of medium, BioImpacts 8 (2018) 81–89, https://doi.org/10.15171/bi.2018.10.
[136] S.K. Bhanja, S.K. Samanta, B. Mondal, S. Jana, J. Ray, A. Pandey, T. Tripathy, Green synthesis of Ag@Au bimetallic composite nanoparticles using a polysaccharide extracted from Ramaria botrytis mushroom and performance in catalytic reduction of 4-nitrophenol and antioxidant, antibacterial activity, Environ, Nanotechnology, Monit. Manag. 14 (2020), 100341, https://doi.org/10.1016/j.enmm.2020.100341.
[137] W. Xiao, S. Li, S. Wang, C.T. Ho, Chemistry and bioactivity of Gardenia jasminoides, J. Food Drug Anal. 25 (2017) 43–61, https://doi.org/10.1016/j.jfda.2016.11.005.
[138] T. Riaz, P. Mughal, T. Shahzadi, S. Shahid, M.A. Abbasi, Green synthesis of silver nickel bimetallic nanoparticles using plant extract of Salvadora persica and evaluation of their various biological activities, Mater. Res. Express. 6 (2019), https://doi.org/10.1088/2053-1591/ab74fc.
[139] A.L. Padilla-Cruz, J.A. Garza-Cervantes, X.G. Vasto-Anzaldo, G. García-Rivas, A. León-Buitimea, J.R. Morones-Ramírez, Synthesis and design of Ag–Fe bimetallic nanoparticles as antimicrobial synergistic combination therapies against clinically relevant pathogens, Sci. Rep. 11 (2021) 1–10, https://doi.org/10.1038/s41598-021-84768-8.
[140] M.A. Malik, A.A. Alshehri, R. Patel, Facile one-pot green synthesis of Ag-Fe bimetallic nanoparticles and their catalytic capability for 4-nitrophenol reduction, J. Mater. Res. Technol. 12 (2021) 455–470, https://doi.org/10.1016/j.jmrt.2021.02.063.
[141] H. Wang, G.J. Provan, K. Helliwell, Determination of rosmarinic acid and caffeic acid in aromatic herbs by HPLC, Food Chem. 87 (2004) 307–311, https://doi.org/10.1016/j.foodchem.2003.12.029.
[142] H.J.D. Dorman, A. Peltoketo, R. Hiltunen, M.J. Tikkanen, Characterisation of the antioxidant properties of de-odourised aqueous extracts from selected Lamiaceae herbs, Food Chem. 83 (2003) 255–262, https://doi.org/10.1016/S0308-8146(03)00088-8.
[143] J. Al-Haddad, F. Alzaabi, P. Pal, K. Rambabu, F. Banat, Green synthesis of bimetallic copper–silver nanoparticles and their application in catalytic and antibacterial activities, Clean Technol. Environ. Policy. 22 (2020) 269–277, https://doi.org/10.1007/s10098-019-01765-2.
[144] X. Weng, M. Guo, F. Luo, Z. Chen, One-step green synthesis of bimetallic Fe/Ni nanoparticles by eucalyptus leaf extract: biomolecules identification, characterization and catalytic activity, Chem. Eng. J. 308 (2017) 904–911, https://doi.org/10.1016/j.cej.2016.09.134.
[145] Sunita Verma, Rajbala, Study on phytochemical and pharmacological activity of miswak tree salvadora persica (salvadoraceae), Int. J. Current Res. Modern Education 3 (2018) 11–14.
[146] A.A. Olajire, A.A. Mohammed, Green synthesis of bimetallic PdcoreAushell nanoparticles for enhanced solid-phase photodegradation of low-density polyethylene film, J. Mol. Struct. 1206 (2020), 127724, https://doi.org/10.1016/j.molstruc.2020.127724.
[147] W.P. Wicaksono, G.T.M. Kadja, D. Amalia, L. Uyun, W.P. Rini, A. Hidayat, R. L. Fahmi, D. Nasriyanti, S.G.V. Leun, H.A. Ariyanta, T.A. Ivandini, A green synthesis of gold–palladium core–shell nanoparticles using orange peel extract through two-step reduction method and its formaldehyde colorimetric sensing performance, Nano-Structures and Nano-Objects 24 (2020), 100535, https://doi.org/10.1016/j.nanoso.2020.100535.
[148] M. Nasrollahzadeh, Z. Issaabadi, S.M. Sajadi, Green synthesis of a Cu/MgO nanocomposite by: cassytha filiformis L. extract and investigation of its catalytic activity in the reduction of methylene blue, congo red and nitro compounds in aqueous media, RSC Adv. 8 (2018) 3723–3735, https://doi.org/10.1039/c7ra13491f.
[149] S. Kulkarni, M. Jadhav, P. Raikar, S. Raikar, U. Raikar, Core-shell novel composite metal nanoparticles for hydrogenation and dye degradation applications, Ind. Eng. Chem. Res. 58 (2019) 3630–3639, https://doi.org/10.1021/acs.iecr.8b06094.
[150] M.S. Alwhibi, K.M.O. Ortashi, A.A. Hendi, M.A. Awad, D.A. Soliman, M. El-Zaidy, Green synthesis, characterization and biomedical potential of Ag@Au core-shell noble metal nanoparticles, J. King Saud Univ. - Sci. 34 (2022), 102000, https://doi.org/10.1016/j.jksus.2022.102000.
[151] R.N.E. Tiri, F. Gulbagca, A. Aygun, A. Cherif, F. Sen, Biosynthesis of Ag–Pt bimetallic nanoparticles using propolis extract: antibacterial effects and catalytic activity on NaBH4 hydrolysis, Environ. Res. 206 (2022), 112622, https://doi.org/10.1016/j.envres.2021.112622.
[152] A. Tkaczyk, K. Mitrowska, A. Posyniak, Synthetic organic dyes as contaminants of the aquatic environment and their implications for ecosystems: a review, Sci. Total Environ. 717 (2020), 137222.
[153] S. Benkhaya, S. M' rabet, A. El Harfi, A review on classifications, recent synthesis and applications of textile dyes, Inorg. Chem. Commun. 115 (2020), 107891.
[154] S. Varjani, P. Rakholiya, H.Y. Ng, S. You, J.A. Teixeira, Microbial degradation of dyes: an overview, Bioresour. Technol. 314 (2020), 123728.
[155] T. Shindhal, P. Rakholiya, S. Varjani, A. Pandey, H.H. Ngo, W. Guo, H.Y. Ng, M. J. Taherzadeh, A critical review on advances in the practices and perspectives for the treatment of dye industry wastewater, Bioengineered 12 (1) (2021) 70–87.
[156] D. Nayeri, S.A. Mousavi, Dye removal from water and wastewater by nanosized metal oxides - modified activated carbon: a review on recent researches, J. Environ. Health Sci. Eng. 18 (2) (2020) 1671–1689.
[157] B.D. Deshpande, P.S. Agrawal, M.K.N. Yenkie, S.J. Dhoble, Prospective of nanotechnology in degradation of waste water: a new challenges, Nano-Structures & Nano-Objects 22 (2020), 100442.
[158] S. Cheriyamundath, S.L. Vavilala, Nanotechnol.-Based Wastewater Treatment 35 (1) (2021) 123–132.
[159] D. Hebbalalu, J. Lalley, M.N. Nadagouda, R.S. Varma, Greener techniques for the synthesis of silver nanoparticles using plant extracts, enzymes, bacteria, biodegradable polymers, and microwaves, ACS Sustain. Chem. Eng. 1 (7) (2013) 703–712.
[160] P.C. Nagajyothi, S.V. Prabhakar Vattikuti, K.C. Devarayapalli, K. Yoo, J. Shim, T. V.M. Sreekanth, Green synthesis: photocatalytic degradation of textile dyes using metal and metal oxide nanoparticles-latest trends and advancements, Crit. Rev. Environ. Sci. Technol. 50 (24) (2020) 2617–2723.
[161] A. Rana, K. Yadav, S. Jagadevan, A comprehensive review on green synthesis of nature-inspired metal nanoparticles: mechanism, application and toxicity, J. Clean. Prod. 272 (2020), 122880.
[162] A. Singh, P.K. Gautam, A. Verma, V. Singh, P.M. Shivapriya, S. Shivalkar, A. K. Sahoo, S.K. Samanta, Green synthesis of metallic nanoparticles as effective alternatives to treat antibiotics resistant bacterial infections: a review, Biotechnol. Reports 25 (2020) e00427.
[163] A. Gellé, G.D. Price, F. Voisard, N. Brodusch, R. Gauvin, Z. Amara, A. Moores, Enhancing Singlet Oxygen Photocatalysis with Plasmonic Nanoparticles, ACS Appl. Mater. Interfaces 13 (30) (2021) 35606–35616.
[164] G.K. Weldegebrieal, Synthesis method, antibacterial and photocatalytic activity of ZnO nanoparticles for azo dyes in wastewater treatment: a review, Inorg. Chem. Commun. 120 (2020), 108140.
[165] Z. Zhang, X. He, C. Zhou, M. Reaume, M. Wu, B. Liu, B.P. Lee, Iron magnetic nanoparticle-induced ros generation from catechol-containing microgel for environmental and biomedical applications, ACS Appl. Mater. Interfaces 12 (19) (2020) 21210–21220.
[166] J. Yu, A.C. Wang, M. Zhang, Z. Lin, Water treatment via non-membrane inorganic nanoparticles/cellulose composites, Mater. Today (2021).
[167] W.S. Koe, J.W. Lee, W.C. Chong, Y.L. Pang, L.C. Sim, An overview of photocatalytic degradation: photocatalysts, mechanisms, and development of photocatalytic membrane, Environ. Sci. Pollut. Res. 27 (3) (2020) 2522–2565.

[168] L.V. Bora, R.K. Mewada, Visible/solar light active photocatalysts for organic effluent treatment: fundamentals, mechanisms and parametric review, Renew. Sustain. Energy Rev. 76 (2017) 1393–1421.
[169] T. de Oliveira Guidolin, N.M. Possolli, M.B. Polla, T.B. Wermuth, T. Franco de Oliveira, S. Eller, O.R. Klegues Montedo, S. Arcaro, M.A.P. Cechinel, Photocatalytic pathway on the degradation of methylene blue from aqueous solutions using magnetite nanoparticles, J. Clean. Prod. 318 (2021), 128556.
[170] M.P. Ajith, M. Aswathi, E. Priyadarshini, P. Rajamani, Recent innovations of nanotechnology in water treatment: a comprehensive review, Bioresour. Technol. 342 (2021), 126000.
[171] M.A. Islam, M.V. Jacob, E. Antunes, A critical review on silver nanoparticles: from synthesis and applications to its mitigation through low-cost adsorption by biochar, J. Environ. Manag. 281 (2021), 111918.
[172] C.V. Restrepo, C.C. Villa, Synthesis of silver nanoparticles, influence of capping agents, and dependence on size and shape: a review, Environ. Nanotechnol. Monitoring & Manag. 15 (2021), 100428.
[173] L. Sherin, A. Sohail, U.-e.-S. Amjad, M. Mustafa, R. Jabeen, A. Ul-Hamid, Facile green synthesis of silver nanoparticles using Terminalia bellerica kernel extract for catalytic reduction of anthropogenic water pollutants, Colloid and Interface Sci. Commun. 37 (2020), 100276.
[174] M. Mavaei, A. Chahardoli, Y. Shokoohinia, A. Khoshroo, A. Fattahi, One-step synthesized silver nanoparticles using isoimperatorin: evaluation of photocatalytic, and electrochemical activities, Sci. Rep. 10 (1) (2020) 1762.
[175] E.F. Aboelfetoh, A.H. Gemeay, R.G. El-Sharkawy, Effective disposal of methylene blue using green immobilized silver nanoparticles on graphene oxide and reduced graphene oxide sheets through one-pot synthesis, Environ. Monit. Assess. 192 (6) (2020) 355.
[176] K. Varghese Alex, P. Tamil Pavai, R. Rugmini, M. Shiva Prasad, K. Kamakshi, K. C. Sekhar, Green synthesized Ag nanoparticles for bio-sensing and photocatalytic applications, ACS Omega 5 (22) (2020) 13123–13129.
[177] J.F. Li, Y.C. Liu, M. Chokkalingam, E.J. Rupa, R. Mathiyalagan, J. Hurh, J.C. Ahn, J.K. Park, J. Yu Pu, D.C. Yang, Phytosynthesis of silver nanoparticles using rhizome extract of Alpinia officinarum and their photocatalytic removal of dye under UV and visible light irradiation, Optik (Stuttg) 208 (2020), 164521.
[178] K. Muthu, S. Rajeswari, B. Akilandaeaswari, S.M. Nagasundari, R. Rangasamy, Synthesis, characterisation and photocatalytic activity of silver nanoparticles stabilised by Punica granatum seeds extract, Mater. Technol. 36 (11) (2021) 684–693.
[179] P. Rani, V. Kumar, P.P. Singh, A.S. Matharu, W. Zhang, K.-H. Kim, J. Singh, M. Rawat, Highly stable AgNPs prepared via a novel green approach for catalytic and photocatalytic removal of biological and non-biological pollutants, Environ. Int. 143 (2020), 105924.
[180] M.A. Awad, A. Hendi, K.M. Ortashi, B. Alzahrani, D. Soliman, A. Alanazi, W. Alenazi, R.M. Taha, R. Ramadan, M. El-Tohamy, N. AlMasoud, T.S. Alomar, Biogenic synthesis of silver nanoparticles using Trigonella foenum-graecum seed extract: characterization, photocatalytic and antibacterial activities, Sensors and Actuators A: Phys. 323 (2021), 112670.
[181] Á.d.J. Ruíz-Baltazar, Kinetic adsorption models of silver nanoparticles biosynthesized by Cnicus Benedictus: study of the photocatalytic degradation of methylene blue and antibacterial activity, Inorg. Chem. Commun. 120 (2020), 108158.
[182] V. Ravichandran, S. Vasanthi, S. Shalini, S.A.A. Shah, M. Tripathy, N. Paliwal, Green synthesis, characterization, antibacterial, antioxidant and photocatalytic activity of Parkia speciosa leaves extract mediated silver nanoparticles, Results in Phys. 15 (2019), 102565.
[183] A.C. Ekennia, D.N. Uduagwu, N.N. Nwaji, O.J. Olowu, O.L. Nwanji, M. Ejimofor, C.U. Sonde, O.O. Oje, D.O. Igwe, Green synthesis of silver nanoparticles using leaf extract of Euphorbia sanguine: an in vitro study of its photocatalytic and melanogenesis inhibition activity, Inorganic and Nano-Metal Chem. (2021) 1–9.
[184] V.-.D. Doan, M.-.T. Phung, T.L.-H. Nguyen, T.-.C. Mai, T.-.D. Nguyen, Noble metallic nanoparticles from waste Nypa fruticans fruit husk: biosynthesis, characterization, antibacterial activity and recyclable catalysis, Arabian J. Chem. 13 (10) (2020) 7490–7503.
[185] K. Chand, D. Cao, D. Eldin Fouad, A. Hussain Shah, A. Qadeer Dayo, K. Zhu, M. Nazim Lakhan, G. Mehdi, S. Dong, Green synthesis, characterization and photocatalytic application of silver nanoparticles synthesized by various plant extracts, Arabian J. Chem. 13 (11) (2020) 8248–8261.
[186] Z.U.H. Khan, N.S. Shah, J. Iqbal, A.U. Khan, M. Imran, S.M. Alshehri, N. Muhammad, M. Sayed, N. Ahmad, A. Kousar, M. Ashfaq, F. Howari, K. Tahir, Biomedical and photocatalytic applications of biosynthesized silver nanoparticles: ecotoxicology study of brilliant green dye and its mechanistic degradation pathways, J. Mol. Liq. 319 (2020), 114114.
[187] V. Seerangaraj, S. Sathiyavimal, S.N. Shankar, J.G.T. Nandagopal, P. Balashanmugam, F.A. Al-Misned, M. Shanmugavel, P. Senthilkumar, A. Pugazhendhi, Cytotoxic effects of silver nanoparticles on Ruellia tuberosa: photocatalytic degradation properties against crystal violet and coomassie brilliant blue, J. Environ. Chem. Eng. 9 (2) (2021), 105088.
[188] G.N. Rajivgandhi, M. Maruthupandy, J.-.L. Li, L. Dong, N.S. Alharbi, S. Kadaikunnan, J.M. Khaled, K.F. Alanzi, W.-.J. Li, Photocatalytic reduction and anti-bacterial activity of biosynthesized silver nanoparticles against multi drug resistant Staphylococcus saprophyticus BDUMS 5 (MN310601), Mater. Sci. Eng.: C 114 (2020), 111024.
[189] M.E. Taghavizadeh Yazdi, M. Darroudi, M.S. Amiri, H. Zarrinfar, H.A. Hosseini, M. Mashreghi, H. Mozafarri, A. Ghorbani, S.H. Mousavi, Antimycobacterial, anticancer, antioxidant and photocatalytic activity of biosynthesized silver nanoparticles using berberis integerrima, Iranian J. Sci. Technol. Trans. A: Sci. (2021).
[190] J. Kadam, P. Dhawal, S. Barve, S. Kakodkar, Green synthesis of silver nanoparticles using cauliflower waste and their multifaceted applications in photocatalytic degradation of methylene blue dye and Hg2+ biosensing, SN Appl. Sci. 2 (4) (2020) 738.
[191] H.M. Mehwish, M.S.R. Rajoka, Y. Xiong, H. Cai, R.M. Aadil, Q. Mahmood, Z. He, Q. Zhu, Green synthesis of a silver nanoparticle using Moringa oleifera seed and its applications for antimicrobial and sun-light mediated photocatalytic water detoxification, J. Environ. Chem. Eng. 9 (4) (2021), 105290.
[192] D.B. Manikandan, A. Sridhar, R. Krishnasamy Sekar, B. Perumalsamy, S. Veeran, M. Arumugam, P. Karuppaiah, T. Ramasamy, Green fabrication, characterization of silver nanoparticles using aqueous leaf extract of Ocimum americanum (Hoary Basil) and investigation of its in vitro antibacterial, antioxidant, anticancer and photocatalytic reduction, J. Environ. Chem. Eng. 9 (1) (2021), 104845.
[193] N. El-Desouky, K.R. Shoueir, I. El-Mehasseb, M. El-Kemary, Bio-inspired green manufacturing of plasmonic silver nanoparticles/Degussa using Banana Waste Peduncles: photocatalytic, antimicrobial, and cytotoxicity evaluation, J. Mater. Res. Technol. 10 (2021) 671–686.
[194] K. Chand, C. Jiao, M.N. Lakhan, A.H. Shah, V. Kumar, D.E. Fouad, M.B. Chandio, A. Ali Maitlo, M. Ahmed, D. Cao, Green synthesis, characterization and photocatalytic activity of silver nanoparticles synthesized with Nigella Sativa seed extract, Chem. Phys. Lett. 763 (2021), 138218.
[195] M. Chandhru, R. Logesh, S. Kutti Rani, N. Ahmed, N. Vasimalai, Green synthesis of silver nanoparticles from plant latex and their antibacterial and photocatalytic studies, Environ. Technol. (2021) 1–11.
[196] A.R. Deshmukh, P.K. Dikshit, B.S. Kim, Green in situ immobilization of gold and silver nanoparticles on bacterial nanocellulose film using Punica granatum peels extract and their application as reusable catalysts, Int. J. Biol. Macromol. 205 (2022) 169–177.
[197] S.D. Roy, K.C. Das, S.S. Dhar, Conventional to green synthesis of magnetic iron oxide nanoparticles; its application as catalyst, photocatalyst and toxicity: a short review, Inorg. Chem. Commun. 134 (2021), 109050.
[198] N. Beheshtkhoo, M.A.J. Kouhbanani, A. Savardashtaki, A.M. Amani, S. Taghizadeh, Green synthesis of iron oxide nanoparticles by aqueous leaf extract of Daphne mezereum as a novel dye removing material, Appl. Phys. A 124 (5) (2018) 363.
[199] A. Taha, E. Da'na, M. Hessien, Evaluation of catalytic and adsorption activity of iron nanoparticles greenly prepared under different conditions: box–Behnken design, Mol. Simul. (2020) 1–11.
[200] M.Y. Rather, S. Sundarapandian, Magnetic iron oxide nanorod synthesis by Wedelia urticifolia (Blume) DC. leaf extract for methylene blue dye degradation, Appl. Nanosci. 10 (7) (2020) 2219–2227.
[201] M. Zulfikar, R. Nadeem, T. Javed, M.I. Jilani, I. Javed, Green synthesis of Fe nanoparticles by using Mangifera indica extract and its application in photo-catalytic degradation of dyes, Water Sci. Technol. 83 (7) (2021) 1739–1752.
[202] U. Khunjan, P. Kasikamphaiboon, Green synthesis of kaolin-supported nanoscale zero-valent iron using ruellia tuberosa leaf extract for effective decolorization of Azo Dye reactive black 5, Arabian J. Sci. Eng. 46 (1) (2021) 383–394.
[203] C.D. Raman, K. Sellappa, M. Mkandawire, Facile one step green synthesis of iron nanoparticles using grape leaves extract: textile dye decolorization and wastewater treatment, Water Sci. Technol. 83 (9) (2021) 2242–2258.
[204] C. Xiao, H. Li, Y. Zhao, X. Zhang, X. Wang, Green synthesis of iron nanoparticle by tea extract (polyphenols) and its selective removal of cationic dyes, J. Environ. Manag. 275 (2020), 111262.
[205] M. Yuan, X. Fu, J. Yu, Y. Xu, J. Huang, Q. Li, D. Sun, Green synthesized iron nanoparticles as highly efficient fenton-like catalyst for degradation of dyes, Chemosphere 261 (2020), 127618.
[206] J. Das, S.S. Dhar, Camellia sinensis mediated synthesis of zero valent iron nanoparticles and study of their efficacy in dye degradation and antibacterial activity, Int. J. Environ. Anal. Chem. (2020) 1–14.
[207] C. Wang, R. Huang, R. Sun, Green one-spot synthesis of hydrochar supported zero-valent iron for heterogeneous Fenton-like discoloration of dyes at neutral pH, J. Mol. Liq. 320 (2020), 114421.
[208] A.S.Y. Ting, J.E. Chin, Biogenic Synthesis of iron nanoparticles from apple peel extracts for decolorization of malachite green dye, Water, Air, & Soil Pollut. 231 (6) (2020) 278.
[209] S. Vasantharaj, S. Sathiyavimal, P. Senthilkumar, F. LewisOscar, A. Pugazhendhi, Biosynthesis of iron oxide nanoparticles using leaf extract of Ruellia tuberosa: antimicrobial properties and their applications in photocatalytic degradation, J. Photochem. Photobiol. B: Biol. 192 (2019) 74–82.
[210] D. Patiño-Ruiz, L. Sánchez-Botero, L. Tejeda-Benitez, J. Hinestroza, A. Herrera, Green synthesis of iron oxide nanoparticles using Cymbopogon citratus extract and sodium carbonate salt: nanotoxicological considerations for potential environmental applications, Environ. Nanotechnol. Monitoring & Manag. 14 (2020), 100377.
[211] S. Qasim, A. Zafar, M.S. Saif, Z. Ali, M. Nazar, M. Waqas, A.U. Haq, T. Tariq, S. G. Hassan, F. Iqbal, X.-.G. Shu, M. Hasan, Green synthesis of iron oxide nanorods using Withania coagulans extract improved photocatalytic degradation and antimicrobial activity, J. Photochem. Photobiol. B: Biol. 204 (2020), 111784.
[212] P. Karpagavinayagam, C. Vedhi, Green synthesis of iron oxide nanoparticles using Avicennia marina flower extract, Vacuum 160 (2019) 286–292.
[213] S.M. Shalaby, F.F. Madkour, H.Y. El-Kassas, A.A. Mohamed, A.M. Elgarahy, Green synthesis of recyclable iron oxide nanoparticles using Spirulina platensis microalgae for adsorptive removal of cationic and anionic dyes, Environ. Sci. Pollut. Res. (2021).

[214] L.V. Prakash, A. Gopinath, R. Gandhimathi, S. Velmathi, S.T. Ramesh, P. V. Nidheesh, Ultrasound aided heterogeneous Fenton degradation of Acid Blue 15 over green synthesized magnetite nanoparticles, Sep. Purif.Technol. 266 (2021), 118230.
[215] M.V. Arasu, S. Arokiyaraj, P. Viayaraghavan, T.S.J. Kumar, V. Duraipandiyan, N. A. Al-Dhabi, K. Kaviyarasu, One step green synthesis of larvicidal, and azo dye degrading antibacterial nanoparticles by response surface methodology, J. Photochem. Photobiol. B: Biol. 190 (2019) 154–162.
[216] A.M. Abdelfatah, M. Fawzy, A.S. Eltaweil, M.E. El-Khouly, Green synthesis of nano-zero-valent iron using ricinus communis seeds extract: characterization and application in the treatment of methylene blue-polluted water, ACS Omega 6 (39) (2021) 25397–25411.
[217] S. Eslami, M.A. Ebrahimzadeh, P. Biparva, Green synthesis of safe zero valent iron nanoparticles by Myrtus communis leaf extract as an effective agent for reducing excessive iron in iron-overloaded mice, a thalassemia model, RSC Adv. 8 (46) (2018) 26144–26155.
[218] U. Shanker, V. Jassal, M. Rani, Green synthesis of iron hexacyanoferrate nanoparticles: potential candidate for the degradation of toxic PAHs, Journal of Environmental Chemical Engineering 5 (4) (2017) 4108–4120.
[219] B. Sharma, S. Menon, S. Mathur, N. Kumari, V. Sharma, Decolorization of malachite green dye from aqueous solution using biosurfactant-stabilized iron oxide nanoparticles: process optimization and reaction kinetics, Int. J. Environ. Sci. Technol. 18 (7) (2021) 1739–1752.
[220] M.S.H. Bhuiyan, M.Y. Miah, S.C. Paul, T.D. Aka, O. Saha, M.M. Rahaman, M.J. I. Sharif, O. Habiba, M. Ashaduzzaman, Green synthesis of iron oxide nanoparticle using Carica papaya leaf extract: application for photocatalytic degradation of remazol yellow RR dye and antibacterial activity, Heliyon 6 (8) (2020) e04603.
[221] I. Bibi, N. Nazar, S. Ata, M. Sultan, A. Ali, A. Abbas, K. Jilani, S. Kamal, F. M. Sarim, M.I. Khan, F. Jalal, M. Iqbal, Green synthesis of iron oxide nanoparticles using pomegranate seeds extract and photocatalytic activity evaluation for the degradation of textile dye, J. Mater. Res. Technol. 8 (6) (2019) 6115–6124.
[222] M.V. Arularasu, J. Devakumar, T.V. Rajendran, An innovative approach for green synthesis of iron oxide nanoparticles: characterization and its photocatalytic activity, Polyhedron 156 (2018) 279–290.
[223] S. Pai, S.M. Kini, M.K. Narasimhan, A. Pugazhendhi, R. Selvaraj, Structural characterization and adsorptive ability of green synthesized Fe3O4 nanoparticles to remove Acid blue 113 dye, Surfaces and Interfaces 23 (2021), 100947.
[224] Bashir Ahmmad, Kwati Leonard, Md Shariful Islam, Junichi Kurawaki, Manickavachagam Muruganandham, Takahiro Ohkubo, Yasushige Kuroda, Green synthesis of mesoporous hematite (α-Fe2O3) nanoparticles and their photocatalytic activity, Adv. Powder Technol. 24 (1) (2013) 160–167.
[225] A.V. Ramesh, D. Rama Devi, S. Mohan Botsa, K. Basavaiah, Facile green synthesis of Fe3O4 nanoparticles using aqueous leaf extract of Zanthoxylum armatum DC. for efficient adsorption of methylene blue, J. Asian Ceramic Soc. 6 (2) (2018) 145–155.
[226] Z. Li, S. Khuje, A. Chivate, Y. Huang, Y. Hu, L. An, Z. Shao, J. Wang, S. Chang, S. Ren, Printable copper sensor electronics for high temperature, ACS Appl. Electronic Mater. 2 (7) (2020) 1867–1873.
[227] P. Vaid, P. Raizada, A.K. Saini, R.V. Saini, Biogenic silver, gold and copper nanoparticles - A sustainable green chemistry approach for cancer therapy, Sustain. Chem. Pharmacy 16 (2020), 100247.
[228] L. Wang, J. Jiang, J. Ma, S. Pang, T. Zhang, A review on advanced oxidation processes homogeneously initiated by copper(II), Chem. Eng. J. 427 (2022), 131721.
[229] H.N. Cuong, S. Pansambal, S. Ghotekar, R. Oza, N.T. Thanh Hai, N.M. Viet, V.-. H. Nguyen, New frontiers in the plant extract mediated biosynthesis of copper oxide (CuO) nanoparticles and their potential applications: a review, Environ. Res. 203 (2022), 111858.
[230] J. Singh, V. Kumar, K.-.H. Kim, M. Rawat, Biogenic synthesis of copper oxide nanoparticles using plant extract and its prodigious potential for photocatalytic degradation of dyes, Environ. Res. 177 (2019), 108569.
[231] S.K. Chandraker, M. Lal, M.K. Ghosh, V. Tiwari, T.K. Ghorai, R. Shukla, Green synthesis of copper nanoparticles using leaf extract of Ageratum houstonianum Mill. and study of their photocatalytic and antibacterial activities, Nano Express 1 (1) (2020), 010033.
[232] R.M. Kiriyanthan, S.A. Sharmili, R. Balaji, S. Jayashree, S. Mahboob, K.A. Al-Ghanim, F. Al-Misned, Z. Ahmed, M. Govindarajan, B. Vaseeharan, Photocatalytic, antiproliferative and antimicrobial properties of copper nanoparticles synthesized using Manilkara zapota leaf extract: a photodynamic approach, Photodiagnosis Photodyn. Ther. 32 (2020), 102058.
[233] S.K. Karuppannan, R. Ramalingam, S.B. Mohamed Khalith, M.J.H. Dowlath, G. I. Darul Raiyaan, K.D. Arunachalam, Characterization, antibacterial and photocatalytic evaluation of green synthesized copper oxide nanoparticles, Biocatal. Agric. Biotechnol. 31 (2021), 101904.
[234] P. Chawla, N. Kumar, A. Bains, S.B. Dhull, M. Kumar, R. Kaushik, S. Punia, Gum arabic capped copper nanoparticles: synthesis, characterization, and applications, Int. J. Biol. Macromol. 146 (2020) 232–242.
[235] N. Sarwar, U.B. Humayoun, M. Kumar, S.F.A. Zaidi, J.H. Yoo, N. Ali, D.I. Jeong, J. H. Lee, D.H. Yoon, Citric acid mediated green synthesis of copper nanoparticles using cinnamon bark extract and its multifaceted applications, J. Clean. Prod. 292 (2021), 125974.
[236] S. Raina, A. Roy, N. Bharadvaja, Degradation of dyes using biologically synthesized silver and copper nanoparticles, Environ. Nanotechnol., Monitoring & Manag. 13 (2020), 100278.
[237] D.B. Manikandan, M. Arumugam, S. Veeran, A. Sridhar, R. Krishnasamy Sekar, B. Perumalsamy, T. Ramasamy, Biofabrication of ecofriendly copper oxide nanoparticles using Ocimum americanum aqueous leaf extract: analysis of in vitro antibacterial, anticancer, and photocatalytic activities, Environ. Sci. Pollut. Res. 28 (26) (2021) 33927–33941.
[238] S. Sharma, K. Kumar, Aloe-vera leaf extract as a green agent for the synthesis of CuO nanoparticles inactivating bacterial pathogens and dye, J. Dispers. Sci. Technol. 42 (13) (2021) 1950–1962.
[239] M. Rafique, F. Shafiq, S.S. Ali Gillani, M. Shakil, M.B. Tahir, I. Sadaf, Eco-friendly green and biosynthesis of copper oxide nanoparticles using Citrofortunella microcarpa leaves extract for efficient photocatalytic degradation of Rhodamin B dye form textile wastewater, Optik (Stuttg) 208 (2020), 164053.
[240] S. Sharma, K. Kumar, N. Thakur, S. Chauhan, M.S. Chauhan, Eco-friendly Ocimum tenuiflorum green route synthesis of CuO nanoparticles: characterizations on photocatalytic and antibacterial activities, J. Environ. Chem. Eng. 9 (4) (2021), 105395.
[241] M.B. Zaman, R. Poolla, P. Singh, T. Gudipati, Biogenic synthesis of CuO nanoparticles using Tamarindus indica L. and a study of their photocatalytic and antibacterial activity, Environ. Nanotechnol. Monitoring & Manag. 14 (2020), 100346.
[242] A. Muthuvel, M. Jothibas, C. Manoharan, Synthesis of copper oxide nanoparticles by chemical and biogenic methods: photocatalytic degradation and in vitro antioxidant activity, Nanotechnol. Environ. Eng. 5 (2) (2020) 14.
[243] S. Kayalvizhi, A. Sengottaiyan, T. Selvankumar, B. Senthilkumar, C. Sudhakar, K. Selvam, Eco-friendly cost-effective approach for synthesis of copper oxide nanoparticles for enhanced photocatalytic performance, Optik (Stuttg) 202 (2020), 163507.
[244] S.A. Akintelu, A.S. Folorunso, A Review on green synthesis of zinc oxide nanoparticles using plant extracts and its biomedical applications, Bionanoscience 10 (4) (2020) 848–863.
[245] A.M. Pillai, V.S. Sivasankarapillai, A. Rahdar, J. Joseph, F. Sadeghfar, R. Anuf A, K. Rajesh, G.Z. Kyzas, Green synthesis and characterization of zinc oxide nanoparticles with antibacterial and antifungal activity, J. Mol. Struct. 1211 (2020), 128107.
[246] Yashni, G.; Al-Gheethi, A.; Mohamed, R.; Hossain, M.S.; Kamil, A.F.; Abirama Shanmugan, V., Photocatalysis of xenobiotic organic compounds in greywater using zinc oxide nanoparticles: a critical review. 2021, 35 (1), 190–217.
[247] A. Narayana, S.A. Bhat, A. Fathima, S.V. Lokesh, S.G. Surya, C.V. Yelamaggad, Green and low-cost synthesis of zinc oxide nanoparticles and their application in transistor-based carbon monoxide sensing, RSC Adv. 10 (23) (2020) 13532–13542.
[248] R. Vinayagam, R. Selvaraj, P. Arivalagan, T. Varadavenkatesan, Synthesis, characterization and photocatalytic dye degradation capability of Calliandra haematocephala-mediated zinc oxide nanoflowers, J. Photochem. Photobiol. B: Biol. 203 (2020), 111760.
[249] N.A. Mirgane, V.S. Shivankar, S.B. Kotwal, G.C. Wadhawa, M.C. Sonawale, Degradation of dyes using biologically synthesized zinc oxide nanoparticles, in: Materials Today: Proceedings 37, 2021, pp. 849–853.
[250] S. Chakraborty, J.J. Farida, R. Simon, S. Kasthuri, N.L. Mary, Averrhoe carrambola fruit extract assisted green synthesis of zno nanoparticles for the photodegradation of congo red dye, Surfaces and Interfaces 19 (2020), 100488.
[251] P. Debnath, N.K. Mondal, Effective removal of congo red dye from aqueous solution using biosynthesized zinc oxide nanoparticles, Environ. Nanotechnol., Monitoring & Manag. 14 (2020), 100320.
[252] Y.C. Liu, J. Li, J. Ahn, J. Pu, E.J. Rupa, Y. Huo, D.C. Yang, Biosynthesis of zinc oxide nanoparticles by one-pot green synthesis using fruit extract of Amomum longiligulare and its activity as a photocatalyst, Optik (Stuttg) 218 (2020), 165245.
[253] S.M. Tabrizi Hafez Moghaddas, B. Elahi, V. Javanbakht, Biosynthesis of pure zinc oxide nanoparticles using Quince seed mucilage for photocatalytic dye degradation, J. Alloys Compd. 821 (2020), 153519.
[254] J.K. Park, E.J. Rupa, M.H. Arif, J.F. Li, G. Anandapadmanaban, J.P. Kang, M. Kim, J.C. Ahn, R. Akter, D.C. Yang, S.C. Kang, Synthesis of zinc oxide nanoparticles from Gynostemma pentaphyllum extracts and assessment of photocatalytic properties through malachite green dye decolorization under UV illumination-A Green Approach, Optik (Stuttg) 239 (2021), 166249.
[255] C. Mallikarjunaswamy, V. Lakshmi Ranganatha, R. Ramu, G. Udayabhanu; Nagaraju, Facile microwave-assisted green synthesis of ZnO nanoparticles: application to photodegradation, antibacterial and antioxidant, J. Mater. Sci.: Mater. Electron. 31 (2) (2020) 1004–1021.
[256] K. Rambabu, G. Bharath, F. Banat, P.L. Show, Green synthesis of zinc oxide nanoparticles using Phoenix dactylifera waste as bioreductant for effective dye degradation and antibacterial performance in wastewater treatment, J. Hazard. Mater. 402 (2021), 123560.
[257] M. Shabaani, S. Rahaiee, M. Zare, S.M. Jafari, Green synthesis of ZnO nanoparticles using loquat seed extract; Biological functions and photocatalytic degradation properties, LWT 134 (2020), 110133.
[258] A.C. Ekennia, D.N. Uduagwu, N.N. Nwaji, O.O. Oje, C.O. Emma-Uba, S.I. Mgbii, O.J. Olowo, O.L. Nwanji, Green Synthesis of Biogenic Zinc Oxide Nanoflower as Dual Agent for Photodegradation of an Organic Dye and Tyrosinase Inhibitor, J. Inorg. Organomet. Polym. Mater. 31 (2) (2021) 886–897.
[259] P.N.V.K. Pallela, L.K. Ruddaraju, S.C. Veerla, R. Matangi, P. Kollu, S. Ummey, S.V. N. Pammi, Synergetic antibacterial potential, dye degrading capability and biocompatibility of Asperagus racemosus root assisted ZnO nanoparticles, Mater. Today Commun. 25 (2020), 101574.

[260] M. Rafique, R. Tahir, S.S.A. Gillani, M.B. Tahir, M. Shakil, T. Iqbal, M. O. Abdellahi, Plant-mediated green synthesis of zinc oxide nanoparticles from Syzygium Cumini for seed germination and wastewater purification, Int. J. Environ. Anal. Chem. (2020) 1–16.
[261] D. Achudhan, S. Vijayakumar, B. Malaikozhundan, M. Divya, M. Jothirajan, K. Subbian, Z.I. González-Sánchez, S. Mahboob, K.A. Al-Ghanim, B. Vaseeharan, The antibacterial, antibiofilm, antifogging and mosquitocidal activities of titanium dioxide (TiO2) nanoparticles green-synthesized using multiple plants extracts, J. Environ. Chem. Eng. 8 (6) (2020), 104521.
[262] A. Singh, V. Goyal, J. Singh, M. Rawat, Structural, morphological, optical and photocatalytic properties of green synthesized TiO2 NPs, Current Res. Green and Sustain. Chem. 3 (2020), 100033.
[263] G. Nabi, A. Majid, A. Riaz, T. Alharbi, M. Arshad Kamran, M. Al-Habardi, Green synthesis of spherical TiO2 nanoparticles using Citrus Limetta extract: excellent photocatalytic water decontamination agent for RhB dye, Inorg. Chem. Commun. 129 (2021), 108618.
[264] G. Nabi, Q.-.U. Ain, M.B. Tahir, K. Nadeem Riaz, T. Iqbal, M. Rafique, S. Hussain, W. Raza, I. Aslam, M. Rizwan, Green synthesis of TiO2 nanoparticles using lemon peel extract: their optical and photocatalytic properties, Int. J. Environ. Anal. Chem. (2020) 1–9.
[265] H. Kaur, S. Kaur, S. Kumar, J. Singh, M. Rawat, Eco-friendly approach: synthesis of novel green TiO2 nanoparticles for degradation of reactive green 19 dye and replacement of chemical synthesized TiO2, J. Cluster Sci. 32 (5) (2021) 1191–1204.
[266] E.T. Helmy, E.M. Abouellef, U.A. Soliman, J.H. Pan, Novel green synthesis of S-doped TiO2 nanoparticles using Malva parviflora plant extract and their photocatalytic, antimicrobial and antioxidant activities under sunlight illumination, Chemosphere 271 (2021), 129524.
[267] M. Najjar, H.A. Hosseini, A. Masoudi, Z. Sabouri, A. Mostafapour, M. Khatami, M. Darroudi, Green chemical approach for the synthesis of SnO2 nanoparticles and its application in photocatalytic degradation of Eriochrome Black T dye, Optik (Stuttg) 242 (2021), 167152.
[268] M. Honarmand, M. Golmohammadi, A. Naeimi, Biosynthesis of tin oxide (SnO2) nanoparticles using jujube fruit for photocatalytic degradation of organic dyes, Adv. Powder Technol. 30 (8) (2019) 1551–1557.
[269] J. Singh, N. Kaur, P. Kaur, S. Kaur, J. Kaur, P. Kukkar, V. Kumar, D. Kukkar, M. Rawat, Piper betle leaves mediated synthesis of biogenic SnO2 nanoparticles for photocatalytic degradation of reactive yellow 186 dye under direct sunlight, Environ. Nanotechnol., Monitoring & Manag. 10 (2018) 331–338.
[270] J. Ebrahimian, M. Mohsennia, M. Khayatkashani, Photocatalytic-degradation of organic dye and removal of heavy metal ions using synthesized SnO2 nanoparticles by Vitex agnus-castus fruit via a green route, Mater. Lett. 263 (2020), 127255.
[271] E. Gomathi, M. Jayapriya, M. Arulmozhi, Environmental benign synthesis of tin oxide (SnO2) nanoparticles using Actinidia deliciosa (Kiwi) peel extract with enhanced catalytic properties, Inorg. Chem. Commun. 130 (2021), 108670.
[272] P.A. Luque, H.E. Garrafa-Gálvez, O. Nava, A. Olivas, M.E. Martínez-Rosas, A. R. Vilchis-Nestor, A. Villegas-Fuentes, M.J. Chinchillas-Chinchillas, Efficient sunlight and UV photocatalytic degradation of methyl orange, methylene blue and rhodamine B, using Citrus×paradisi synthesized SnO2 semiconductor nanoparticles, Ceram. Int. 47 (17) (2021) 23861–23874.
[273] B. Khodadadi, M. Bordbar, M. Nasrollahzadeh, Green synthesis of Pd nanoparticles at Apricot kernel shell substrate using Salvia hydrangea extract: catalytic activity for reduction of organic dyes, J. Colloid Interface Sci. 490 (2017) 1–10.
[274] M.I. Din, M. Tariq, Z. Hussain, R. Khalid, Single step green synthesis of nickel and nickel oxide nanoparticles from Hordeum vulgare for photocatalytic degradation of methylene blue dye, Inorganic and Nano-Metal Chem. 50 (4) (2020) 292–297.
[275] L.A. Wali, A.M. Alwan, A.B. Dheyab, D.A. Hashim, Excellent fabrication of Pd-Ag NPs/PSi photocatalyst based on bimetallic nanoparticles for improving methylene blue photocatalytic degradation, Optik (Stuttg) 179 (2019) 708–717.
[276] C. Sharma, S. Ansari, M.S. Ansari, S.P. Satsangee, M.M. Srivastava, Single-step green route synthesis of Au/Ag bimetallic nanoparticles using clove buds extract: enhancement in antioxidant bio-efficacy and catalytic activity, Mater. Sci. Eng.: C 116 (2020), 111153.
[277] H. Hu, Y. Lin, Y.H. Hu, Synthesis, structures and applications of single component core-shell structured TiO2: a review, Chem. Eng. J. 375 (2019), 122029.
[278] S. Ghosh, S. Roy, J. Naskar, R.K. Kole, Process optimization for biosynthesis of mono and bimetallic alloy nanoparticle catalysts for degradation of dyes in individual and ternary mixture, Sci. Rep. 10 (1) (2020) 277.
[279] D. Bhardwaj, R. Singh, Green biomimetic synthesis of Ag–TiO2 nanocomposite using Origanum majorana leaf extract under sonication and their biological activities, Bioresour. Bioprocess. 8 (1) (2021) 1–12.
[280] A. Al-Asfar, Z. Zaheer, E.S. Aazam, Eco-friendly green synthesis of Ag@Fe bimetallic nanoparticles: antioxidant, antimicrobial and photocatalytic degradation of bromothymol blue, J. Photochem. Photobiol. B: Biol. 185 (2018) 143–152.
[281] X. He, D.-.P. Yang, X. Zhang, M. Liu, Z. Kang, C. Lin, N. Jia, R. Luque, Waste eggshell membrane-templated CuO-ZnO nanocomposites with enhanced adsorption, catalysis and antibacterial properties for water purification, Chem. Eng. J. 369 (2019) 621–633.
[282] J. Al-Haddad, F. Alzaabi, P. Pal, K. Rambabu, F. Banat, Green synthesis of bimetallic copper–silver nanoparticles and their application in catalytic and antibacterial activities, Clean Technol. Environ. Policy 22 (1) (2020) 269–277.
[283] M. Yang, F. Lu, T. Zhou, J. Zhao, C. Ding, A. Fakhri, V.K. Gupta, Biosynthesis of nano bimetallic Ag/Pt alloy from Crocus sativus L. extract: biological efficacy and catalytic activity, J. Photochem. Photobiol. B: Biol. 212 (2020), 112025.
[284] A. Velidandi, N.P.P. Pabbathi, S. Dahariya, R.R. Baadhe, Green synthesis of novel Ag–Cu and Ag–Znbimetallic nanoparticles and their in vitro biological, eco-toxicity and catalytic studies, Nano-Structures & Nano-Objects 26 (2021), 100687.
[285] A.K. Prajapati, M.K. Mondal, Novel green strategy for CuO–ZnO–C nanocomposites fabrication using marigold (Tagetes spp.) flower petals extract with and without CTAB treatment for adsorption of Cr (VI) and Congo red dye, J. Environ. Manag. 290 (2021), 112615.
[286] A. Fouda, S.S. Salem, A.R. Wassel, M.F. Hamza, T.I. Shaheen, Optimization of green biosynthesized visible light active CuO/ZnO nano-photocatalysts for the degradation of organic methylene blue dye, Heliyon 6 (9) (2020) e04896.
[287] A. Nayak, J.K. Sahoo, S.K. Sahoo, D. Sahu, Removal of congo red dye from aqueous solution using zinc oxide nanoparticles synthesised from Ocimum sanctum (Tulsi leaf): a green approach, Int. J. Environ. Anal. Chem. (2020) 1–22.
[288] B. Fatima, S.I. Siddiqui, R.K. Nirala, K. Vikrant, K.-.H. Kim, R. Ahmad, S. A. Chaudhry, Facile green synthesis of ZnO–CdWO4 nanoparticles and their potential as adsorbents to remove organic dye, Environ. Pollut. 271 (2021), 116401.
[289] M.H. Sayadi, S. Ghollasimood, N. Ahmadpour, S. Homaeigohar, Biosynthesis of the ZnO/SnO2 nanoparticles and characterization of their photocatalytic potential for removal of organic water pollutants, J. Photochem. Photobiol. A: Chem. 425 (2022), 113662.
[290] L. Gnanasekaran, A.K. Priya, F. Gracia, Orange peel extract influenced partial transformation of SnO2 to SnO in green 3D-ZnO/SnO2 system for chlorophenol degradation, J. Hazard. Mater. 424 (2022), 127464.
[291] M.A. Malik, A.A. Alshehri, R. Patel, Facile one-pot green synthesis of Ag–Fe bimetallic nanoparticles and their catalytic capability for 4-nitrophenol reduction, J. Mater. Res. Technol. 12 (2021) 455–470.
[292] S. Mohan, M.V. Devan, S. Sambathkumar, V. Shanmugam, K. Ravikumar, R. Marnadu, B. Palanivel, H.H. Hegazy, Dual probes of Ag/Pd bimetallic NPs facilely synthesized by green process using Catharanthus leaf extract on textile dye removal and free radical capability, Appl. Nanosci. 11 (5) (2021) 1565–1574.
[293] Younas, U.; Hassan, S.T.; Ali, F.; Hassan, F.; Saeed, Z.; Pervaiz, M.; Khan, S.; Jannat, F.T.; Bibi, S.; Sadiqa, A.; Ali, Z.; Iqbal, S.; Ghfar, A.A.; Ouladsmane, M.; AL-Anazy, M.M.; Ali, S., Radical scavenging and catalytic activity of fe-cu bimetallic nanoparticles synthesized from ixora finlaysoniana extract. 2021, 11 (7), 813.
[294] A.R. Suvarna, A. Shetty, S. Anchan, N. Kabeer, S. Nayak, Cyclea peltata leaf mediated green synthesized bimetallic nanoparticles exhibits methyl green dye degradation capability, Bionanoscience 10 (3) (2020) 606–617.
[295] S. Deng, B. Zhao, Y. Xing, Y. Shi, Y. Fu, Z. Liu, Green synthesis of proanthocyanidins-functionalized Au/Ag bimetallic nanoparticles, Green Chem. Lett. Rev. 14 (1) (2021) 45–50.
[296] M. Nasrollahzadeh, Z. Issaabadi, S.M. Sajadi, Green synthesis of a Cu/MgO nanocomposite by Cassytha filiformis L. extract and investigation of its catalytic activity in the reduction of methylene blue, congo red and nitro compounds in aqueous media, RSC Adv. 8 (7) (2018) 3723–3735.
[297] Y. Weng, J. Li, X. Ding, B. Wang, S. Dai, Y. Zhou, R. Pang, Y. Zhao, H. Xu, B. Tian, Y. Hua, Functionalized gold and silver bimetallic nanoparticles using deinococcus radiodurans protein extract mediate degradation of toxic dye malachite green, Int. J. Nanomed. 15 (2020) 1823–1835.
[298] N. Karić, A.S. Maia, A. Teodorović, N. Atanasova, G. Langergraber, G. Crini, M. Đolić, Bio-waste valorisation: agricultural wastes as biosorbents for removal of (in) organic pollutants in wastewater treatment, Chem. Eng. J. Adv. 9 (2022), 100239.
[299] N. Bahadur, P. Das, N. Bhargava, Improving energy efficiency and economic feasibility of photocatalytic treatment of synthetic and real textile wastewater using bagasse fly ash modified TiO2, Chem. Eng. J.Adv. 2 (2020), 100012.
[300] C.V. Rekhate, J.K. Srivastava, Recent advances in ozone-based advanced oxidation processes for treatment of wastewater-A review, Chem. Eng. J. Adv. 3 (2020), 100031.
[301] I. Berruti, S. Nahim-Granados, M.J. Abeledo-Lameiro, I. Oller, M.I. Polo-López, Recent advances in solar photochemical processes for water and wastewater disinfection, Chem. Eng. J. Adv. (2022), 100248.
[302] T. Fatima, S. Husain, M. Khanuja, Superior photocatalytic and electrochemical activity of novel WS2/PANI nanocomposite for the degradation and detection of pollutants: antibiotic, heavy metal ions, and dyes, Chem. Eng. J. Adv. 12 (2022), 100373.
[303] Q. Wang, Y. Wang, L. Yuan, T. Zou, W. Zhang, X. Zhang, X. Huang, Utilization of low-cost watermelon rind for efficient removal of Cd (II) from aqueous solutions: adsorption performance and mechanism elucidation, Chem. Eng. J. Adv. 12 (2022), 100393.
[304] D. Sachan, A. Ramesh, G. Das, Green synthesis of silica nanoparticles from leaf biomass and its application to remove heavy metals from synthetic wastewater: a comparative analysis, Environ. Nanotechnol. Monitoring & Manag. 16 (2021), 100467.
[305] J.D.O. Primo, C. Bittencourt, S. Acosta, A. Sierra-Castillo, J.F. Colomer, S. Jaerger, F.J. Anaissi, Synthesis of zinc oxide nanoparticles by ecofriendly routes: adsorbent for copper removal from wastewater, Front. Chem. 8 (2020), 571790.
[306] J. Ebrahimian, M. Mohsennia, M. Khayatkashani, Photocatalytic-degradation of organic dye and removal of heavy metal ions using synthesized SnO2 nanoparticles by Vitex agnus-castus fruit via a green route, Mater. Lett. 263 (2020), 127255.

[307] S. Altaf, R. Zafar, W.Q. Zaman, S. Ahmad, K. Yaqoob, A. Syed, M. Arshad, Removal of levofloxacin from aqueous solution by green synthesized magnetite (Fe3O4) nanoparticles using Moringa olifera: kinetics and reaction mechanism analysis, Ecotoxicol. Environ. Saf. 226 (2021), 112826.
[308] H.A. Ari, O.A. Alani, Q.R. Zeng, Y.A. Ugya, N.A.O. Offiong, W. Feng, Enhanced UV-assisted Fenton performance of nanostructured biomimetic α-Fe2O3 on degradation of tetracycline, J. Nanostructure in Chem. 12 (1) (2022) 45–58.
[309] G. Gopal, K.V.G. Ravikumar, M. Salma, N. Chandrasekaran, A. Mukherjee, Green synthesized Fe/Pd and in-situ Bentonite-Fe/Pd composite for efficient tetracycline removal, J. Environ. Chem. Eng. 8 (5) (2020), 104126.
[310] S.A. Khan, S. Shahid, B. Shahid, U. Fatima, S.A. Abbasi, Green synthesis of MnO nanoparticles using abutilon indicum leaf extract for biological, photocatalytic, and adsorption activities, Biomolecules 10 (5) (2020) 785.
[311] A.M. Shaik, M. David Raju, D. Rama Sekhara Reddy, Green synthesis of zinc oxide nanoparticles using aqueous root extract of Sphagneticola trilobata Lin and investigate its role in toxic metal removal, sowing germination and fostering of plant growth, Inorganic and Nano-Metal Chem. 50 (7) (2020) 569–579.
[312] A. Verma, N. Bharadvaja, Plant-mediated synthesis and characterization of silver and copper oxide nanoparticles: antibacterial and heavy metal removal activity, J. Cluster Sci. 33 (4) (2022) 1697–1712.
[313] A. Sebastian, A. Nangia, M.N.V. Prasad, Cadmium and sodium adsorption properties of magnetite nanoparticles synthesized from Hevea brasiliensis Muell. Arg. bark: relevance in amelioration of metal stress in rice, J. Hazard Mater. 371 (2019 Jun 5) 261–272.
[314] S. Mahanty, S. Chatterjee, S. Ghosh, P. Tudu, T. Gaine, M. Bakshi, P. Chaudhuri, Synergistic approach towards the sustainable management of heavy metals in wastewater using mycosynthesized iron oxide nanoparticles: biofabrication, adsorptive dynamics and chemometric modeling study, J. Water Process Eng. 37 (2020), 101426.
[315] V.K. Yadav, M.H. Fulekar, Biogenic synthesis of maghemite nanoparticles (γ-Fe2O3) using Tridax leaf extract and its application for removal of fly ash heavy metals (Pb, Cd), Mater. Today: Proceed. 5 (9) (2018) 20704–20710.
[316] S. Venkateswarlu, B.N. Kumar, B. Prathima, Y. SubbaRao, N.V.V. Jyothi, A novel green synthesis of Fe3O4 magnetic nanorods using Punica Granatum rind extract and its application for removal of Pb (II) from aqueous environment, Arabian J. Chem. 12 (4) (2019) 588–596.
[317] M. Honarmand, M. Amini, A. Iranfar, A. Naeimi, Green synthesis of ZnO/SnO2 nanocomposites using pine leaves and their application for the removal of heavy metals from aqueous media, J. Cluster Sci. 33 (1) (2022) 301–310.
[318] N. Barnawi, S. Allehyani, R. Seoudi, Biosynthesis and characterization of gold nanoparticles and its application in eliminating nickel from water, J. Mater. Res. Technol. (2022).
[319] M.A. Irshad, M.B. Shakoor, R. Nawaz, T. Yasmeen, M.S. Arif, M. Rizwan, S. Ali, Green and eco-friendly synthesis of TiO2 nanoparticles and their application for removal of cadmium from wastewater: reaction kinetics study, Zeitschrift für Physikalische Chemie 236 (5) (2022) 637–657.
[320] K.M. Al-Qahtani, Cadmium removal from aqueous solution by green synthesis zero valent silver nanoparticles with Benjamina leaves extract, The Egyptian J. Aquatic Res. 43 (4) (2017) 269–274.
[321] Y. Zhang, Q. Zhao, B. Chen, Reduction and removal of Cr (VI) in water using biosynthesized palladium nanoparticles loaded Shewanella oneidensis MR-1, Sci. e Total Environ. 805 (2022), 150336.
[322] N.K. Sethy, Z. Arif, P.K. Mishra, P. Kumar, Green synthesis of TiO2 nanoparticles from Syzygium cumini extract for photo-catalytic removal of lead (Pb) in explosive industrial wastewater, Green Processing and Synthesis 9 (1) (2020) 171–181.
[323] I. Lung, M. Stan, O. Opris, M.L. Soran, M. Senila, M. Stefan, Removal of lead (II), cadmium (II), and arsenic (III) from aqueous solution using magnetite nanoparticles prepared by green synthesis with Box–Behnken design, Anal. Lett. 51 (16) (2018) 2519–2531.
[324] A.E.D. Mahmoud, K.M. Al-Qahtani, S.O. Alflaij, S.F. Al-Qahtani, F.A. Alsamhan, Green copper oxide nanoparticles for lead, nickel, and cadmium removal from contaminated water, Sci. Rep. 11 (1) (2021) 1–13.
[325] P. Sharma, J. Kherb, J. Prakash, R. Kaushal, A novel and facile green synthesis of SiO2 nanoparticles for removal of toxic water pollutants, Appl. Nanosci. (2021) 1–13.
[326] S. Bhattacharjee, F. Habib, N. Darwish, A. Shanableh, Iron sulfide nanoparticles prepared using date seed extract: green synthesis, characterization and potential application for removal of ciprofloxacin and chromium, Powder Technol. 380 (2021) 219–228.
[327] K.V.G. Ravikumar, S.V. Sudakaran, K. Ravichandran, M. Pulimi, C. Natarajan, A. Mukherjee, Green synthesis of NiFe nano particles using Punica granatum peel extract for tetracycline removal, J. Clean. Prod. 210 (2019) 767–776.
[328] Z. Lin, X. Weng, G. Owens, Z. Chen, Simultaneous removal of Pb (II) and rifampicin from wastewater by iron nanoparticles synthesized by a tea extract, J. Clean. Prod. 242 (2020), 118476.
[329] B. Debnath, M. Majumdar, M. Bhowmik, K.L. Bhowmik, A. Debnath, D.N. Roy, The effective adsorption of tetracycline onto zirconia nanoparticles synthesized by novel microbial green technology, J. Environ. Manag. 261 (2020), 110235.
[330] W. Cai, X. Weng, Z. Chen, Highly efficient removal of antibiotic rifampicin from aqueous solution using green synthesis of recyclable nano-Fe3O4, Environ. Pollut. 247 (2019) 839–846.
[331] A. Makofane, D.E. Motaung, N.C. Hintsho-Mbita, Photocatalytic degradation of methylene blue and sulfisoxazole from water using biosynthesized zinc ferrite nanoparticles, Ceram. Int. 47 (16) (2021) 22615–22626.
[332] P. Debnath, K. Sen, A. Mondal, A. Mondal, N.K. Mondal, Insight into photocatalytic degradation of amoxicillin by biofabricated granular zinc oxide nanoparticle: mechanism, optimization and toxicity evaluation, Int. J. Environ. Res. 15 (3) (2021) 571–583.
[333] K. Pakzad, H. Alinezhad, M. Nasrollahzadeh, Euphorbia polygonifolia extract assisted biosynthesis of Fe3O4@ CuO nanoparticles: applications in the removal of metronidazole, ciprofloxacin and cephalexin antibiotics from aqueous solutions under UV irradiation, Appl. Organomet. Chem. 34 (11) (2020) e5910.